

INFORMATION TO USERS

This manuscript has been reproduced from the microfilm master. UMI films the text directly from the original or copy submitted. Thus, some thesis and dissertation copies are in typewriter face, while others may be from any type of computer printer.

The quality of this reproduction is dependent upon the quality of the copy submitted. Broken or indistinct print, colored or poor quality illustrations and photographs, print bleedthrough, substandard margins, and improper alignment can adversely affect reproduction.

In the unlikely event that the author did not send UMI a complete manuscript and there are missing pages, these will be noted. Also, if unauthorized copyright material had to be removed, a note will indicate the deletion.

Oversize materials (e.g., maps, drawings, charts) are reproduced by sectioning the original, beginning at the upper left-hand corner and continuing from left to right in equal sections with small overlaps.

ProQuest Information and Learning
300 North Zeeb Road, Ann Arbor, MI 48106-1346 USA
800-521-0600

UMI[®]

UNIVERSITY OF ALBERTA

Mathematical Modelling of HTLV-I-Infection Dynamics

by

Horacio Gómez-Acevedo ©

A THESIS SUBMITTED TO THE FACULTY OF GRADUATE STUDIES
AND RESEARCH IN PARTIAL FULFILLMENT OF THE REQUIREMENTS
FOR THE DEGREE OF DOCTOR OF PHILOSOPHY

IN

APPLIED MATHEMATICS

DEPARTMENT OF MATHEMATICAL AND STATISTICAL SCIENCES

EDMONTON, ALBERTA

SPRING 2005



Library and
Archives Canada

Bibliothèque et
Archives Canada

0-494-08240-2

Published Heritage
Branch

Direction du
Patrimoine de l'édition

395 Wellington Street
Ottawa ON K1A 0N4
Canada

395, rue Wellington
Ottawa ON K1A 0N4
Canada

Your file *Votre référence*

ISBN:

Our file *Notre référence*

ISBN:

NOTICE:

The author has granted a non-exclusive license allowing Library and Archives Canada to reproduce, publish, archive, preserve, conserve, communicate to the public by telecommunication or on the Internet, loan, distribute and sell theses worldwide, for commercial or non-commercial purposes, in microform, paper, electronic and/or any other formats.

The author retains copyright ownership and moral rights in this thesis. Neither the thesis nor substantial extracts from it may be printed or otherwise reproduced without the author's permission.

AVIS:

L'auteur a accordé une licence non exclusive permettant à la Bibliothèque et Archives Canada de reproduire, publier, archiver, sauvegarder, conserver, transmettre au public par télécommunication ou par l'Internet, prêter, distribuer et vendre des thèses partout dans le monde, à des fins commerciales ou autres, sur support microforme, papier, électronique et/ou autres formats.

L'auteur conserve la propriété du droit d'auteur et des droits moraux qui protègent cette thèse. Ni la thèse ni des extraits substantiels de celle-ci ne doivent être imprimés ou autrement reproduits sans son autorisation.

In compliance with the Canadian Privacy Act some supporting forms may have been removed from this thesis.

Conformément à la loi canadienne sur la protection de la vie privée, quelques formulaires secondaires ont été enlevés de cette thèse.

While these forms may be included in the document page count, their removal does not represent any loss of content from the thesis.

Bien que ces formulaires aient inclus dans la pagination, il n'y aura aucun contenu manquant.


Canada

Je souhaite seulement que dans une question qui regarde si de près le bien de l'humanité, on ne décide rien qu'avec toute la connaissance de cause qu'un peu d'analyse et de calcul peut fournir.

DANIEL BERNOULLI

Table of Contents

Chapter 1. Introduction	1
1.1. HTLV-I and Related Diseases	1
1.2. HTLV-I and HIV Retroviruses	3
1.3. Modelling HTLV-I Infection	4
1.4. Immune System	6
1.5. Summary of Relevant Literature	9
1.6. Thesis Overview	10
1.7. References	11
Chapter 2. A Basic Model for HTLV-I Infection	18
2.1. Introduction	18
2.2. A Mathematical Model	19
2.3. Equilibrium Points	22
2.4. Global Dynamics	24
2.5. Discussion and Conclusions	29
2.6. References	30
Chapter 3. Mitotic Division of HTLV-I-infected T Cells	33
3.1. Introduction	33
3.2. A Mathematical Model	35
3.3. Local Stability Analysis of the Equilibria	41
3.4. Global Dynamics of a Reduced Model	47
3.5. Numerical Simulations of the Reduced Model	50
3.6. Conclusions	55
3.7. References	57
Chapter 4. CD34 Stem Cells as a Reservoir for HTLV-I Infection	61
4.1. Introduction	61

4.2. A Mathematical Model	62
4.3. Equilibrium Points	65
4.4. Global Dynamics	67
4.5. Numerical Simulations	71
4.6. Conclusions	76
4.7. References	77
Chapter 5. Cytotoxic Response to HTLV-I Infection	81
5.1. Introduction	81
5.2. A Mathematical Model	83
5.3. Local Stability Analysis of the Equilibria	86
5.4. Global Dynamics	87
5.5. Relevance of CTL-related Parameters to HTLV-I Infection	90
5.6. Conclusions	99
5.7. References	101
Chapter 6. Conclusions	106
6.1. General Discussion	106
6.2. Future Research	109
6.3. References	109
Appendix A. Lozinskiĭ Measure and Compound Matrices	111
Appendix B. Li and Muldowney's Method for Global Stability	113

List of Figures

Fig. 1.1. HTLV-I virion structure	2
Fig. 1.2. Classification of the immune responses	7
Fig. 1.3. Immune system responses	8
Fig. 2.1. HTLV-I infection process	19
Fig. 2.2. Transfer diagram	20
Fig. 2.3. Uniqueness of the chronic-infection equilibrium	23
Fig. 2.4. Forward bifurcation	29
Fig. 3.1. Transmission of HTLV-I infection	34
Fig. 3.2. Transfer diagram	35
Fig. 3.3. Roots of $m_\sigma(X)$ when $\sigma > \sigma_0$	39
Fig. 3.4. Positive roots of the polynomials $m_\sigma(X)$ as σ varies	40
Fig. 3.5. Backward bifurcation	45
Fig. 3.6. <i>MATHEMATICA</i> * simulations of system (3.1)	46
Fig. 3.7. Phase-portrait of (3.22) showing multiple stable equilibria	50
Fig. 3.8. <i>MATHEMATICA</i> * simulations of system (3.22)	53
Fig. 3.9. <i>MATHEMATICA</i> * simulations showing a sudden jump of infection level	54
Fig. 4.1. CD34 ⁺ act as a reservoir for HTLV-I infection	62
Fig. 4.2. Transfer diagram	63
Fig. 4.3. Positive roots of $f(x) - g(x)$ when $d \in (0, 1)$	66
Fig. 4.4. Existence of a chronic-infection equilibrium	67
Fig. 4.5. <i>MATHEMATICA</i> * simulations of system (4.1)	73
Fig. 4.6. Graph of $R_0(b)$	74
Fig. 4.7 <i>MATHEMATICA</i> * simulations showing the proviral invasion	75
Fig. 4.8. Hypothesized correlation between the PB and BM proviral load	76
Fig. 5.1. CD8 ⁺ T-cell response in brief	82
Fig. 5.2. Transfer diagram	83
Fig. 5.3. Uniqueness of the chronic-infection equilibrium	86

Fig. 5.4. <i>MATHEMATICA</i> * simulations of the healthy CD4 ⁺ T-cell count	93
Fig. 5.5. <i>MATHEMATICA</i> * simulations of the proviral load	94
Fig. 5.6. <i>MATHEMATICA</i> * simulations of the CD8 ⁺ T-cell level	95
Fig. 5.7. Numerical simulations of healthy CD4 ⁺ T-cell count	97
Fig. 5.8. Numerical simulations of the levels of HTLV-I-infected CD4 ⁺ T cells ...	98
Fig. 5.9. Numerical simulations of the levels of CD8 ⁺ T cells	99

Abbreviations

ATL	Adult T-cell Leukaemia/Lymphoma
AZT	Azidothymidine
CD n	Cluster of Differentiation n
CNS	Central Nervous System
CSF	Cerebrospinal Fluid
CTL	Cytotoxic T Lymphocyte
DNA	Deoxyribonucleic Acid
HAM/TSP	HTVL-I Associated Myelopathy/ Tropical Spastic Paraparesis
HIV	Human Immunodeficiency Virus
HTLV-I	Human T-cell Leukaemia Virus Type I
MHC	Major Histocompatibility Complex
RNA	Ribonucleic Acid
PBMC	Peripheral Blood Mononuclear Cell
tRNA	Transfer RNA

List of Symbols

α	transmission rate at which infected T cells become infectious
b	CD34 ⁺ cell maturation rate
β	contact rate
γ	rate of CTL-mediated elimination
λ	CD4 ⁺ T-cell production rate
Λ	CD34 ⁺ cell production rate
μ_i	removal rate for the i th. compartment
v_i	maximum proliferation rate for the i th compartment
ν	cytotoxic responsiveness
σ	fraction of HTLV-I-infected cells that evade the immune system
$x(t)$	Healthy CD4 ⁺ T cells
$x_h(t)$	Healthy CD34 ⁺ cell
$y(t)$	HTLV-I-infected (latent) CD4 ⁺ T cells
$y_h(t)$	HTLV-I-Infected CD34 ⁺ cell
$z(t)$	HTLV-I-infectious CD4 ⁺ T cells/CD8 ⁺ T cell

TO DR. OLIGERD ALF BIBERSTEIN IN MEMORIAM

Abstract

Human T-cell Leukaemia/Lymphoma Virus Type I (HTLV-I) is a retrovirus identified as the causative agent of the neurological disease HTLV-I-associated myelopathy/tropical spastic paraparesis (HAM/TSP) as well as Adult T-cell leukaemia (ATL). This virus infects primarily $CD4^+$ T cells, but other cell lineages are also susceptible. Using a compartmental approach, some aspects of the infection dynamics are modelled. Since the infectious (horizontal) transmission requires cell-to-cell contact, a model that considers a generalised incidence form was proposed and analysed. It was concluded that the global dynamics is governed by a basic reproduction number R_0 . Clinical experiments show that mitotic division may play a relevant role in HTLV-I infection. A model that considers the mitotic (vertical) transmission was proposed and investigated. Under biologically sound conditions, the model exhibits a backward bifurcation. It has been clinically hypothesized that $CD34^+$ progenitor cells are a reservoir for the virus. A model that contemplates such a reservoir was proposed. The global dynamics of such a model was proved. It also has been observed that HAM/TSP patients harbour high levels of activated $CD8^+$ cytotoxic T cells (CTL). A model that considers the CTL response to HTLV-I was proposed and analysed. The global dynamics depends on the values of the basic reproduction number in the absence (resp. presence) of CTL response. The values on these parameters may help to differentiate HAM/TSP patients from asymptomatic carriers.

Aknowledgments

I would like to thank my supervisor, Dr. Michael Li, for suggesting the topic of this study and guiding me to its completion. Dr. James Muldowney's expertise provided valuable assistance during difficult stages of this work. I appreciate the motivation and support given by Drs. Jack Tuszynski and John Elliott. Also, I want to acknowledge the intellectual input provided by Drs. George Peschke, Herb Freedman and Joseph So in various areas of the research.

This work would not have been possible without the continuous love, support and understanding of my wife Sheila, my parents Alejandra and Teodoro, my parents-in-law Agnes and Michael, my sister Cesandarey, my brothers Gerardo and José, my nephew Uriel, my sisters-in-law Leticia and Rina, my brother-in-law Dave and pet Salma.

I also want to thank my friends, Connie and Jim Hilditch, Nury and Gustavo Carrero, José Calderón and Javier Siller for their encouragement and motivation. My former supervisors Drs. Martha Rzedowski and Gabriel Villa never failed to provide uplifting comments.

Several institutions have supported this research, namely the NCE-MITACS project Mathematical Modeling in Pharmaceutical Development (MMPD) led by Dr. Jack Tuszynski, the National Counsel for Science and Technology of Mexico (CONACyT), and the Superior School of Physics and Mathematics of the National Polytechnique Institute of Mexico (ESFM-IPN).

Finally, I thank thee my Lord for allowing me to come thus far.

Chapter 1

Introduction

1.1. HTLV-I and Related Diseases

Human T-cell Leukaemia/Lymphoma Virus Type I (HTLV-I) is a retrovirus recognized as the causative agent for Adult T-cell Leukaemia/Lymphoma (ATL) and chronic inflammatory disease, termed as HTLV-I-Associated Myelopathy/Tropical Spastic Paraparesis (HAM/TSP) [9, 27, 41]. Recent evidence suggests that HTLV-I is associated with other inflammatory diseases such as uveitis, myositis and alveolitis [28, 39, 42, 51]. HTLV-I-carriers can remain in an asymptomatic stage throughout life and a small proportion (< 5%) develop ATL or HAM/TSP [22, 27].

The number of HTLV-I-infected people is estimated to be between 15 and 25 million worldwide. There are many regions where the infection is endemic, namely Japan, the Caribbean (Jamaica, Trinidad, Martinique, Barbados, Haiti), the equatorial regions of Africa (Ivory Coast, Nigeria, Zaire, Kenya Tanzania), South America (Colombia), Middle East (Iran) and Melanesia [27, 41]. In Japan only, over one million people are infected and more than 700 cases of ATL are reported each year [50].

HTLV-I virions carry viral RNA, tRNA, transcriptase and integrase surrounded by a host-derived lipid envelope embedded with glycoprotein spikes (see Figure 1.1). Viral envelope proteins interact with the host cell receptor GLUT-1 and lead to HTLV-I entry via membrane fusion [36, 47]. Once inside the cell cytoplasm, reverse transcriptase synthesizes viral DNA using RNA as a template. Viral integrase incorporates the viral DNA, which is called *provirus*, into the host-cell genome. Once integrated, the provirus can remain latent for some time after which the cell will produce

viral components [7, 14]. Encoded within HTLV-I genome is the multi-functional protein referred to as Tax. This protein regulates viral transcription, controls cell proliferation, activates cellular oncogenes and inhibits apoptosis [19, 41, 52, 59].

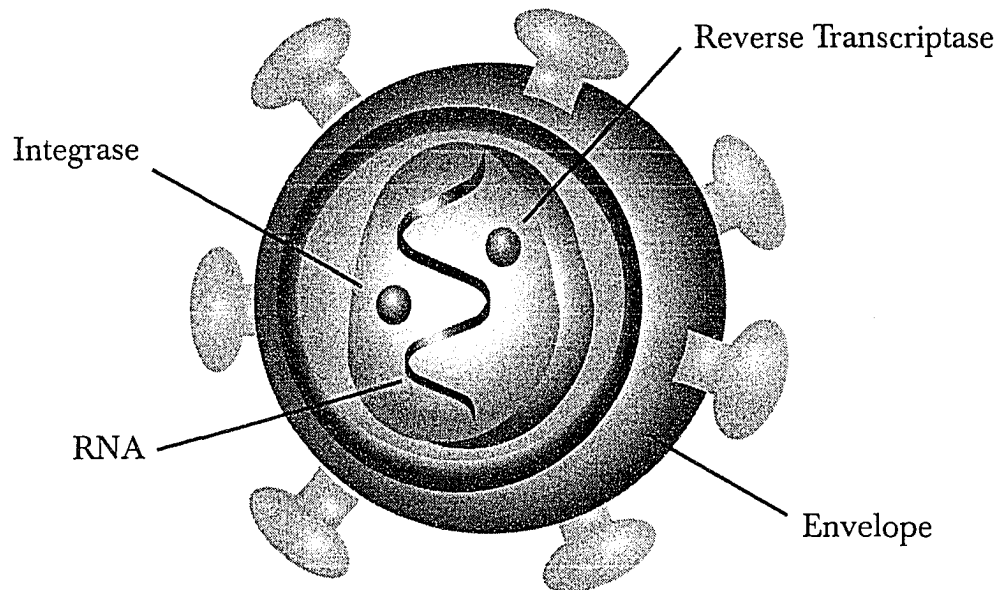


Figure 1.1. HTLV-I virion structure.

HTLV-I targets primarily CD4⁺ T cells, but other T cells can be infected including immature cells [9, 41]. HTLV-I is transmitted by cell-to-cell contact [27, 47]. Free virions are not so infectious and rarely found in plasma [44]. Because of the routes of HTLV-I transmission, proviral loads are crucial for the infection dynamics, and viral loads are normally ignored. Furthermore, the proportion of peripheral blood mononuclear cells (PBMCs) that carry a provirus is particularly high. Normally, asymptomatic carriers have 0.1-1.0 copies per 100 PBMCs, whereas HAM/TSP patients harbour 5-10 copies per 100 PBMCs [4].

Shortly after infection, HTLV-I-infected people show high levels of antibodies [37, 41]. Fifty percent of infected people produce detectable levels of antibodies to the Tax protein. Also, the majority of HTLV-I carriers mount a strong cytotoxic response to the virus, which is mainly directed to the Tax 11-19 peptides [6, 19]. In particular, HAM/TSP patients exhibit remarkably high levels of anti-HTLV-I cytotoxic T lymphocytes in the peripheral blood [27].

1.2. HTLV-I and HIV Retroviruses

A piece of bad news wrapped up in protein.

Sir Peter Medawar

In 1980, Gallo and colleagues discovered the first human retrovirus: HTLV-I. A couple of years later, a second human retrovirus was found by them and named HTLV-II. These discoveries had a tremendous effect on virological research, and promptly another retrovirus was found: HIV, which was formerly designated as HTLV-III [15, 46]. In the rest of the section, we will describe relevant differences between HIV-1 and HTLV-I.

The general genetic structure of HTLV-I is analogous to HIV. However, both retroviruses cause dissimilar diseases, and the two infection processes differ from each other significantly. In HIV, for instance, virions can infect CD4⁺ T cells, and it has been calculated that about 10^{10} viral particles are produced every day [21]. In contrast, HTLV-I transmits mainly by cell-to-cell contact and HTLV-I virions are inefficient at infecting CD4⁺ T cells and are seldom found in plasma [44].

The error-prone process of reverse transcription rapidly generates mutations in the viral genome after few rounds of replication. Despite this, and surprisingly, HTLV-I exhibits an extraordinary genetic stability. It is estimated that the reverse transcriptase misincorporation rate for HTLV-I is 7×10^{-6} bases per replication cycle, whereas for HIV it is 3.5×10^{-5} bases per replication cycle. Furthermore, HTLV-I-infected patients show remarkably high proviral levels. Based on these observations, Wattel et al. [40] hypothesized that mitotic division of infected CD4⁺ T cells plays a relevant role in the infection process.

The high production rate of HIV virions compromises cell integrity and, ultimately, provokes host destruction. In contrast, HTLV-I Tax gene products have the capacity to immortalize T cells by suppressing apoptosis [59]. Moreover, cells carrying HTLV-I proliferate in the absence of external cytokine stimulation. Because of these proliferative effects, HTLV-I is classified as an oncovirus.

1.3. Modelling HTLV-I Infection

Mathematicians are like Frenchmen: whatever you say to them they translate into their own language and forthwith it is something entirely different.

Johann Wolfgang von Goethe

For viral infections, mathematical models try to mimic cellular mechanisms of infection, proliferation and elimination. The analysis of these models reveals the spread of the infection, and may help to elucidate relationships between different observable quantities. The conclusions drawn from the model analysis may suggest mechanisms for viral eradication or control, and, ultimately, help to design vaccination strategies. For instance, in 1995, researchers pasted mathematical modelling and clinical experiments together to study HIV-1 dynamics [21, 55]. Since then, numerous models have been proposed to clarify HIV-infection dynamics, as well as to suggest optimal treatment and vaccination strategies [10, 24, 25, 26, 45, 53, 56, 57].

Throughout this thesis, we will use a compartmental approach to model HTLV-I-infection dynamics. More precisely, from a specific cell population, e.g. $CD4^+$ T cells, we classify each cell depending on its state viz. healthy, infected, etc. This classification partitions the total cell population into different compartments. Note that within each compartment cells may differ by age, activation level, markers specificity, etc. However, these differences are replaced by the simplified abstraction of an average infected or healthy cell. We try to emulate cellular events such as cell proliferation, infection process, cell elimination within the members of the compartments. A system of ordinary differential equations describes the transfer of cells from one compartment to a different one.

Compartmental models have been widely used in epidemiology models. In many of these models, an important threshold is the *basic reproduction number* R_0 , which determines whether a disease can persist in a susceptible population. Anderson and May [2] define R_0 as ‘the average number of secondary infections produced when one infected individual is introduced into a host population where everyone is susceptible’. This definition implicitly assumes that the infected individual spends his whole

infectious period within the susceptible population [20]. This threshold parameter has been adapted to viral infections where individuals are replaced by cells (in our case $CD4^+$ T cells). More precisely:

The basic reproduction number, R_0 , represents the average number of secondary infections caused by a single primary infected $CD4^+$ T cell introduced into a pool of susceptible $CD4^+$ T cells, during its entire infection period.

If $R_0 < 1$, each infected T cell produces, on average, less than one new infected cell over the course of its infectious period, and the infection cannot grow. Conversely, if $R_0 > 1$, each infected T cell produces, on average, more than one new infected cell and the infection will take off.

In any system of ordinary differential equations, the local stability analysis is of primary interest. Roughly speaking, the stability of an equilibrium describes the behaviour of the solutions in a neighbourhood of such a point. Routh-Hurwitz criterion is traditionally used to prove local asymptotic stability of the equilibria. In some models, the basic reproduction number is a sharp threshold parameter; this means that the value of R_0 determines completely the number of equilibria and their stability. In such cases, the models exhibit a ‘forward bifurcation’. However, some of our models have multiple stable equilibria when $R_0 < 1$; thus, there are more parameters involved in the infection control. This phenomenon is referred to as ‘backwards bifurcation’, and it can show catastrophic behaviours.

The determination of the global dynamics in systems of more than two dimensions is mathematically nontrivial. Apparently simple systems can lead to chaotic dynamics e.g. Lorenz system. In our models, we expect a rather simple global behaviour i.e. if $R_0 > 1$ there will be only one equilibrium point and it is globally asymptotically stable in a feasible region. In biological terms, this means that when $R_0 > 1$, any detectable level of HTLV-I-infected cells will reach and stay at an equilibrium level making the infection chronic; such an equilibrium level could be reached

by damped oscillations. Conversely, if $R_0 < 1$ the infection-free equilibrium is globally stable in a feasible region. Biologically this means that HTLV-I-infected cells will die out regardless of their initial level. Lyapunov functions have been used to prove global stability problems in three-dimensional or higher dimensional systems [35], but as Ian Stewart [35] points out ‘Lyapunov functions are extremely powerful –when they exist– although there is a definite art to finding them’. Alternatively, the method developed by Li and Muldowney [29, 32] to prove global stability can also be applied. The method has been used to resolve the global stability in several classes of models [11, 12, 13, 17, 30, 31, 33, 34, 38, 54]. Both the method of Lyapunov functions and that of Li and Muldowney are used in the thesis to tackle the problem of global stability.

We have roughly described the milestones of our mathematical modelling viz. basic reproduction number, stability of the equilibria, global dynamics and bifurcations. It is equally important to interpret our mathematical conclusions in their biological context. Our theoretical implications try to elucidate what the basic mechanisms of the infection are. For example, model conclusions may offer a simple explanation for the high proviral loads found in HTLV-I-infected people. Our theoretical reasoning may even be used for parameter estimation e.g. the responsiveness could be calculated in terms of the proviral load and the CD8⁺ T-cell levels. Recently, some vaccination attempts have been reported targeting the activation of the cytotoxic response [49]. With adequate clinical data, our theoretical results may usher vaccination strategies.

1.4. Immune System

The immune system protects the organism averse to infections; it responds to the presence of pathogens with an innate and if necessary also adaptive immunity. Innate immunity refers to the agents that eliminate foreign organisms based on their ‘typical’ pathogenic structure; it exists even before infection and its responses are always in the same manner. At cellular or molecular level such agents are: phagocytes (neutrophils,

macrophages), natural killer cells, blood proteins (including components of the complement) and cytokines. Adaptive immunity refers to the cells (lymphocytes) that eliminate targeted pathogens. Lymphocytes bind to certain regions of the pathogen, which are called peptides, and induce actions to eliminate cells harbouring such peptide. Adaptive immunity establishes a highly specific response to antigens; it also ‘memorizes’ the antigen to avoid future infections. There are two types of adaptive immune responses: humoral, which is mediated by antibodies produced by B cells, and cell-mediated, which is mediated by T cells. The adaptive responses require time to adjust to the foreign antigen.

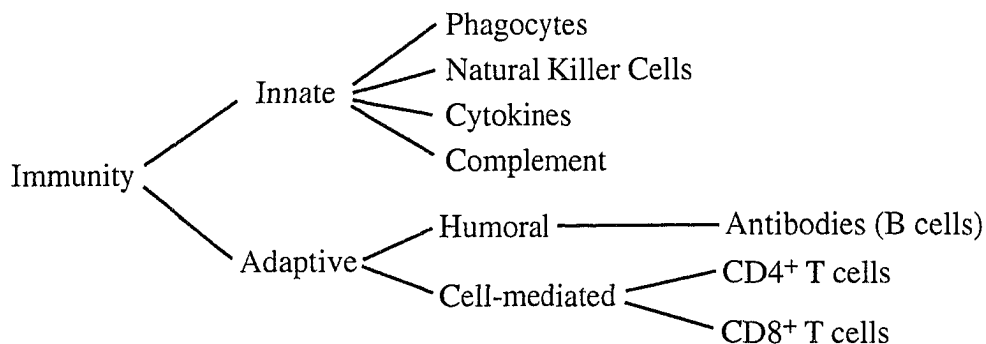


Figure 1.2. Classification of the Immune Responses.

Normally, innate immunity wipes out microbes before adaptive responses activate. In contrast, longer lasting viral infections require the co-operation of both immunities to eliminate infected cells and reduce viral load [8, 16].

Lymphocytes are the most important cells of the adaptive immune system. Adaptive immunity relies on the T-cell capability to distinguish between self and non-self peptides exhibited on the surface of the cells. T lymphocytes attack cells carrying non-self peptides. B and T lymphocytes that have not yet interacted with an antigen are referred to as naïve cells. Interaction of naïve lymphocytes with an antigen induces these cells to proliferate and differentiate into effector or memory cells. Effector cells exit the lymph organs and enter the blood stream to locate and eliminate antigen-bearers at any site.

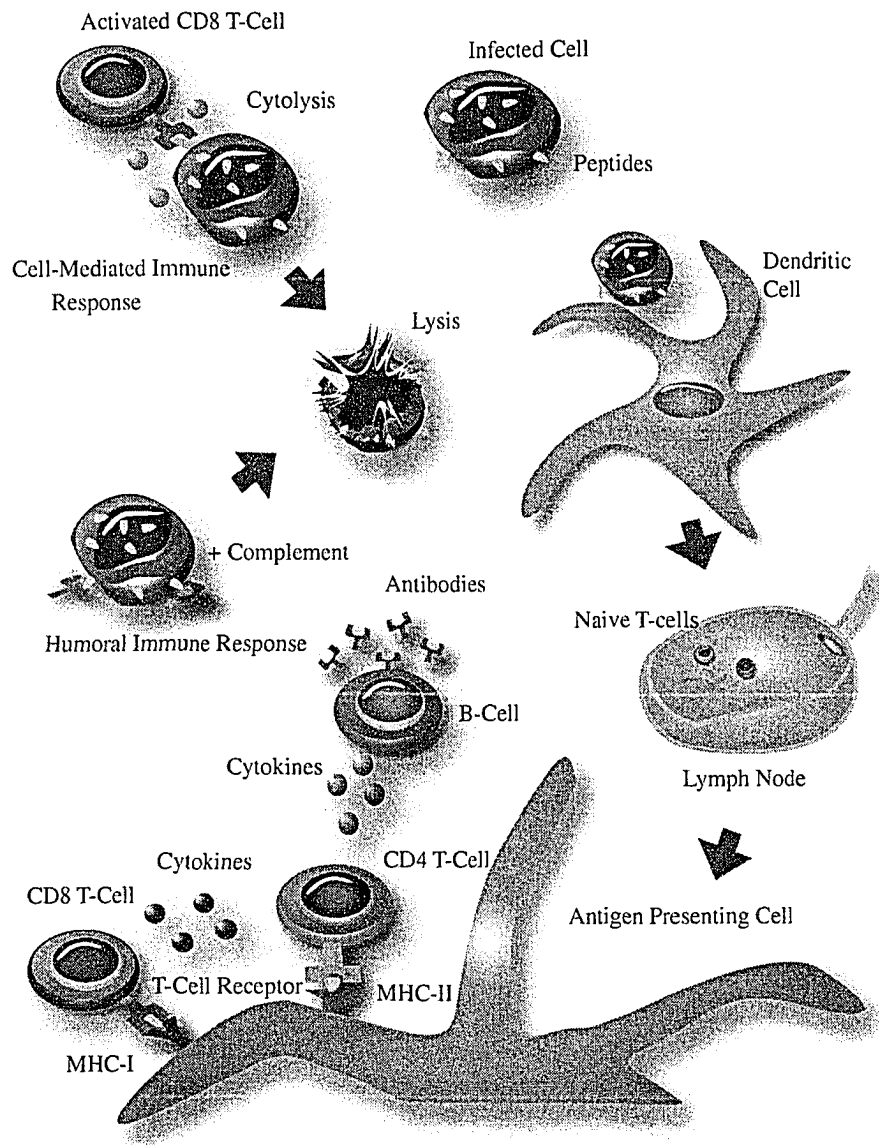


Figure 1.3. Immune System Responses.

T lymphocytes recognize foreign antigen when it is attached to major histocompatibility complex (MHC) molecules on the surface of antigen-presenting cells. T cells expressing the membrane molecule CD4, which are called CD4⁺ T cells or helper cells, recognize antigen bound to class II MHC molecules, whereas T cells expressing the membrane molecule CD8, which are called CD8⁺ T cells or cytotoxic cells, recognize antigen bound to class I MHC molecules. CD4⁺ T cells stimulate

effector mechanisms such as antibodies and phagocytes to eliminate altered cells e.g. virus-infected or tumourous cells. $CD8^+$ T cells eliminate infected cells using proteins (cytokines, cytotoxic granules) that limit the viral replication or lyse infected cells [1, 8]. Figure 1.3 summarizes all these concepts.

1.5. Summary of Related Literature

Literature on the dynamics of HTLV-I infection is scarce. We proceed to describe some of the theoretical work on the subject.

Nowak and colleagues have proposed and investigated several models of viral infections [23, 43, 55, 58]. In particular, [58] considers a model for HTLV-I infection and assumes that $CD4^+$ T cells can be either healthy or actively-infected; latency in the infection is ignored. The CTL response is considered, and conclusions are drawn based on numerical simulations. Using Lyapunov's direct method, [23] establishes the global dynamics of the chronic-infection equilibrium of several models with different type of cytotoxic responses. The analysis does not contemplate the equilibria on the boundaries.

Bangham and Asquit [3, 5] have proposed and analysed different interactions of CTLs with HTLV-I-infected T cells. [3] considers cytokine production of $CD8^+$ T cells and it carries out the local stability analysis.

Stilianakis and Seydel [48] consider a model that includes healthy, latently-infected and actively-infected $CD4^+$ T cells. Progression of $CD4^+$ T cells to ATL is also considered. Local stability analysis and numerical simulations are carried out.

Wang et al. [54] consider Stilianakis and Siedel's model and give a complete mathematical analysis for the global dynamics.

In [18], Gómez-Acevedo and Li consider Stilianakis and Siedel's model with a general incidence form. The global results of Wang et al. [54] are generalised.

1.6. Thesis Overview

In Chapter 2, we start with a basic model for HTLV-I infection. We divide the infected $CD4^+$ T-cell population into two compartments. The first compartment contains cells that are latently-infected; this means that they do not produce viral proteins; thus they cannot transmit the infection. In contrast, the second compartment contains the cells that can infect other cells by contact. We consider a general incidence form of horizontal transmission, in which both the bilinear and standard incidence forms are special cases. We prove that the basic reproduction number R_0 is a sharp threshold parameter for the infection, and it completely determines the global dynamics of the system.

In Chapter 3, we propose and investigate a model that includes the mitotic division of $CD4^+$ T cells. The high proviral loads in the peripheral blood together with the genetic stability of HTLV-I suggest that the mitotic division of HTLV-I-infected T cells may play a role in the infection dynamics. Based on the two-step process hypothesis proposed by Wattel et al. [40], we show that a backwards bifurcation can occur, and we describe some possible consequences of this phenomenon.

In Chapter 4, we propose and analyse a model that incorporates the infection of hematopoietic stem cells by HTLV-I to our basic model. Clinical experiments show that the $CD34^+$ stem cells are susceptible to HTLV-I infection. Since these cells can evade the immune system surveillance, Grant et al. [19] hypothesize that $CD34^+$ act as a reservoir for HTLV-I-infection. We investigate the global dynamics of the model and simulate numerically the solutions. We illustrate how the $CD34^+$ reservoir can induce high levels of provirus in the peripheral blood and bone marrow alike.

In Chapter 5, we analyse a model that includes the cytotoxic response to HTLV-I infection. HAM/TSP patients exhibit remarkably high levels of $CD8^+$ T cells in the peripheral blood. Moreover, there is evidence of $CD8^+$ T cells in the cerebrospinal fluid. The cytokines released by CTLs cause axonal degradation and inflammation. These facts question how protective the CTLs are in the course of infection. We establish the global dynamics of the model. Furthermore, we hypothesize that when

HTLV-I infection is chronic, i.e. $R_0 > 1$, the basic reproduction number in the presence of CTL response, R_1 , may determine the possibilities of an asymptomatic carriers to develop HAM/TSP .

In Chapter 6, we summarize our conclusions and point out lines for future research.

1.7. References

- [1] A. K. ABBAS, A. H. LICHTMAN, AND J. S. POBER, *Cellular and Molecular Immunology*, W. B. Saunders Company, 4 ed., 2000.
- [2] R. M. ANDERSON AND R. M. MAY, *Infectious Diseases in Humans: Dynamics and Control*, Oxford University Press, 1991.
- [3] B. ASQUIT AND C. R. M. BANGHAM, *The role of cytotoxic T lymphocytes in human T-cell lymphotropic virus type 1 infection*, *J. Theor. Biol.*, 207 (2000), pp. 65–79.
- [4] C. M. R. BANGHAM, *The immune response to HTLV-I*, *Curr. Opin. Immunol.*, 12 (2000), pp. 397–402.
- [5] ———, *Genetics and dynamics of the immune response to HTLV-I*, in *Two Decades of Adult T-cell Leukemia and HTLV-I Research*, K. Sugamura, T. Uchiyam, M. Matsuoka, and M. Kannagi, eds., Japan Scientific Societies Press, 2003, pp. 149–170.
- [6] C. R. M. BANGHAM, S. E. HALL, K. J. M. JEFFERY, A. M. VINE, A. WITOKOVER, M. A. NOWAK, K. USUKU, AND M. OSAME, *Genetic control and dynamics of the cellular immune response to the human T-cell leukemia virus, HTLV-I*, *Philos. T. Roy. Soc. B.*, 354 (1999), pp. 691–700.
- [7] K. BARMAK, E. HARHAJ, C. GRANT, T. ALEFANTIS, AND B. WIGDAHL, *Human T cell leukemia virus type I-induced disease: pathways to cancer and neurodegeneration*, *Virology*, 308 (2003), pp. 1–12.

- [8] G. R. BURMESTER AND A. PEZZUTTO, *Color Atlas of Immunology*, Thieme, 2003.
- [9] A. J. CANN AND I. S. Y. CHEN, *Human T-cell leukemia virus type I and II*, in *Fields Virology*, B. N. Fields, D. M. Knipe, and P. M. Howley, eds., Lippincott-Raven Publishers, 1996, pp. 1849–1880.
- [10] R. J. DE BOER AND A. PERELSON, *Target cell limited and immune control models of HIV infection: A comparison.*, *J. Theor. Biol.*, 190 (1999), pp. 201–214.
- [11] P. DE LEEHHEER AND H. L. SMITH, *Virus dynamics: a global analysis*, *SIAM J. Appl. Math.*, 63 (2002), pp. 1313–1327.
- [12] L. ESTEVA AND C. VARGAS, *A model for dengue disease with variable human population*, *J. Math. Biol.*, 38 (1999), pp. 220–240.
- [13] M. FAN, M. Y. LI, AND L. WANG, *Global stability of an SEIS epidemic model with recruitment and varying total population size*, *Math. Biosci.*, 170 (2001), pp. 199–208.
- [14] S. J. FLINT, L. W. ENQUIST, R. M. KRUG, V. R. RACANIELLO, AND A. M. SKALKKA, *Principles of Virology: Molecular Biology, Pathogenesis, and Control*, American Society of Microbiology Press, 2000.
- [15] R. C. GALLO, *Discoveries of human retroviruses*, in *Two Decades of Adult T-cell Leukemia and HTLV-I Research*, K. Sugamura, T. Uchiyam, M. Matsuoka, and M. Kannagi, eds., Japan Scientific Societies Press, 2003, pp. 19–28.
- [16] R. A. GOLDSBY, T. J. KINDT, B. A. OSBORNE, AND J. KUBY, *Immunology*, W. H. Freeman and Company, 5th. ed., 2003.
- [17] H. GÓMEZ-ACEVEDO, *Global stability in a model for diseases transmitted by ixodid ticks*, *Canad. Appl. Math. Quart.*, (2003). In press.
- [18] H. GÓMEZ-ACEVEDO AND M. Y. LI, *Global dynamics of a mathematical model for HTLV-I infection of T cells*, *Canad. Appl. Math. Quart.*, 10 (2002), pp. 71–86.

- [19] C. GRANT, K. BARMAN, T. ALEFANTIS, J. YAO, S. JACOBSON, AND B. WIGDAHL, *Human T cell leukemia virus type I and neurologic disease: events in bone marrow, peripheral blood, and central nervous system during normal immune surveillance and neuroinflammation*, *J. Cell. Physiol.*, 190 (2002), pp. 133–159.
- [20] H. W. HETHCOTE, *The mathematics of infectious diseases*, *SIAM Rev.*, 42 (2000), pp. 599–653.
- [21] D. D. HO, A. U. NEUMAN, A. S. PERELSON, W. CHEN, J. LEONARD, AND M. MARKOWITZ, *Rapid turnover of plasma virions and CD4 lymphocytes in HIV-1 infection*, *Nature*, 373 (1995), pp. 123–126.
- [22] P. HÖLLSBERG AND D. A. HAFNER, *Pathogenesis of diseases induced by human lymphotropic virus type I infection.*, *N. Engl. J. Med.*, 328 (1993), pp. 1173–1182.
- [23] Y. IWASA, F. MICHOR, AND M. NOWAK, *Some basic properties of immune selection*, *J. Theor. Biol.*, (2004). In press.
- [24] D. E. KIRSCHNER, S. LENHART, AND S. SERBIN, *Optimal control of the chemotherapy of HIV*, *J. Math. Biol.*, 35 (1997), pp. 775–792.
- [25] D. E. KIRSCHNER AND G. F. WEBB, *Understanding drug resistance for monotherapy treatment of HIV infection*, *Bull. Math. Biol.*, 59 (1997), pp. 763–785.
- [26] ———, *Immunotherapy of HIV-1 infection*, *J. Biol. Systems*, 6 (1998), pp. 71–83.
- [27] R. KUBOTA, M. OSAME, AND S. JACOBSON, *Retrovirus: Human T-cell lymphotropic virus type I-associated diseases and immune dysfunction*, in *Effects of Microbes on the Immune System*, M. W. Cunningham and R. S. Fujinami, eds., Lippincott Williams & Wilkins, 2000, pp. 349–371.
- [28] M. LEON-MONZON, I. ILLA, AND C. DALAKAS, *Polymyositis in patients infected with human T-cell lymphotropic virus type I: the role of the virus in the cause of the disease.*, *Ann. Neurol.*, 36 (1994), pp. 643–649.

- [29] M. Y. LI, *Geometrical Studies on the Global Asymptotic Behaviour of Dissipative Dynamical Systems*, PhD thesis, University of Alberta, 1993.
- [30] M. Y. LI, J. R. GRAEF, L. WANG, AND J. KARSAI, *Global dynamics of an SEIR model with varying population size*, *Math. Biosci.*, 160 (1999), pp. 191–213.
- [31] M. Y. LI AND J. S. MULDOWNNEY, *Global stability for the SEIR model in epidemiology*, *Math. Biosci.*, 125 (1995), pp. 155–164.
- [32] ———, *A geometric approach to global-stability problems*, *SIAM J. Math. Anal.*, 27 (1996), pp. 1070–1083.
- [33] M. Y. LI, J. S. MULDOWNNEY, AND P. VAN DEN DRIESSCHE, *Global stability for the SEIRS models in epidemiology*, *Canad. Appl. Math. Quart.*, 7 (1999), pp. 409–425.
- [34] M. Y. LI, H. L. SMITH, AND L. WANG, *Global dynamics of an SEIR model with vertical transmission*, *SIAM J. Appl. Math.*, 62 (2001), pp. 58–69.
- [35] A. M. LYAPUNOV, *The General Problem of the Stability of Motion*, Taylor & Francis, 1992.
- [36] N. MANEL, F. J. KIM, S. KINET, N. TAYLOR, M. SITBON, AND J.-L. BATTINI, *The ubiquitous glucose transporter GLUT-1 is a receptor for HTLV*, *Cell*, 115 (2003), pp. 449–459.
- [37] A. MANNS, E. L. MURPHY, R. WILK, G. HAYNES, J. P. FIGUEROA, B. HANCHARD, M. BARNETT, J. DRUMMOND, D. WATERS, M. CERNEY, J. R. SEALS, S. S. ALEXANDER, H. LEE, AND W. A. BLATTNER, *Detection of early human T-cell lymphotropic virus type I antibody patterns during seroconversion among transfusion recipients*, *Blood*, 77 (1991), pp. 896–905.
- [38] C. C. MCCLUSKEY, *Global Stability in Epidemiological Models*, PhD thesis, University of Alberta, 2002.

- [39] O. S. MORGAN, P. RODGERS-JOHNSON, C. MORA, AND G. CHAR, *HTLV-I and polymyositis in Jamaica*, *Lancet*, 334 (1989), pp. 1184–1187.
- [40] F. MORTREUX, M. KAZANJI, A.-S. GABET, B. DE THOISY, AND E. WATTEL, *Two-step nature of human T-cell leukemia virus type 1 replication in experimentally infected squirrel monkeys (*saimiri sciureus*)*, *J. Virol.*, 75 (2001), pp. 1083–1089.
- [41] N. E. MUELLER AND W. A. BLATTNER, *Retroviruses-human T-cell lymphotropic virus*, in *Viral Infections in Humans: Epidemiology and Control*, A. S. Evans and R. A. Kaslow, eds., Plenum Medical Book Company, 1997, pp. 785–813.
- [42] K. NISHIOKA, I. MARUYAMA, K. SATO, I. KITAJIMA, Y. NAKAJIMA, AND M. OSAME, *Chronic inflammatory arthropathy associated with HTLV-I*, *Lancet*, 333 (1989), p. 441.
- [43] M. A. NOWAK AND C. R. M. BANGHAM, *Population dynamics of immune responses to persistent viruses*, *Science*, 272 (1996), pp. 74–79.
- [44] K. OKOCHI, H. SATO, AND Y. HINUMA, *A retrospective study on transmission of adult T-cell leukemia virus by blood transfusion: seroconversion in recipients*, *Vox Sang.*, 46 (1984), pp. 245–253.
- [45] A. S. PERELSON AND P. W. NELSON, *Mathematical analysis of HIV-I dynamics in vivo*, *SIAM Rev.*, 41 (1999), pp. 3–44.
- [46] B. J. POIESZ, F. W. RUSCETTI, A. F. GAZDAR, P. A. BUNN, J. D. MINNA, AND R. C. GALLO, *Detection and isolation of type C retrovirus particles from fresh and cultured lymphocytes of a patient with cutaneous T cell lymphoma*, *Pro. Natl. Acad. Sci. USA*, 77 (1980), pp. 7415–7419.
- [47] H. SHIRAKI, Y. SAGARA, AND Y. INOUE, *Cell-to-cell transmission of HTLV-I*, in *Two Decades of Adult T-cell Leukemia and HTLV-I Research*, K. Sugamura, T. Uchiyam, M. Matsuoka, and M. Kannagi, eds., Japan Scientific Societies Press, 2003, pp. 303–316.

- [48] N. I. STILIANAKIS AND J. SEYDEL, *Modeling the T-cell dynamics and pathogenesis of htlv-i infection*, Bull. Math. Biol., 61 (1999), pp. 935–947.
- [49] R. SUNDARAM, Y. SUN, C. M. WALKER, F. A. LEMONNIER, S. JACOBSON, AND P. T. P. KAUMAYA, *A novel multivalent human CTL peptide construct elicits robust cellular immune responses in HLA-A*0201 transgenic mice: implications for HTLV-I vaccine design*, Vaccine, 21 (2003), pp. 2767–2781.
- [50] K. TAKATSUJI, *Discovery of adult T-cell leukemia: reminiscences*, in Two Decades of Adult T-cell Leukemia and HTLV-I Research, K. Sugamura, T. Uchiyam, M. Matsuoka, and M. Kannagi, eds., Japan Scientific Societies Press, 2003, pp. 7–9.
- [51] K. TERADA, S. KATAMINE, K. EGUCHI, R. MORIUCHI, M. KITA, H. SHIMADA, I. YAMASHITA, K. IWATA, Y. TSUJI, S. NAGATAKI, AND T. MIYAMOTO, *Prevalence of serum and salivary antibodies to HTLV-I in Sjögren's syndrome*, Lancet, 344 (1994), pp. 1116–1119.
- [52] T. TSUKAHARA, M. KANNAGI, T. OHASHI, H. KATO, M. ARAI, G. NUNEZ, Y. IWANAGA, N. YAMAMOTO, K. OHTANI, M. NAKAMURA, AND M. FUJII, *Induction of Bcl-x(L) expression by human T-cell leukemia virus type 1 Tax through NF- κ B in apoptosis resistant T-cell transfectants with Tax*, J. Virol., 73 (1999), pp. 7981–7987.
- [53] J. X. VELASCO-HERNÁNDEZ, J. A. GARCÍA, AND D. E. KIRSCHNER, *Remarks on modeling host-viral dynamics and treatment*, in Mathematical Approaches for Emerging and Reemerging Infectious Diseases: An introduction, C. Castillo-Chávez, S. Blower, P. van den Driessche, D. Kirschner, and A.-A. Yakubu, eds., vol. 125 of IMA Volumes in Mathematics and its Applications, Springer-Verlag, 2002, pp. 287–308.
- [54] L. WANG, M. Y. LI, AND D. E. KIRSCHNER, *Mathematical analysis of the global dynamics of a model for HTLV-I infection and ATL progression*, Math. Biosci., 179 (2002), pp. 207–217.

- [55] X. WEI, S. K. GHOSH, M. E. TAYLOR, V. A. JOHNSON, E. A. EMINI, P. DEUTSCH, J. D. LIFSON, S. BONHOEFFER, M. A. NOWAK, AND B. H. HAHN, *Viral dynamics in human immunodeficiency virus type 1 infection*, Nature, 373 (1995), pp. 117–122.
- [56] L. M. WEIN, S. A. ZENIOS, AND M. A. NOWAK, *Dynamic multidrug therapies for HIV: a control theoretic approach*, J. Theor. Biol., 185 (1997), pp. 15–29.
- [57] D. WODARZ AND M. A. NOWAK, *Specific therapies could lead to long-term immunological control of HIV*, Proc. Natl. Acad. Sci. USA, 96 (1999), pp. 464–469.
- [58] D. WODARZ, M. A. NOWAK, AND C. R. M. BANGHAM, *The dynamics of HTLV-I and the CTL response*, Immunol. Today, 20 (1999), pp. 220–227.
- [59] M. YOSHIDA, *Molecular biology of HTLV-1 pleiotropic function of Tax protein in cell regulation*, in Two Decades of Adult T-cell Leukemia and HTLV-I Research, K. Sugamura, T. Uchiyam, M. Matsuoka, and M. Kannagi, eds., Japan Scientific Societies Press, 2003, pp. 11–18.

Chapter 2

A Basic Model for HTLV-I Infection

2.1. Introduction

Human T-cell Leukaemia/Lymphoma Virus Type I (HTLV-I) was the first human retrovirus identified. HTLV-I causes several illnesses, mainly Adult T-cell Leukaemia/Lymphoma (ATL) and HTLV-I-Associated Myelopathy/Tropical Spastic Paraparesis (HAM/TSP) [7, 13]. Free HTLV-I viruses are not very infectious and rarely found in plasma. The infection spreads mostly through cell-to-cell contact [22].

HTLV-I virions have an almost spherical core of about 100 nm in diameter. Inside the core, virions carry viral RNA, tRNA and enzymes such as reverse transcriptase and integrase. The interaction between the virus surface and the receptor GTLU-1 allows virus attachment and entry [20]. Following entry, reverse transcriptase transcribes a chain of DNA from the viral RNA. Subsequently, a double-stranded DNA is formed and viral integrase places it into the host DNA. The integrated viral DNA, which is called *provirus*, can remain without producing viral proteins for a period of time. During this latency period, the host cell cannot transmit the infection. Upon stimulation, a provirus-carrier cell starts expressing viral proteins on its surface and transmitting HTLV-I infection to bystander cells [4].

More than 90% of the proviral load in peripheral blood from infected patients is found in CD4⁺ T cells [13]. HTLV-I carriers show high levels of antibodies soon after the infection [15]. Experiments also show that the bulk of the proviral load comes out from relatively few clones [7]. This clinical evidence may suggest that few HTLV-I-infected cells are able to survive the immune system attack.

Using a compartmental approach, we propose and analyse a basic model for HTLV-I infection. We assume that newly infected cells can stay in a latent state for some period of time. We also consider a general expression for the horizontal incidence that includes both the bilinear and the standard incidence as particular cases.

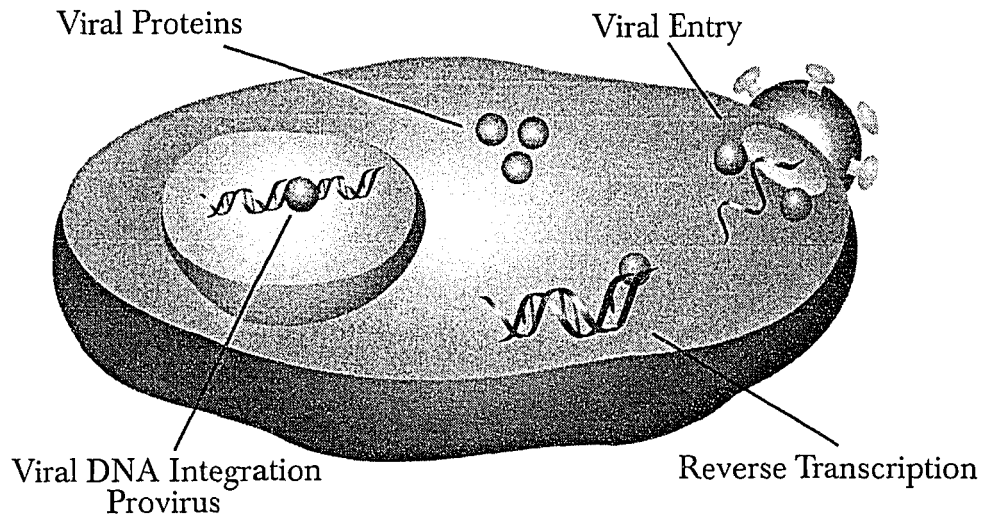


Figure 2.1. HTLV-I Infection Process.

2.2. A Mathematical Model

We partition $CD4^+$ T cells into three compartments: healthy, latently-infected, and actively-infected. Latently-infected cells are not infectious because they are either integrating the provirus into their own DNA or not producing viral proteins. Actively-infected cells can infect healthy ones. Let x , y , z denote the number of susceptible, latently-infected, and actively-infected $CD4^+$ T cells, respectively. Let N denote the total number of $CD4^+$ T cells that participate in the infection transmission. Since HTLV-I infection occurs by the infectious route i.e. cell-to-cell contact between actively-infected cells and uninfected ones, the incidence term can be modelled analogously as in the population models for infectious diseases. Two common incidence forms are the bilinear βxz , and the standard $\tilde{\beta}xz/N$. In our model, we assume the incidence form depends on the total $CD4^+$ T-cell population. More precisely, we define the incidence form as $\beta C(N)xz/N$, where β is the number of adequate contacts,

i.e. contacts sufficient for transmission, of a cell per unit of time, and $C(N)$ is the contact function $C(N) = N^{1-\varepsilon}$ with $\varepsilon \in [0, 1]$. The contact function represents the rate of effective contacts between a susceptible and an actively-infected T cell [23]. For the sake of simplicity, we write our incidence form as $\beta x z f(N)$, where $f(N) = N^{-\varepsilon}$ with $\varepsilon \in [0, 1]$. When $\varepsilon = 0$ and 1, our incidence form reduces to the bilinear and the standard incidence, respectively. Soon after the primary infection, HTLV-I-carrier cells confront a strong humoral response (targeted mainly to Tax proteins) [3, 15]. Moreover, the low mutation rate observed during HTLV-I replication, compared to the mutation rate observed during HIV-1 replication [16, 19], suggests that only a fraction $\sigma \in [0, 1]$ of newly infected cells by contact will survive the humoral immune response. The transmission dynamics is depicted in the following diagram:

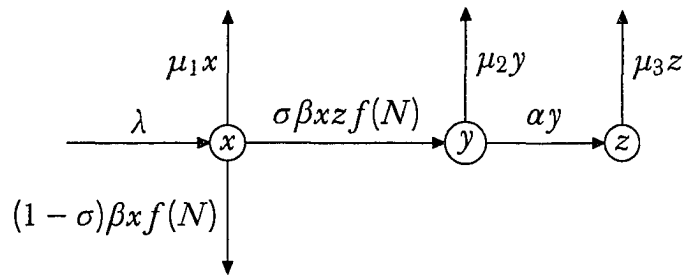


Figure 2.2. Transfer diagram.

The maintenance of the T-cell population may involve proliferation of mature cells in the periphery or maturation of progenitor stem cells [8]. In this model, we assume the simplest scenario in which $CD4^+$ T cells are produced at constant rate λ and all of them are susceptible. Since the probability of lymphocyte elimination in function of time is not known [21], we assume that the per capita elimination rate is a constant μ_1 . This condition means that the probability of cell elimination at time t is given by an exponential distribution with expectancy $1/\mu_1$ [5, 9]. The parameters μ_2 and μ_3 may include the loss resulting from the adaptive-immunity attack. The parameter α is the transmission rate at which latently-infected $CD4^+$ T cells become actively-infected; thus $1/\alpha$ can be regarded as the mean latent period. All parameters in the model are positive constants.

Based on the transfer diagram and our assumptions, we derive the following system of nonlinear differential equations:

$$\begin{aligned}x' &= \lambda - \mu_1 x - \beta x z f(N), \\y' &= \sigma \beta x z f(N) - (\mu_2 + \alpha)y, \\z' &= \alpha y - \mu_3 z.\end{aligned}\tag{2.1}$$

Here

$$f(N) = N^{-\varepsilon}, \quad 0 \leq \varepsilon \leq 1.\tag{2.2}$$

From (2.1), we obtain:

$$\begin{aligned}x' &\leq \lambda - \mu_1 x, \\N' &\leq \lambda - \bar{\mu}(x + y + z),\end{aligned}$$

where $\bar{\mu} = \min\{\mu_1, \mu_2, \mu_3\}$. It follows that

$$\limsup_{t \rightarrow \infty} x(t) \leq \frac{\lambda}{\mu_1} \quad \text{and} \quad \limsup_{t \rightarrow \infty} N(t) \leq \frac{\lambda}{\bar{\mu}}.$$

The feasible region for (2.1) is

$$\Delta = \left\{ (x, y, z) \in \mathbb{R}_+^3 : x \leq \frac{\lambda}{\mu_1}, x + y + z \leq \frac{\lambda}{\bar{\mu}} \right\}.$$

The region Δ is positively invariant with respect to (2.1) and the model is well-posed.

The basic reproduction number for (2.1) is given by:

$$R_0 = \frac{\sigma \alpha \beta}{(\mu_2 + \alpha) \mu_3} \left(\frac{\lambda}{\mu_1} \right)^{1-\varepsilon}.$$

Heuristically, we derive R_0 as follows: in the absence of infection, T-cell population approaches the constant $N^* = \lambda/\mu_1$, thus, the contact function approaches $G(N^*) = N^* f(N^*)$. A fraction $\alpha/(\mu_2 + \alpha)$ of cells leave latency and become infectious. The average infectious period of actively-infected cells is $1/\mu_3$. A fraction σ of newly infected CD4⁺ T cells that evade the immune system. Finally, multiplying the previous quantities by the contact rate β gives R_0 [12, 18, 24].

2.3. Equilibrium Points

We will establish that when $R_0 \leq 1$, no chronic HTLV-I infection of T cells is possible, and the only infection-free equilibrium $P_0 = (\lambda/\mu_1, 0, 0)$ is globally asymptotically stable in the feasible region. When $R_0 > 1$, a primary HTLV-I infection in T cells always leads to chronic infection, and a unique chronic-infection equilibrium $P_1 = (x^*, y^*, z^*)$ is globally asymptotically stable in the interior of the feasible region.

Theorem 2.1. If $R_0 \leq 1$, system (2.1) has only the infection-free equilibrium $P_0 = (\lambda/\mu_1, 0, 0)$. If $R_0 > 1$, there exists exactly one chronic-infection equilibrium $P_1 = (x^*, y^*, z^*)$.

Proof. Clearly P_0 exists for all the positive parameters. Any chronic-infection equilibrium point should satisfy:

$$\begin{aligned} x^* &= \frac{\lambda}{\mu_1} - \frac{(\mu_2 + \alpha)\mu_3}{\sigma\alpha\mu_1} z^*, \\ y^* &= \frac{\mu_3}{\alpha} z^*, \\ x^* f(N^*) &= \frac{(\mu_2 + \alpha)\mu_3}{\sigma\alpha\beta}, \end{aligned} \tag{2.3}$$

where $N^* = x^* + y^* + z^*$. Define

$$h(X) = \frac{\lambda}{\mu_1} - \frac{(\mu_2 + \alpha)\mu_3}{\sigma\alpha\mu_1} X \tag{2.4},$$

and

$$\begin{aligned} g(X) &= \frac{(\mu_2 + \alpha)\mu_3}{\sigma\alpha\beta} \left(\frac{\lambda}{\mu_1} + \left(1 + \frac{\mu_3}{\alpha} - \frac{(\mu_2 + \alpha)\mu_3}{\sigma\alpha\mu_1} \right) X \right)^\varepsilon \\ &= \frac{\lambda}{\mu_1 R_0} (1 + dX)^\varepsilon, \end{aligned} \tag{2.5}$$

where

$$d = \frac{\mu_1}{\lambda} \left(1 + \frac{\mu_3}{\alpha} - \frac{(\mu_2 + \alpha)\mu_3}{\sigma\alpha\mu_1} \right).$$

In terms of (2.4) and (2.5), conditions (2.3) imply

$$h(z^*) = g(z^*). \tag{2.6}$$

Note that $h(0) = \lambda/\mu_1$, and $g(0) = \lambda/(\mu_1 R_0) = h(0)/R_0$. Also $h(X)$ is a straight line of negative slope, whereas $g(X)$ is increasing or decreasing depending on the sign of d .

I: $d \geq 0$. In this case g is non-decreasing. Graphs of g and h have no intersection point if $g(0) > h(0)$, i.e. if $R_0 < 1$, and have exactly one intersection if $g(0) \leq h(0)$, i.e. if $R_0 \geq 1$, and when $g(0) = h(0)$, i.e. when $R_0 = 1$, the only intersection is at $z^* = 0$.

II: $d < 0$. In this case g is decreasing and concave down in its domain $[0, -1/d]$. Moreover, $h(X_1) = 0$ implies $X_1 = \frac{\sigma\alpha\lambda}{(\mu_2 + \alpha)\mu_3}$, and $g(X_2) = 0$ implies

$$X_2 = -\frac{1}{d} = \frac{\sigma\alpha\lambda}{(\mu_2 + \alpha)\mu_3} \cdot \frac{1}{\left(1 - \frac{\sigma\alpha\mu_1 + \sigma\mu_1\mu_3}{(\mu_2 + \alpha)}\right)} > X_1.$$

Therefore, the possible intersections of the graphs of g and h are:

- (a) no intersection when $R_0 < 1$;
- (b) exactly one intersection when $R_0 \geq 1$. When $R_0 = 1$ the only intersection is at $z^* = 0$. See Figure 2.3.

q.e.d.

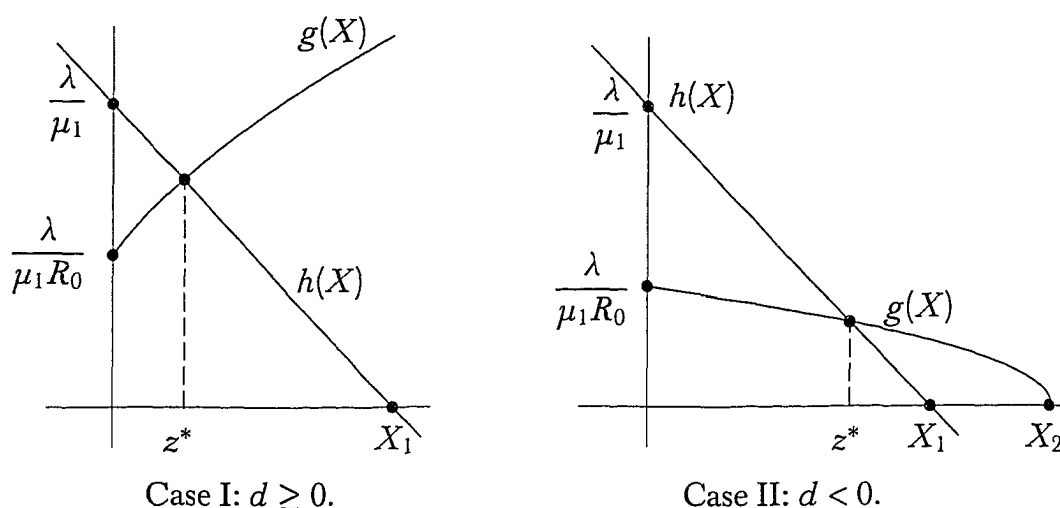


Figure 2.3. Uniqueness of the chronic-infection equilibrium when $R_0 > 1$.

2.4. Global Dynamics

In ecology, it is important to determine the survival or extinction of species within the same environment. A particular species of size $x(t)$ *persists* (coexists) when

$$\liminf_{t \rightarrow \infty} x(t) > 0 \quad \text{provided } x(0) > 0.$$

However, persistence does not guarantee the survival in biological terms [5]. A more precise definition is *uniform persistence* that requires a positive bound for population size. We proceed to define this concept formally.

Definition. Suppose the mapping $x \mapsto F(x)$ from an open subset $B \subset \mathbb{R}^n$ to \mathbb{R}^n is such that each solution $x(t, x_0)$ to the differential equation

$$x' = F(x), \tag{2.7}$$

is uniquely determined by its initial value $x(0) = x_0$. Furthermore, suppose that a closed set $A \subset B$ is positively invariant with respect to (2.7). The system (2.7) is called *uniformly persistent* in $\overset{\circ}{A}$ (see [6, 10]), if there exists $\varepsilon_0 > 0$ such that for all $x_0 \in \overset{\circ}{A}$,

$$\liminf_{t \rightarrow \infty} d(x(t, x_0), \partial A) > \varepsilon_0, \tag{2.8}$$

where d is a distance function and ∂A is the boundary of A .

Uniform persistence can be used to characterize chronic infection of CD4⁺ T cells. More specifically, condition (2.8) means that levels of CD4⁺ T cells will never reach the boundary of the feasible region Δ . In particular, the infected cells will remain at positive levels, provided that there were originally infected cells in the blood.

Theorem 2.2. If $R_0 \leq 1$, the infection-free equilibrium P_0 is globally stable in the closed region Δ . If $R_0 > 1$, then P_0 is unstable and system (1) is uniformly persistent in the interior of Δ .

Proof. Consider a Lyapunov function $L = \alpha y + (\mu_2 + \alpha)z$. We have

$$\begin{aligned} L' &= \alpha y' + (\mu_2 + \alpha)z' = z[\sigma\alpha\beta x f(N) - (\mu_2 + \alpha)\mu_3] \\ &= (\mu_2 + \alpha)\mu_3 z \left(\frac{\sigma\alpha\beta x f(N)}{(\mu_2 + \alpha)\mu_3} - 1 \right) \\ &\leq (\mu_2 + \alpha)\mu_3 z (R_0 - 1) \leq 0, \quad \text{if } R_0 \leq 1. \end{aligned}$$

The maximal compact invariant set in $\{(x, y, z) \in \Delta : L' = 0\}$ is the singleton $\{P_0\}$ when $R_0 \leq 1$. The global stability of P_0 follows from the LaSalle Invariance Principle [14]. Moreover, if $R_0 > 1$, then $L' > 0$ for those points in the interior of Δ that are sufficiently close to P_0 . Solutions in Δ starting sufficiently close to P_0 leave a neighborhood of P_0 except those on the invariant x -axis, where solutions converge to the infection-free equilibrium point P_0 . In particular, the largest compact invariant set on the boundary of Δ is the singleton $\{P_0\}$. The uniform persistence follows from Theorem 4.3 of [10] by setting $X = \mathbb{R}^3$, $E = \Delta$ and noticing that the singleton $\{P_0\}$ is isolated, and P_0 is unstable when $R_0 > 1$.

q.e.d.

Theorem 2.2 establishes the basic reproduction number R_0 as a sharp threshold parameter; when $R_0 \leq 1$, the infection of T cells always dies out, whereas when $R_0 > 1$, it becomes chronic.

Theorem 2.3. Suppose that $R_0 > 1$. Then the unique chronic-infection equilibrium $P_1 = (x^*, y^*, z^*)$ is globally stable in the interior of Δ .

Proof. We will use the general method of Li and Muldowney to establish the global stability of P_1 (see Appendix B). We note that uniform persistence of (2.1), together with boundedness of solutions, implies the existence of a compact absorbing set in $\overset{\circ}{\Delta}$ (see [6]). Moreover, since P_1 is the only equilibrium in $\overset{\circ}{\Delta}$, conditions (H1) and (H2) of Theorem B.1 are fulfilled (see Appendix B). We need to construct a 3×3 matrix-valued function Q , and choose a suitable vector norm $|\cdot|$ in $\mathbb{R}^3 \cong \mathbb{R}^{\binom{3}{2}}$ such that the corresponding Lozinskiĭ measure μ and \bar{q}_2 satisfies $\bar{q}_2 < 0$ (see Appendices A and B).

The Jacobian matrix of (2.1) along a solution (x, y, z) is given by:

$$J = \begin{pmatrix} -\mu_1 - \beta z(f(N) + x f'(N)) & -\beta x z f'(N) & -\beta x(f(N) + z f'(N)) \\ \sigma \beta z(f(N) + x f'(N)) & \sigma \beta x z f'(N) - (\mu_2 + \alpha) & \sigma \beta x(f(N) + z f'(N)) \\ 0 & \alpha & -\mu_3 \end{pmatrix},$$

and its second additive compound matrix (see Appendix A)

$$J^{[2]} = \begin{pmatrix} j_{11} & \sigma \beta x(f(N) + z f'(N)) & \beta x(f(N) + z f'(N)) \\ \alpha & j_{22} & -\beta x z f'(N) \\ 0 & \sigma \beta z(f(N) + x f'(N)) & j_{33} \end{pmatrix},$$

where

$$j_{11} = -\mu_1 - \beta z f(N) - (\mu_2 + \alpha) - \beta x z f'(N)(1 - \sigma),$$

$$j_{22} = -\mu_1 - \beta z f(N) - \beta x z f'(N) - \mu_3, \text{ and}$$

$$j_{33} = \sigma \beta x z f'(N) - (\mu_2 + \alpha) - \mu_3.$$

Define the matrix $Q = Q(x, y, z) = \text{diag} \{ \sigma, \sigma y/z, y/z \}$. Then

$$Q_f Q^{-1} = \text{diag} \{ 0, y'/y - z'/z, y'/y - z'/z \},$$

where Q_f is the matrix obtained by replacing each entry q_{ij} in Q by its directional derivative in the direction of f . Thus, the matrix $B = Q_f Q^{-1} + Q J^{[2]} Q^{-1}$ can be written in block form as

$$\begin{pmatrix} B_{11} & B_{12} \\ B_{21} & B_{22} \end{pmatrix},$$

where

$$B_{11} = -\mu_1 - \beta z f(N) - (\mu_2 + \alpha) - \beta x z f'(N)(1 - \sigma),$$

$$B_{12} = \left((\sigma \beta x z f'(N) + \sigma \beta x f(N)) \frac{z}{y}, -(\sigma \beta x z f'(N) + \sigma \beta x f(N)) \frac{z}{y} \right),$$

$$B_{21} = \left(\alpha \frac{y}{z}, 0 \right)^T, \text{ and}$$

$$B_{22} = \text{diag} \left\{ \frac{y'}{y} - \frac{z'}{z}, \frac{y'}{y} - \frac{z'}{z} \right\} + \begin{pmatrix} -\mu_1 - \beta z f(N) - \beta x z f'(N) - \mu_3 & -\sigma \beta x z f'(N) \\ \beta x z f'(N) + \beta z f(N) & \sigma \beta x z f'(N) - (\mu_2 + \alpha) - \mu_3 \end{pmatrix}.$$

Choose a vector norm in \mathbb{R}^3

$$|(x, y, z)| = \max\{|x|, |y| + |z|\}$$

and let μ denote the corresponding Lozinskiĭ measure. We have the estimate (see [17])

$$\mu(B) \leq \max\{g_1, g_2\}, \quad (2.9)$$

where

$$g_1 = \mu_*(B_{11}) + |B_{12}|, \quad g_2 = |B_{21}| + \mu_*(B_{22}).$$

Note that $\mu_*(B_{22})$ is the Lozinskiĭ measure of the 2×2 matrix B_{22} with respect to the ℓ_1 norm in \mathbb{R}^2 , $|B_{12}|$ and $|B_{21}|$ are the operator norms of B_{12} and B_{21} when they are regarded as mappings from \mathbb{R}^2 to \mathbb{R} and from \mathbb{R} to \mathbb{R}^2 , respectively, and \mathbb{R}^2 is endowed with the ℓ_1 norm. Note that

$$\mu_*(B_{11}) = B_{11} = -\mu_1 - \beta z f(N) - (\mu_2 + \alpha) - \beta x z f'(N)(1 - \sigma). \quad (2.10)$$

The function $f(X) = X^{-\varepsilon}$ ($\varepsilon \in [0, 1]$) satisfies $f'(X) \leq 0$ and for $X > 0$

$$|X f'(X)| \leq f(X).$$

Since $x \leq N$, the previous expression yields

$$f(N) + x f'(N) \geq f(N) + N f'(N) \geq 0. \quad (2.11)$$

Thus, $\beta z f(N) + \beta x z f'(N) \geq 0$ and

$$|B_{12}| = |\sigma \beta x z f'(N) + \sigma \beta x f(N)| \frac{z}{y} = (\sigma \beta x z f'(N) + \sigma \beta x f(N)) \frac{z}{y}.$$

Rewriting the second equation in (2.1) as

$$\frac{y'}{y} = \sigma x f(N) \frac{z}{y} - (\mu_2 + \alpha),$$

and substituting into g_1 , we obtain

$$\begin{aligned}
 g_1 &= -\mu_1 - \beta z f(N) - (\mu_2 + \alpha) - \beta x z f'(N)(1 - \sigma) + \\
 &\quad (\sigma \beta x z f'(N) + \sigma \beta x f(N)) \frac{z}{y} \\
 &= -\mu_1 + \frac{y'}{y} - \beta z f(N) - \beta x z f'(N)(1 - \sigma) + (\sigma \beta x z f'(N)) \frac{z}{y} \\
 &\leq -\mu_1 + \frac{y'}{y}, \quad \text{by (2.11)}.
 \end{aligned} \tag{2.12}$$

On the other hand, we have

$$\mu_*(B_{22}) = \frac{y'}{y} - \frac{z'}{z} - \mu_3 - \min\{\mu_1, \mu_2 + \alpha\}.$$

and $|B_{21}| = \alpha y/z$. Rewriting the third equation in (2.1) as

$$\frac{z'}{z} = \alpha \frac{y}{z} - \mu_3,$$

and substituting into g_2 , we obtain

$$\begin{aligned}
 g_2 &= \alpha \frac{y}{z} + \frac{y'}{y} - \frac{z'}{z} - \mu_3 - \min\{\mu_1, \mu_2 + \alpha\} \\
 &= \frac{y'}{y} - \min\{\mu_1, \mu_2 + \alpha\}.
 \end{aligned} \tag{2.13}$$

From (2.9), (2.12) and (2.13), we conclude

$$\mu_*(B) \leq \frac{y'}{y} - \delta,$$

where $\delta = \min\{\mu_1, \mu_2 + \alpha\} > 0$. Let $K \subset \overset{\circ}{\Delta}$ be the compact absorbing set. Then there exists $\bar{t} > 0$ such that $(x(0), y(0), z(0)) \in K$ implies $(x(t), y(t), z(t)) \in K$ for all $t > \bar{t}$. Therefore, for $t > \bar{t}$,

$$\frac{1}{t} \int_0^t \mu(B) ds \leq \frac{1}{t} \ln \frac{y(t)}{y(\bar{t})} + \frac{1}{t} \int_0^{\bar{t}} \mu(B) ds - \delta \frac{t - \bar{t}}{t}$$

for all $(x(0), y(0), z(0)) \in K$, which implies $\bar{q}_2 \leq -\delta/2 < 0$, proving Theorem 2.3.

q.e.d.

2.5. Discussion and Conclusions

In this Chapter, we present a complete mathematical analysis for the global dynamics of a model for HTLV-I infection of CD4⁺ T cells. In our basic model, the CD4⁺ T-cell population is partitioned into three subclasses: uninfected (susceptible) x , latently-infected (infected but not yet infectious) y , and actively-infected (infectious) z . Unlike other retroviruses, HTLV-I requires cell-to-cell contact to infect other cells *in vivo* [13]. Once an infectious contact is established, it may take some time for the newly infected cell to start the production of viral proteins and become infectious.

We consider a generalized incidence form that includes the standard and bilinear incidences. More precisely, the incidence form is $\beta C(N)xz/N$, where β is the number of adequate contacts and $C(N) = N^{1-\varepsilon}$ with $\varepsilon \in [0, 1]$ is the contact function. This function represents the rate of effective contacts between a susceptible and an actively-infected T cell. When $\varepsilon = 0$, we have a bilinear incidence, whereas when $\varepsilon = 1$, we get a standard incidence. Also, based on clinical evidence, we assume that the immune system is able to eliminate a proportion of newly infected cells.

Our analysis proves that the basic reproduction number R_0 governs HTLV-I infection dynamics. If $R_0 \leq 1$ no chronic infection is possible, and the HTLV-I-infected T cells are wiped out. When $R_0 > 1$, a chronic infection is established and the unique chronic-infection equilibrium is globally stable. Thus, our model exhibits a forward bifurcation (see Figure 2.4). This implies that changes in R_0 gradually modify the proviral load.

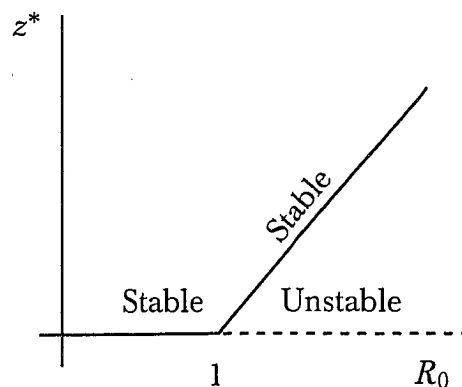


Figure 2.4. Forward Bifurcation.

We will show how R_0 and z^* change with different choices of $f(N)$ in the incidence, as defined in (2.2). Assuming that all the parameters are fixed except ε . The normal $CD4^+$ T-cell count in a healthy individual is about 1000 cells/mm³ [11]. Thus, it is reasonable to assume that $\lambda/\mu_1 > 1$. From its definition, we can see that R_0 is a decreasing function of ε . Furthermore, since HTLV-I-infected cells keep most of their functional capabilities [7], we can assume that $\mu_1 = \mu_2 = \mu_3$. Thus, at the chronic-infection equilibrium we have

$$\frac{\lambda}{\mu_1} > N^* = x^* + y^* + z^* = \frac{\lambda}{\mu_1}(1 + dz^*),$$

This implies $d < 0$, and analyzing the intersection of the graphs of g and h (see Figure 2.3), we conclude that z^* is an increasing function of ε . Hence, changes in the contact function can reduce the basic reproduction number, but they will increase the level of HTLV-I-infected T cells. It is worth mentioning that, for epidemics in human populations, experimental data seem to indicate that $\varepsilon = 1$, i.e. the standard incidence, is more realistic [1, 2, 12].

2.6. References

- [1] R. M. ANDERSON, *Transmission dynamics and control of infectious diseases*, in Population Biology of Infectious Diseases, R. M. Anderson and R. M. May, eds., Springer-Verlag, 1982, pp. 149–176.
- [2] R. M. ANDERSON AND R. M. MAY, *Infectious Diseases in Humans: Dynamics and Control*, Oxford University Press, 1991.
- [3] C. M. R. BANGHAM, *The immune response to HTLV-I*, Curr. Opin. Immunol., 12 (2000), pp. 397–402.
- [4] K. BARMAK, E. HARHAJ, C. GRANT, T. ALEFANTIS, AND B. WIGDAHL, *Human T cell leukemia virus type I-induced disease: pathways to cancer and neurodegeneration*, Virology, 308 (2003), pp. 1–12.

- [5] F. BRAUER AND C. CASTILLO-CHÁVEZ, *Mathematical Models in Population Biology and Epidemiology*, Springer-Verlag, 2000.
- [6] G. BUTLER, H. I. FREEDMAN, AND P. WALTMAN, *Uniformly persistent systems*, Proc. Amer. Math. Soc., 96 (1986), pp. 425–430.
- [7] A. J. CANN AND I. S. Y. CHEN, *Human T-cell leukemia virus type I and II*, in Fields Virology, B. N. Fields, D. M. Knipe, and P. M. Howley, eds., Lippincott-Raven Publishers, 1996, pp. 1849–1880.
- [8] D. R. CLARK, R. J. DE BOER, K. C. WOLTHERS, AND F. MIEDEMA, *T cell dynamics in HIV-1 infection*, in Advances in Immunology, F. J. Dixon, ed., Academic Press, 1999, pp. 301–327.
- [9] O. DIEKMANN AND J. A. P. HEESTERBEEK, *Mathematical Epidemiology of Infectious Diseases: Model building, analysis and interpretation*, John Wiley & Sons, 2000.
- [10] H. I. FREEDMAN, S. RUAN, AND M. TANG, *Uniform persistence and flows near a closed positively invariant set*, J. Dynam. Differential Equations, 6 (1994), pp. 583–600.
- [11] R. A. GOLDSBY, T. J. KINDT, B. A. OSBORNE, AND J. KUBY, *Immunology*, W. H. Freeman and Company, 5th. ed., 2003.
- [12] H. W. HETHCOTE, *The mathematics of infectious diseases*, SIAM Rev., 42 (2000), pp. 599–653.
- [13] R. KUBOTA, M. OSAME, AND S. JACOBSON, *Retrovirus: Human T-cell lymphotropic virus type I-associated diseases and immune dysfunction*, in Effects of Microbes on the Immune System, M. W. Cunningham and R. S. Fujinami, eds., Lippincott Williams & Wilkins, 2000, pp. 349–371.
- [14] J. P. LASALLE, *The Stability of Dynamical Systems*, Regional Conference Series in Applied Mathematics, SIAM, 1976.

- [15] A. MANNS, E. L. MURPHY, R. WILK, G. HAYNES, J. P. FIGUEROA, B. HAN-
CHARD, M. BARNETT, J. DRUMMOND, D. WATERS, M. CERNEY, J. R.
SEALS, S. S. ALEXANDER, H. LEE, AND W. A. BLATTNER, *Detection of early
human T-cell lymphotropic virus type I antibody patterns during seroconversion among trans-
fusion recipients*, *Blood*, 77 (1991), pp. 896–905.
- [16] L. M. MANSKY, *In vivo analysis of human T-cell leukemia virus type 1 reverse transcrip-
tion accuracy*, *J. Virol.*, 74 (2000), pp. 9525–9531.
- [17] R. H. MARTIN JR., *Logarithmic norms and projections applied to linear differential
systems*, *J. Math. Anal. Appl.*, 45 (1974), pp. 432–454.
- [18] J. MENA-LORCA AND H. W. HETHCOTE, *Dynamic models in infectious diseases as
regulators of population sizes*, *J. Math. Biol.*, 30 (1992), pp. 693–716.
- [19] F. MORTREUX, M. KAZANJI, A.-S. GABET, B. DE THOISY, AND E. WATTEL,
*Two-step nature of human T-cell leukemia virus type 1 replication in experimentally infected
squirrel monkeys (*saimiri sciureus*)*, *J. Virol.*, 75 (2001), pp. 1083–1089.
- [20] J. OVERBAUGH, *HTLV-I sweet-talks its way into cells*, *Nat. Med.*, 10 (2004), pp. 20–
21.
- [21] A. S. PERELSON AND P. W. NELSON, *Mathematical analysis of HIV-I dynamics in
vivo*, *SIAM Rev.*, 41 (1999), pp. 3–44.
- [22] H. SHIRAKI, Y. SAGARA, AND Y. INOUE, *Cell-to-cell transmission of HTLV-I*, in
Two Decades of Adult T-cell Leukemia and HTLV-I Research, K. Sugamura,
T. Uchiyam, M. Matsuoka, and M. Kannagi, eds., Japan Scientific Societies Press,
2003, pp. 303–316.
- [23] H. R. THIEME, *Persistence under relaxed point-dissipativity (with application to an
endemic model)*, *SIAM J. Math. Anal.*, 24 (1993), pp. 407–435.
- [24] P. VAN DEN DRIESSCHE AND J. WATMOUGH, *Reproduction numbers and sub-
threshold endemic equilibria for compartmental models of disease transmission*, *Math.
Biosci.*, 180 (2002), pp. 29–48.

Chapter 3

Mitotic Division of HTLV-I-infected T Cells

3.1. Introduction

Lymphocytes reproduce by duplicating their contents and then dividing into two. Cell division, or *mitosis*, involves several phases, one of which is the nuclear division. During nuclear division, cellular polymerases replicate the DNA with a particularly low mutation rate.

HTLV-I-infected cells that undergo mitosis will produce clones with (almost) identical provirus. In contrast with this meticulous proviral copy, HTLV-I infectious transmission, i.e. by cell-to-cell contact, involves the error-prone viral reverse transcription (see Figure 3.1). Consequently, newly infected cells will show proviral mutations after a few rounds of (infectious) transmission. In comparison with other retroviruses, HTLV-I exhibits an extraordinary genetic stability. For instance, the average mutation rate per base per replication cycle for HTLV-I is 7×10^{-6} and that for HIV is 3.5×10^{-5} [23, 36].

Generally, HTLV-I-infected patients harbour a remarkably high proviral load –asymptomatic carriers can have up to 1% of peripheral mononuclear blood cells (PBMCs) infected [27, 37]. Moreover, most of the proviral load emanates from few clones [28].

To reconcile the paradox of having a retroviral infection with high proviral loads and genetically stable proviruses, E. Wattel and colleagues [28, 35] hypothesize that HTLV-I infection is a two-step process consisting of a transient phase of reverse transcription followed by a persistent clonal expansion of HTLV-I-bearing T cells.

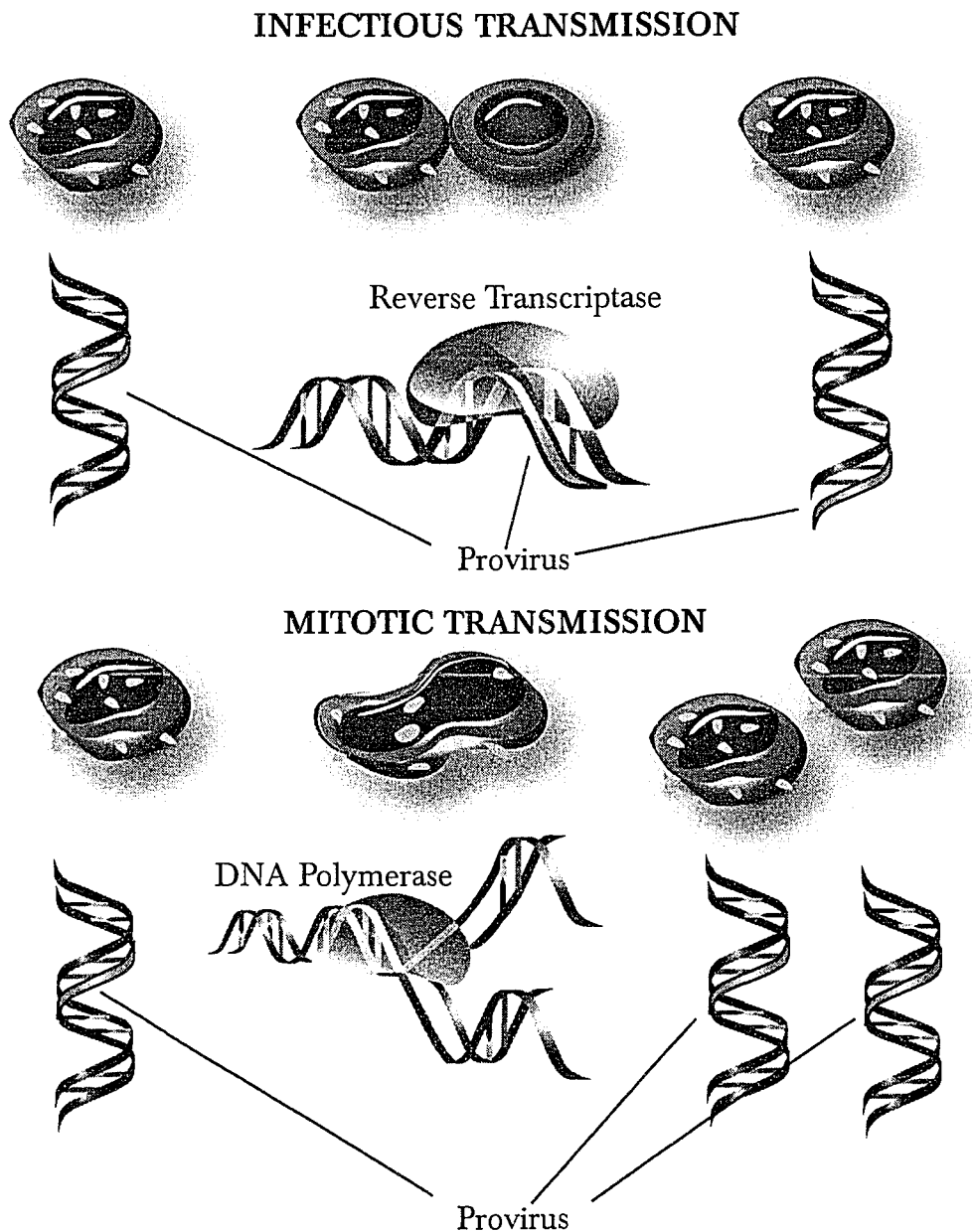


Figure 3.1. Transmission of HTLV-I infection.

In this Chapter, we propose and investigate a model that incorporates mitotic division of cells. Since HTLV-I antigens continuously restimulate the cellular immune system *in vivo* [38], we allow the infectious transmission to be present during the whole course of infection. As in Chapter 2, we incorporate the genetic stability to the model by

reducing the infection rate. Recall that such an infection rate summarizes the overall effects of infectious transmission, e.g. contact rate and effectivity of transmission.

Under biologically sound conditions, we show that our model exhibits a *backward bifurcation*. Thus, multiple stable equilibria exist when the basic reproduction number is below one. This bifurcation has “catastrophic” behaviours, e.g. abrupt changes in the solutions when parameters are slightly perturbed. We will simulate numerically a reduced model. Finally, we will explore the plausibility that such a bifurcation occurs in the HTLV-I-infection dynamics.

3.2. A Mathematical Model

We partition CD4⁺ T-cell population into compartments as in Chapter 2, i.e. susceptible (x), latently-infected (y), and actively-infected (z). We assume a bilinear incidence βxz for the infectious transmission, i.e. cell-to-cell transmission. Moreover, we consider that only a fraction $\sigma \in [0, 1]$ of newly infected cells by contact will survive the immune response. Clinical evidence suggests that T-cell division is density-dependent, and it slows as the T-cell count gets higher [18, 31]. Therefore, it is reasonable to assume that cell proliferation obeys a logistic type of growth. More specifically, we represent cell division in the susceptible compartment as $v_1 x(1 - N/K)$, where v_1 is the maximum proliferation rate, $N = x + y + z$ is the total CD4⁺ T-cell population, and K is the level at which mitotic division stops. We include an analogous growth term for the latently-infected compartment. We depict the transmission dynamics in the following transfer diagram:

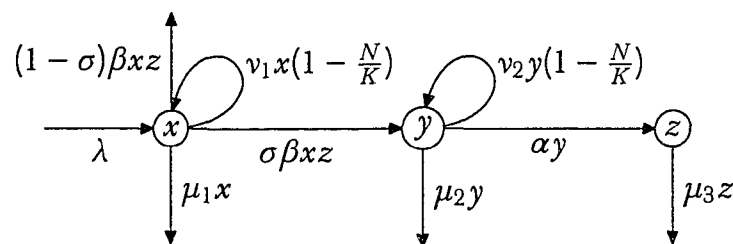


Figure 3.2. Transfer diagram.

In contrast with the model (2.1) in Chapter 2, here λ denotes the production of T cells exclusively by maturation within the lymph organs, viz. thymus, bone marrow and spleen; we assume that such a cell production is constant. The removal rates for uninfected, latently-infected, and actively-infected CD4⁺ T cells are μ_1 , μ_2 , and μ_3 , respectively. The removal rates μ_2 and μ_3 may include the loss resulting from natural causes or induced by the humoral- or adaptive-immunity. The rate at which infected cells leave latency and become actively-infected is α ; therefore, the average latent period is $1/\alpha$. All parameters in the model are positive constants.

Based on the transfer diagram and our assumptions, we obtain the following system of differential equations:

$$\begin{aligned}x' &= \lambda + v_1 x \left(1 - \frac{x + y + z}{K}\right) - \mu_1 x - \beta x z, \\y' &= \sigma \beta x z + v_2 y \left(1 - \frac{x + y + z}{K}\right) - \mu_2 y - \alpha y, \\z' &= \alpha y - \mu_3 z.\end{aligned}\tag{3.1}$$

In the absence of infection, i.e. $y = 0$ and $z = 0$, system (3.1) reduces to

$$x' = f(x),\tag{3.2}$$

where

$$f(X) = \lambda + (v_1 - \mu_1)X - \frac{v_1}{K}X^2.\tag{3.3}$$

Let x_0 be the positive root of $f(x)$. Then, a phase-line analysis shows that solutions of (3.2) satisfy $\limsup_{t \rightarrow \infty} x(t) = x_0$

Adding up the equations from (3.1) we get

$$(x + y + z)' \leq \lambda + v(x + y) \left(1 - \frac{x + y + z}{K}\right) - \mu(x + y + z),$$

where $v = \max\{v_1, v_2\}$, and $\mu = \min\{\mu_1, \mu_2, \mu_3\}$. It follows that

$$\limsup_{t \rightarrow \infty} x(t) + y(t) + z(t) \leq \bar{N},$$

where \bar{N} is the positive root of the quadratic equation $\lambda + (\nu - \mu)N - \frac{\nu}{K}N^2$. Thus, a feasible region for (3.1) is:

$$\Gamma = \left\{ (x, y, z) \in \mathbb{R}_+^3 : x \leq x_0, x + y + z \leq \bar{N} \right\}.$$

The region Γ is positively invariant with respect to (3.1) and the model is well-posed.

HTLV-I-proviral DNA production (amplification) has two sources: infectious transmission (cell-to-cell contact), and mitotic transmission (cell division) [11, 28]. Accordingly, the basic reproduction number consists of summands for each one of these transmissions; we label the infectious (horizontal) and mitotic (vertical) transmissions by $R_0^h(\sigma)$, and R_0^v , respectively. Thus,

$$R_0(\sigma) = R_0^h(\sigma) + R_0^v = \frac{\sigma \alpha \beta x_0}{(\mu_2 + \alpha) \mu_3} + \frac{\nu_2}{\mu_2 + \alpha} \left(1 - \frac{x_0}{K} \right), \quad (3.4)$$

where x_0 is the positive root of the polynomial f defined in (3.3).

Heuristically, we obtain $R_0^h(\sigma)$ as in Chapter 2; that is: $R_0^h(\sigma)$ is the product of the contact rate β , the average latent period of infected cells $\alpha/(\mu_2 + \alpha)$, the fraction σ of newly-infected $CD4^+$ T cells that evade the immune system, the average infectious period of actively-infected cells $1/\mu_3$, and the T-cell population x_0 in the absence of infection. We obtain R_0^v as the product of the mean (death-adjusted) latent period $1/(\mu_2 + \alpha)$, and the average number of latently-infected T cells produced by the division of a primary latently-infected cell $\nu_2(1 - x_0/K)$ (see [17, 26, 33]).

We will show that, under certain conditions, the model exhibits a backward bifurcation. Roughly speaking, this means that there exist multiple stable equilibria when $R_0(\sigma) \leq 1$, and “close” solutions may approach abruptly to different steady states.

An equilibrium point (x, y, z) satisfies:

$$\begin{aligned} 0 &= \lambda + \nu_1 x \left(1 - \frac{x + y + z}{K} \right) - \mu_1 x - \beta x z, \\ 0 &= \sigma \beta x z + \nu_2 y \left(1 - \frac{x + y + z}{K} \right) - \mu_2 y - \alpha y, \\ 0 &= \alpha y - \mu_3 z. \end{aligned} \quad (3.5)$$

For any choice of parameters, there exists the infection-free equilibrium point $P_0 = (x_0, 0, 0)$, where x_0 is the positive root of f .

Assume $y > 0$. From the third equation of (3.5) we have:

$$z = \frac{\alpha}{\mu_3} y. \quad (3.6)$$

Substituting (3.6) into the second equation of (3.5) gives

$$\frac{\sigma\beta\alpha}{\mu_3} x + v_2 \left(1 - \frac{x+y+z}{K} \right) - (\mu_2 + \alpha) = 0,$$

which leads to

$$z = \frac{\alpha K}{v_2(\mu_3 + \alpha)} \left[\left(\frac{\sigma\beta\alpha K - v_2\mu_3}{\mu_3 K} \right) x + v_2 - (\mu_2 + \alpha) \right]. \quad (3.7)$$

From the first equation of (3.5), we obtain

$$\lambda + (v_1 - \mu_1)x - \frac{v_1}{K} x^2 = \left[\frac{v_1(\mu_3 + \alpha) + \beta\alpha K}{\alpha K} \right] xz. \quad (3.8)$$

Combining (3.7) and (3.8), we conclude that a chronic-infection equilibrium must satisfy:

$$f(x) = g_\sigma(x), \quad (3.9)$$

where

$$g_\sigma(X) = \vartheta \left[\left(\frac{\sigma\beta\alpha K - v_2\mu_3}{\mu_3 K} \right) X + v_2 - (\mu_2 + \alpha) \right] X, \quad (3.10)$$

and

$$\vartheta = \frac{v_1\mu_3 + v_1\alpha + \beta\alpha K}{v_2(\mu_3 + \alpha)}. \quad (3.11)$$

Define the polynomial

$$m_\sigma(X) = f(X) - g_\sigma(X) = \lambda + m_1 X + m_2(\sigma) X^2, \quad (3.12)$$

where

$$m_1 = v_1 - \mu_1 - \vartheta[v_2 - (\mu_2 + \alpha)], \quad (3.13)$$

$$m_2(\sigma) = -\frac{v_1}{K} - \vartheta \left[\frac{\sigma\beta\alpha K - v_2\mu_3}{\mu_3 K} \right]. \quad (3.14)$$

The positive roots of $m_\sigma(X)$ represent the x -co-ordinate of the equilibria. Multiple chronic-infection equilibria can occur only when

$$m_1 < 0 \quad \text{and} \quad m_2(\sigma) > 0. \quad (3.15)$$

Note that $m_2(\sigma) > 0$ implies

$$\sigma \beta \alpha K < \nu_2 \mu_3. \quad (3.16)$$

When (3.15) holds, the global minimum of $m_\sigma(X)$ occurs at

$$\bar{X}(\sigma) = -\frac{m_1}{2m_2(\sigma)} = \frac{\mu_3 K m_1}{2[\nu_1 \mu_3 + \vartheta(\sigma \beta \alpha K - \nu_2 \mu_3)]} > 0.$$

Note that $\bar{X}(\sigma)$ is an increasing function of its parameter. Moreover, the value of $m_\sigma(\bar{X}(\sigma))$ increases as σ increases. The graph of m_σ intersects exactly once the positive X -axis when:

$$\exists \sigma_0 \text{ such that } m_1^2 - 4\lambda m_2(\sigma_0) = 0.$$

Or equivalently, when

$$\sigma_0 = \frac{\nu_2 \mu_3}{\beta \alpha K} - \frac{\mu_3}{\beta \alpha \vartheta} \left[\frac{m_1^2}{4\lambda} + \frac{\nu_1}{K} \right] = \frac{\nu_2 \mu_3 (4\lambda \beta \alpha - (\mu_3 + \alpha) m_1^2)}{4\lambda \beta \alpha (\nu_1 (\mu_3 + \alpha) + \beta \alpha K)}. \quad (3.17)$$

Thus, when $\sigma < \sigma_0$, the polynomial m_σ has no real roots; when $\sigma = \sigma_0$, the polynomial m_σ has exactly one positive root. Finally, when $\sigma > \sigma_0$ we will have two positive roots $x^*(\sigma) < \bar{X}(\sigma) < x_*(\sigma)$ (see Figures 3.3 and 3.4).

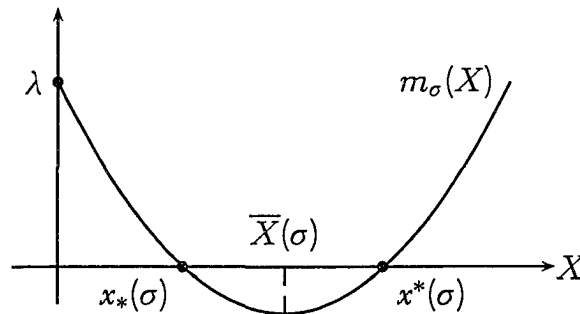


Figure 3.3. Roots of $m_\sigma(X)$ when $\sigma > \sigma_0$.

Note that $x^*(\sigma)$ is an increasing function. Therefore, there exists $\sigma_c \geq \sigma_0$ such that $m_{\sigma_c}(x_0) = 0$. More precisely,

$$\sigma_c = \frac{v_2 \mu_3}{\beta \alpha K} - \frac{\mu_3(v_2 - (\mu_2 + \alpha))}{\beta \alpha x_0}. \quad (3.18)$$

Remark. Formally, σ_0 and σ_c can assume any value. However, we impose the condition

$$\sigma_0 > 0 \quad \text{and} \quad \sigma_c \leq 1. \quad (3.19)$$

As parameter σ varies, we obtain the following cases (see Figure 3.4)

- (i) $0 < \sigma < \sigma_0$. There is no chronic-infection equilibrium point.
- (ii) $\sigma = \sigma_0$. There is exactly one chronic-infection equilibrium point.
- (iii) $\sigma_0 < \sigma < \sigma_c$. There are two chronic-infection equilibria $P_* = (x_*, y_*, z_*)$ and $P^* = (x^*, y^*, z^*)$, $x_* < x^*$, $y_* > y^*$, $z_* > z^*$.
- (iv) $\sigma \geq \sigma_c$. There is a unique chronic-infection equilibrium $P_* = (x_*, y_*, z_*)$ in the feasible region Γ .

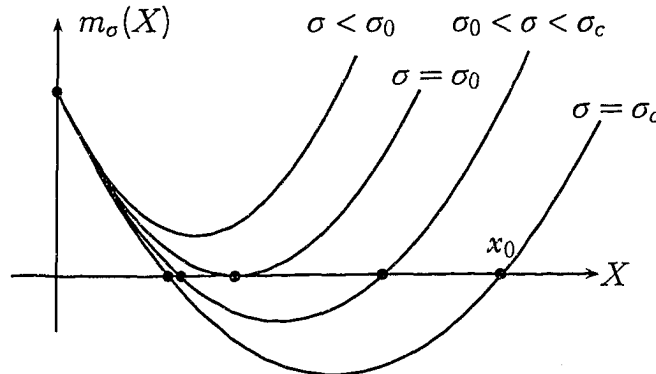


Figure 3.4. Positive roots of the polynomials $m_\sigma(X)$ as σ varies.

We summarize this analysis in the following result.

Theorem 3.1. System (1) always has the infection-free equilibrium $P_0 = (x_0, 0, 0)$. Assume the conditions (3.15) and (3.19) are satisfied. Then the number of chronic-infection equilibria is determined by σ . More specifically,

- (i) if $0 < \sigma < \sigma_0$, there are no chronic-infection equilibria;
- (ii) if $\sigma = \sigma_0$, there is a unique chronic-infection equilibrium;
- (iii) if $\sigma_0 < \sigma < \sigma_c$, there are two chronic-infection equilibria P_* and P^* ;
- (iv) if $\sigma \geq \sigma_c$, there is a unique chronic-infection equilibrium P_* .

3.3. Local Stability Analysis of the Equilibria

We will prove the local stability of the equilibria using *Routh-Hurwitz criterion*. Suppose the mapping $\mathbf{x} \mapsto F(\mathbf{x})$ from an open subset $B \subset \mathbb{R}^3$ to \mathbb{R}^3 is C^1 . Let $J(\mathbf{x}) = DF(\mathbf{x})$ be the Jacobian matrix of F . Suppose \mathbf{x}_0 is an equilibrium point of the differential equation

$$\mathbf{x}' = F(\mathbf{x}).$$

Then, by the Routh-Hurwitz criterion (see [6]), \mathbf{x}_0 is locally asymptotically stable if and only if

- (i) $\text{Tr } J(\mathbf{x}_0) < 0$,
- (ii) $\text{Det } J(\mathbf{x}_0) < 0$,
- (iii) $\text{Tr } J(\mathbf{x}_0) \cdot c_2 < \text{Det } J(\mathbf{x}_0)$,

where c_2 is the sum of the principal 2×2 minors of $J(\mathbf{x}_0)$.

Theorem 3.2. The infection-free equilibrium point P_0 is locally asymptotically stable when $R_0(\sigma) < 1$, and is a saddle when $R_0(\sigma) > 1$.

Proof. We can write the Jacobian matrix of (3.1) at P_0 as

$$J(P_0) = \begin{pmatrix} -\frac{\lambda}{x_0} - \frac{v_1 x_0}{K} & -\frac{v_1 x_0}{K} & -\frac{v_1 x_0}{K} - \beta x_0 \\ 0 & v_2 \left[1 - \frac{x_0}{K}\right] - (\mu_2 + \alpha) & \sigma \beta x_0 \\ 0 & \alpha & -\mu_3 \end{pmatrix}.$$

Note that $v_2 \left[1 - \frac{x_0}{K}\right] - (\mu_2 + \alpha) \leq (\mu_2 + \alpha)(R_0(\sigma) - 1)$. Thus, condition (i) is fulfilled when $R_0(\sigma) < 1$. We also have

$$\text{Det } J(P_0) = - \left(\frac{\lambda}{x_0} + \frac{v_1 x_0}{K} \right) \text{Det } A, \quad (3.20)$$

where

$$A = \begin{pmatrix} v_2 \left[1 - \frac{x_0}{K}\right] - (\mu_2 + \alpha) & \sigma \beta x_0 \\ \alpha & -\mu_3 \end{pmatrix}.$$

Using the definition of the basic reproduction number (3.4), we get

$$\text{Det } A = -\mu_3(\mu_2 + \alpha)[R_0(\sigma) - 1].$$

Therefore, condition (ii) holds if and only if $R_0(\sigma) < 1$. Moreover, this implies the instability of P_0 when $R_0(\sigma) > 1$. From the definition of c_2 , we obtain

$$c_2 = - \left[\frac{\lambda}{x_0} + \frac{v_1 x_0}{K} \right] \left[v_2 \left[1 - \frac{x_0}{K} \right] - (\mu_2 + \alpha) - \mu_3 \right] + \text{Det } A. \quad (3.21)$$

Condition (iii) follows from (3.20), (3.21) and condition (i). Therefore, by Routh-Hurwitz criterion, the disease-free equilibrium point is stable when $R_0(\sigma) < 1$ and unstable for $R_0(\sigma) > 1$. *q.e.d.*

Theorem 3.3. (i) If $R_0(\sigma_0) < R_0(\sigma) < 1$, then P_* is locally stable whereas P^* is a saddle. (ii) If $R_0(\sigma) > 1$, then P_* is locally asymptotically stable.

Proof. The Jacobian matrix of (3.1) at the equilibrium point $\widehat{P} = (\widehat{x}, \widehat{y}, \widehat{z})$ is given by:

$$J(\widehat{P}) = \begin{pmatrix} j_{11} & -\frac{v_1}{K} \widehat{x} & -\left(\frac{v_1}{K} + \beta\right) \widehat{x} \\ \sigma \beta \widehat{z} - \frac{v_2}{K} \widehat{y} & j_{22} & \sigma \beta \widehat{x} - \frac{v_2}{K} \widehat{y} \\ 0 & \alpha & -\mu_3 \end{pmatrix},$$

where the diagonal elements are given by:

$$j_{11} = v_1 \left[1 - \frac{\widehat{x} + \widehat{y} + \widehat{z}}{K} \right] - \mu_1 - \beta \widehat{z} - \frac{v_1}{K} \widehat{x}, \quad \text{and}$$

$$j_{22} = v_2 \left[1 - \frac{\widehat{x} + \widehat{y} + \widehat{z}}{K} \right] - (\mu_2 + \alpha) - \frac{v_2}{K} \widehat{y}.$$

Note that \widehat{x} , \widehat{y} , \widehat{z} are positive. Thus, condition (i) of the Routh-Hurwitz criterion holds because

$$j_{11} = -\frac{\lambda}{\widehat{x}} - \frac{v_1}{K} \widehat{x} < 0 \quad \text{and} \quad j_{22} = -\sigma \beta \frac{\widehat{x} \widehat{z}}{\widehat{y}} - \frac{v_2}{K} \widehat{y} < 0.$$

The determinant of $J(\widehat{P})$ is given by

$$\begin{aligned} & \text{Det } J(\widehat{P}) \\ &= - \left(\sigma \beta \widehat{z} - \frac{v_2}{K} \widehat{y} \right) \left[\mu_3 \frac{v_1}{K} \widehat{x} + \alpha \left(\frac{v_1}{K} + \beta \right) \widehat{x} \right] + j_{11} \left[-\mu_3 j_{22} - \alpha \left(\sigma \beta \widehat{x} - \frac{v_2}{K} \widehat{y} \right) \right] \\ &= - \left(\sigma \beta \widehat{z} - \frac{v_2}{K} \widehat{y} \right) \left[\mu_3 \frac{v_1}{K} \widehat{x} + \alpha \left(\frac{v_1}{K} + \beta \right) \widehat{x} \right] \end{aligned}$$

$$\begin{aligned}
 & +j_{11} \left[-\mu_3 \left(-\sigma\beta \frac{\hat{x}\hat{z}}{\hat{y}} - \frac{\nu_2}{K} \hat{y} \right) - \alpha \left(\sigma\beta\hat{x} - \frac{\nu_2}{K} \hat{y} \right) \right] \\
 = & - \left(\frac{\sigma\beta\alpha K - \nu_2\mu_3}{\alpha K} \right) \left[(\mu_3 + \alpha) \frac{\nu_1}{K} + \beta\alpha \right] \hat{x}\hat{z} + j_{11}(\mu_3 + \alpha) \frac{\nu_2}{K} \hat{y} \\
 = & \frac{\hat{z}}{\alpha K} \left\{ -(\sigma\beta\alpha K - \nu_2\mu_3) \left[(\mu_3 + \alpha) \frac{\nu_1}{K} + \beta\alpha \right] \hat{x} \right. \\
 & \left. + (\mu_3 + \alpha)\nu_2\mu_3 \left[\nu_1 \left(1 - \frac{\hat{x}}{K} \right) - \frac{\nu_1}{K} \hat{x} - \mu_1 - \frac{\nu_1}{K} (\hat{y} + \hat{z}) - \beta\hat{z} \right] \right\} \\
 = & \frac{(\mu_3 + \alpha)\nu_2\mu_3\hat{z}}{\alpha K} \left\{ -\frac{\sigma\beta\alpha K - \nu_2\mu_3}{\mu_3 K} \vartheta \hat{x} \right. \\
 & \left. + \nu_1 \left(1 - \frac{\hat{x}}{K} \right) - \mu_1 - \frac{\nu_1}{K} \hat{x} - \vartheta \left[\frac{\sigma\beta\alpha K - \nu_2\mu_3}{\mu_3 K} \hat{x} + \nu_2 - (\mu_2 + \alpha) \right] \right\} \\
 = & \frac{(\mu_3 + \alpha)\nu_2\mu_3\hat{z}}{\alpha K} \left\{ -\vartheta \left[2 \frac{\sigma\beta\alpha K - \nu_2\mu_3}{\mu_3 K} \hat{x} + \nu_2 - (\mu_2 + \alpha) \right] \right. \\
 & \left. + \nu_1 \left(1 - \frac{\hat{x}}{K} \right) - \mu_1 - \frac{\nu_1}{K} \hat{x} \right\} \\
 = & \frac{(\mu_3 + \alpha)\nu_2\mu_3\hat{z}}{\alpha K} \{-g'_\sigma(\hat{x}) + f'(\hat{x})\} = \frac{(\mu_3 + \alpha)\nu_2\mu_3\hat{z}}{\alpha K} m'_\sigma(\hat{x}).
 \end{aligned}$$

Note that $m'_\sigma(x_*) < 0$ implies condition (ii) of the Routh-Hurwitz criterion, whereas $m'_\sigma(x^*) > 0$ implies the instability of P^* (see Figure 3.3). Since $j_{11} < 0$, we obtain:

$$\begin{aligned}
 c_2 = & j_{11}j_{22} + \frac{\nu_1}{K} \hat{x} \left(\sigma\beta\hat{z} - \frac{\nu_2}{K} \hat{y} \right) - \mu_3(j_{11} + j_{22}) - \alpha \left(\sigma\beta\hat{x} - \frac{\nu_2}{K} \hat{y} \right) \\
 = & j_{11}j_{22} + \frac{\nu_1}{K} \hat{x} \left(\sigma\beta\hat{z} - \frac{\nu_2}{K} \hat{y} \right) - \mu_3j_{11} - \left(\mu_3j_{22} + \alpha \left(\sigma\beta\hat{x} - \frac{\nu_2}{K} \hat{y} \right) \right) \\
 = & j_{11}j_{22} + \frac{\nu_1}{K} \hat{x} \left(\sigma\beta\hat{z} - \frac{\nu_2}{K} \hat{y} \right) - \mu_3j_{11} + \frac{(\mu_3 + \alpha)\nu_2}{K} \hat{y} \\
 = & \left(-\frac{\lambda}{\hat{x}} - \frac{\nu_1}{K} \hat{x} \right) \left(-\frac{\sigma\beta\alpha}{\mu_3} \hat{x} - \frac{\nu_2}{K} \hat{y} \right) + \frac{\nu_1}{K} \hat{x} \left(\sigma\beta\hat{z} - \frac{\nu_2}{K} \hat{y} \right) - \mu_3j_{11} + \frac{(\mu_3 + \alpha)\nu_2}{K} \hat{y} \\
 = & \frac{\sigma\beta\alpha}{\mu_3} \left(\lambda + \frac{\nu_1}{K} \hat{x}^2 \right) + \frac{\lambda\nu_2}{K} \frac{\hat{y}}{\hat{x}} + \frac{\nu_1\sigma\beta}{K} \hat{x}\hat{z} - \mu_3j_{11} + \frac{(\mu_3 + \alpha)\nu_2}{K} \hat{y} > 0.
 \end{aligned}$$

Finally, we will show that the condition (iii) of the Routh-Hurwitz criterion holds.

Write

$$-\text{Tr } J(\hat{P}) \cdot c_2 = (-j_{11} - j_{22} + \mu_3) c_2$$

$$\begin{aligned}
 &= (-j_{11} - j_{22})c_2 + \mu_3 \left(j_{11}(j_{22} - \mu_3) + \frac{v_1}{K} \hat{x} \left(\sigma \beta \hat{z} - \frac{v_2}{K} \hat{y} \right) + \frac{(\mu_3 + \alpha)v_2}{K} \hat{y} \right) \\
 &= (-j_{11} - j_{22})c_2 + \mu_3 \left(j_{11}(j_{22} - \mu_3) + \frac{(\mu_3 + \alpha)v_2}{K} \hat{y} \right) + \frac{\mu_3 v_1}{K} \left(\frac{\sigma \beta \alpha K - v_2 \mu_3}{\mu_3 K} \right) \hat{x} \hat{y} \\
 &\stackrel{(3.16)}{>} (-j_{11} - j_{22})c_2 + \mu_3 \left(j_{11}(j_{22} - \mu_3) + \frac{(\mu_3 + \alpha)v_2}{K} \hat{y} \right) + \\
 &\quad + \left(\frac{(\mu_3 + \alpha)v_1}{K} + \beta \alpha \right) \left(\frac{\sigma \beta \alpha K - v_2 \mu_3}{\mu_3 K} \right) \hat{x} \hat{y} \\
 &= -j_{11}^2(j_{22} - \mu_3) - \frac{(\mu_3 + \alpha)v_2}{K} \hat{y} j_{11} - \frac{v_1}{K} \left(\frac{\sigma \beta \alpha K - v_2 \mu_3}{\mu_3 K} \right) \hat{x} \hat{y} j_{11} - j_{22}c_2 \\
 &\quad + \mu_3 \left(j_{11}(j_{22} - \mu_3) + \frac{(\mu_3 + \alpha)v_2}{K} \hat{y} \right) + \left(\frac{(\mu_3 + \alpha)v_1}{K} + \beta \alpha \right) \left(\frac{\sigma \beta \alpha K - v_2 \mu_3}{\mu_3 K} \right) \hat{x} \hat{y} \\
 &= -j_{11}^2(j_{22} - \mu_3) - \frac{v_1}{K} \left(\frac{\sigma \beta \alpha K - v_2 \mu_3}{\mu_3 K} \right) \hat{x} \hat{y} j_{11} - j_{22}c_2 \\
 &\quad + \mu_3 \left(j_{11}(j_{22} - \mu_3) + \frac{(\mu_3 + \alpha)v_2}{K} \hat{y} \right) - \text{Det } J(\hat{P}) \\
 &= -j_{11} \left(j_{11} j_{22} + \frac{v_1}{K} \left(\frac{\sigma \beta \alpha K - v_2 \mu_3}{\mu_3 K} \right) \hat{x} \hat{y} \right) + j_{11}^2 \mu_3 - j_{22}c_2 \\
 &\quad + \mu_3 \left(j_{11}(j_{22} - \mu_3) + \frac{(\mu_3 + \alpha)v_2}{K} \hat{y} \right) - \text{Det } J(\hat{P}) \\
 &= -j_{11} \left(j_{11} j_{22} - \frac{v_1 v_2}{K^2} \hat{x} \hat{y} \right) - \frac{v_1 \sigma \beta \alpha}{\mu_3 K} \hat{x} \hat{y} j_{11} + j_{11}^2 \mu_3 - j_{22}c_2 \\
 &\quad + \mu_3 \left(j_{11}(j_{22} - \mu_3) + \frac{(\mu_3 + \alpha)v_2}{K} \hat{y} \right) - \text{Det } J(\hat{P}) \\
 &= -j_{11} \left(\frac{\sigma \beta \alpha}{\mu_3} \left(\lambda + \frac{v_1}{K} \hat{x}^2 \right) + \frac{\lambda v_2}{K} \frac{\hat{y}}{\hat{x}} \right) - \frac{v_1 \sigma \beta \alpha}{v_3 K} \hat{x} \hat{y} j_{11} + j_{11}^2 \mu_3 \\
 &\quad - j_{22}c_2 + \mu_3 \left(j_{11}(j_{22} - \mu_3) + \frac{(\mu_3 + \alpha)v_2}{K} \hat{y} \right) - \text{Det } J(\hat{P}) \\
 &= B - \text{Det } J(\hat{P}),
 \end{aligned}$$

where $B > 0$; thus, P_* is locally stable.

q.e.d.

We summarize the preceding analysis in the bifurcation diagram shown in Figure 3.5, in which solid lines indicate stable equilibria, and dashed lines indicate unstable equilibria. Note that P^* has a smaller y^* and lies in the middle branch,

whereas y_* lies on the top branch. By its definition, $R_0(\sigma)$ is an increasing function of σ ; moreover, $R_0(\sigma_c) = 1$. Thus, $\sigma_0 < \sigma < \sigma_c \iff R_0(\sigma_0) < R_0(\sigma) < 1$, and $\sigma > \sigma_c \iff R_0(\sigma) > 1$. We see that $R_0(\sigma)$ still behaves as a threshold parameter in that if $R_0(\sigma) < 1$, the infection-free equilibrium P_0 is stable, whereas if $R_0(\sigma) > 1$, P_0 becomes unstable and a unique chronic-infection equilibrium P_* is stable.

The bifurcation diagram in figure in Figure 3.5 shows the standard features of a backward bifurcation (see [7, 8, 12, 13, 21, 20, 24, 25, 32]); namely, multiple chronic-infection equilibria exist when the basic reproduction number is below unity. Such a bifurcation possesses certain “catastrophic” behaviours:

- When $R_0(\sigma)$ increases through 1, the number of infected cells can suddenly change from low level to a high persistent level. This may lead to a sudden infection outbreak among T-cell population.
- When $R_0(\sigma)$ decreases through 1, the level of chronic-infection remains high.

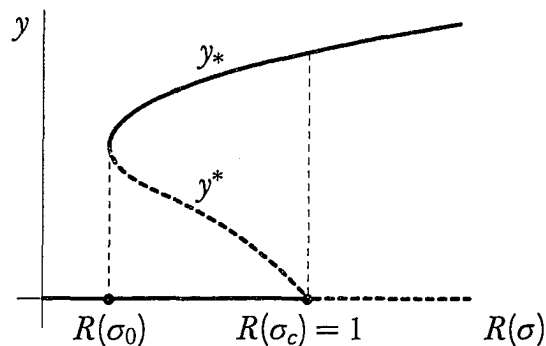


Figure 3.5. Backward Bifurcation.

This is in a sharp contrast to the standard forward bifurcation as the one obtained in Chapter 2. A serious complication associated with a backward bifurcation is: lowering the basic reproduction number R_0 below unity may no longer be a viable control measure, hence, different prevention and control measures have to be contemplated.

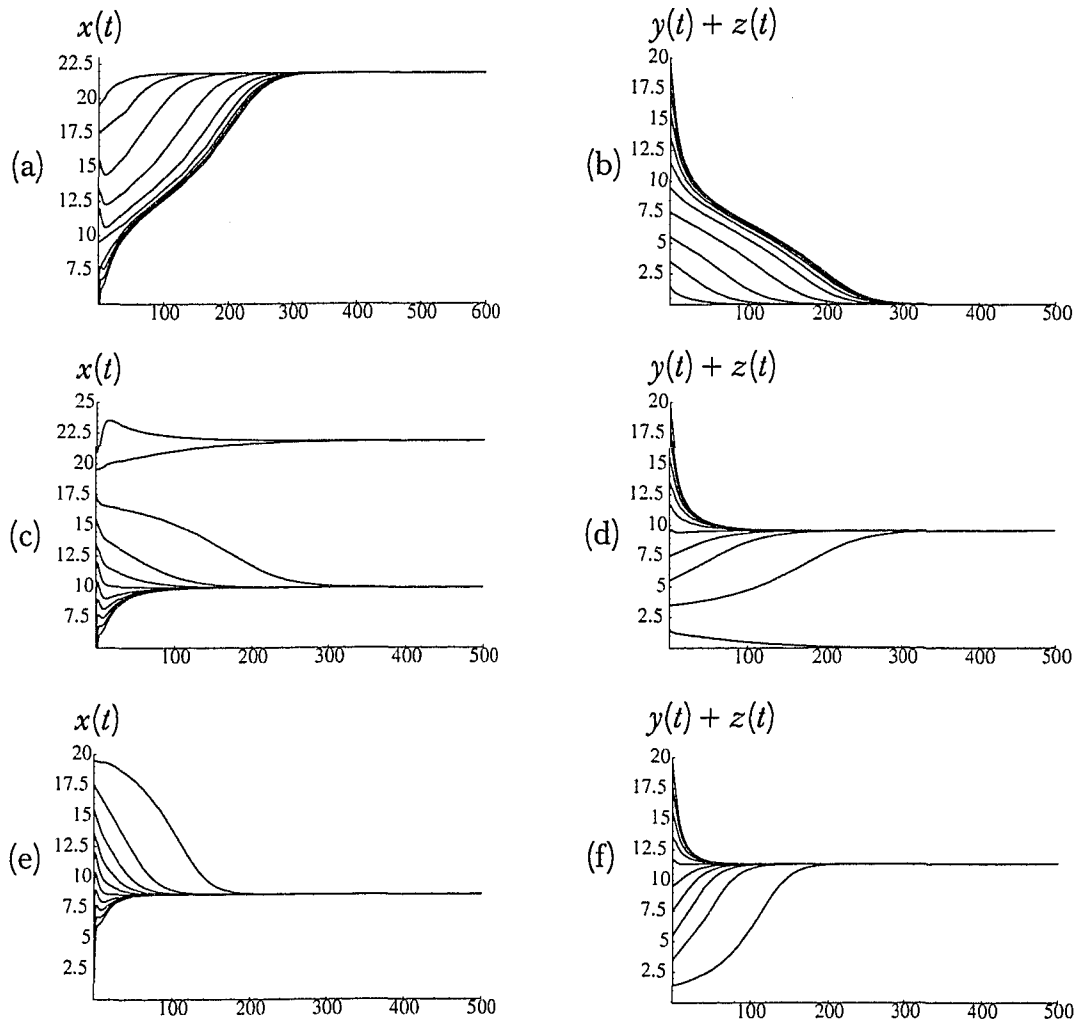


Figure 3.6. *MATHEMATICA** simulations of system (3.1). In (a) and (b) $R(\sigma) < R(\sigma_0)$, all the solutions approach to P_0 . In (c) and (d), $R(\sigma_0) < R(\sigma) < 1$, the solutions approach either P_0 or P_* depending on the initial conditions. Finally, in (e) and (f) $R(\sigma) > 1$, all the solutions approach P_* .

3.4. Global Dynamics of a Reduced Model

In this section, we amalgamate the two compartments of latently- and actively-infected cells into one, which, generically, we refer to as infected-cells compartment (y). There are several benefits from this reduction. Firstly, the dynamics of the reduced model mimics that of the “full” model in the sense that a backward bifurcation can also occur. Secondly, it facilitates the global analysis of the system.

It is worth mentioning that the relevance of latency for HTLV-I infection is hitherto unclear. Bangham and colleagues [2, 16] claim that HTLV-I is not latent based on the following facts:

- Newly HTLV-I-infected cells express viral proteins within 6 hours which contrasts to the average lifespan of a naïve CD4⁺ T cell (normally scaled in years [5]).
- There are persistent humoral and cell-mediated immune responses to Tax viral proteins in asymptomatic carriers and HAM/TSP patients [19, 22].

Thus, our reduced model can be interpreted as a model without latency.

Theorems 3.1 and 3.3 underpin reduced model’s local stability. We will sketch relevant changes. The reduced model is given by:

$$\begin{aligned} x' &= \lambda + v_1 x \left(1 - \frac{x+y}{K}\right) - \mu_1 x - \beta xy, \\ y' &= \sigma \beta xy + v_2 y \left(1 - \frac{x+y}{K}\right) - \mu_2 y. \end{aligned} \tag{3.22}$$

A feasible region for (3.22) is

$$\Gamma_1 = \left\{ (x, y) \in \mathbb{R}_+^2 : x \leq x_0, x + y \leq \widetilde{N} \right\},$$

where x_0 is the positive root of (3.2), \widetilde{N} is the positive root of the polynomial $\lambda + (\widetilde{v} - \widetilde{\mu})N - \frac{\widetilde{v}}{K}N^2$, $\widetilde{v} = \max\{v_1, v_2\}$, and $\widetilde{\mu} = \min\{\mu_1, \mu_2\}$. The basic reproduction number for system (3.22) is given by:

$$R_0(\sigma) = R_0^h(\sigma) + R_0^v = \frac{\sigma \beta x_0}{\mu_2} + \frac{v_2}{\mu_2} \left(1 - \frac{x_0}{K}\right). \tag{3.23}$$

An interpretation of this basic reproduction number follows that of (3.4). For any choice of positive parameters, system (3.22) has the infection-free equilibrium point $P_0 = (x_0, 0)$. A chronic-infection equilibrium point (x, y) must satisfy

$$f(x) = \tilde{g}_\sigma(x), \quad (3.24)$$

where

$$\tilde{g}_\sigma(X) = \vartheta_1 \left[\left(\frac{\sigma\beta K - \nu_2}{K} \right) X + \nu_2 - \mu_2 \right] X, \quad (3.25)$$

and

$$\vartheta_1 = \frac{\nu_1 + \beta K}{\nu_2}. \quad (3.26)$$

The positive roots of the following polynomial give the x -co-ordinate of the equilibria

$$\tilde{m}_\sigma(X) = f(X) - \tilde{g}_\sigma(X) = \lambda + \tilde{m}_1 X + \tilde{m}_2(\sigma) X^2,$$

where

$$\tilde{m}_1 = \nu_1 - \mu_1 - \vartheta_1[\nu_2 - \mu_2], \quad (3.27)$$

$$\tilde{m}_2(\sigma) = -\frac{\nu_1}{K} - \vartheta_1 \left[\frac{\sigma\beta K - \nu_2}{K} \right]. \quad (3.28)$$

Multiple chronic-infection equilibria occur when the following conditions hold

$$\tilde{m}_1 < 0 \quad \text{and} \quad \tilde{m}_2(\sigma) > 0, \quad (3.29)$$

and

$$\sigma_0 > 0 \quad \text{and} \quad \sigma_c \leq 1. \quad (3.30)$$

The corresponding expressions for σ_0 and σ_c are given by

$$\sigma_0 = \frac{\nu_2(4\lambda\beta - \tilde{m}_1^2)}{4\lambda\beta(\nu_1 + \beta K)} \quad \text{and} \quad \sigma_c = \frac{\nu_2}{\beta K} - \frac{\nu_2 - \mu_2}{\beta x_0}.$$

The following theorem establishes the global dynamics of the system (3.22).

Theorem 3.4. Assume that conditions (3.29) and (3.30) are satisfied. Then

- (i) when $0 < R_0(\sigma) < R_0(\sigma_0)$, the infection-free equilibrium P_0 is globally asymptotically stable in $\bar{\Gamma}_1$;
- (ii) when $R_0(\sigma_0) < R_0(\sigma) < 1$, system (3.22) has two attractors in $\bar{\Gamma}_1$, the infection-free equilibrium P_0 and the chronic-infection P_* . Their basins of attraction in the interior of Γ_1 are separated by the stable manifolds of the saddle point P^* ;
- (iii) when $R_0(\sigma) > 1$, the unique chronic-infection equilibrium P_* is globally asymptotically stable in the interior of Γ_1 .

Proof. We first rule out periodic orbits in the interior of Γ_1 using Dulac's criterion (see [14, 15]). We choose a Dulac multiplier $\alpha(x, y) = 1/xy$. Let $(P(x, y), Q(x, y))$ denote the right-hand-side of (3.22). We have

$$\frac{\partial(\alpha P)}{\partial x} + \frac{\partial(\alpha Q)}{\partial y} = - \left(\frac{\lambda}{x^2 y} + \frac{v_1}{K y} + \frac{v_2}{K x} \right) < 0,$$

for all $x > 0, y > 0$. Thus, (3.22) has no periodic orbits in $\bar{\Gamma}_1$. A simple application of the classical Poincaré-Bendixson theory shows that every solution in $\bar{\Gamma}_1$ converges to a single equilibrium. The rest of the theorem follows from the local stability of equilibria as stated in Theorem 3.3. *q.e.d.*

In Figure 3.7, a phase-portrait of (3.22) for case (ii) of Theorem 3.4 is numerically generated using *MATHEMATICA*[®]. Three equilibria are marked with dots, with P_0 on the x -axis, and P^* sitting between P_* and P_0 . The heteroclinic orbits from P^* to P_* and P_0 are identifiable, as well as the basin boundaries, which are the stable manifolds of the saddle point P^* . In this case, $R_0(\sigma) < 1$, but the fate of the infection critically depends on the initial conditions. If the initial point lies in the basin of attraction of P_0 , then the infection will die out, whereas the infection will persist if the initial point lies in the basin of attraction of P_* . This behaviour does not occur in virus-host models that

have forward bifurcation [10, 34].

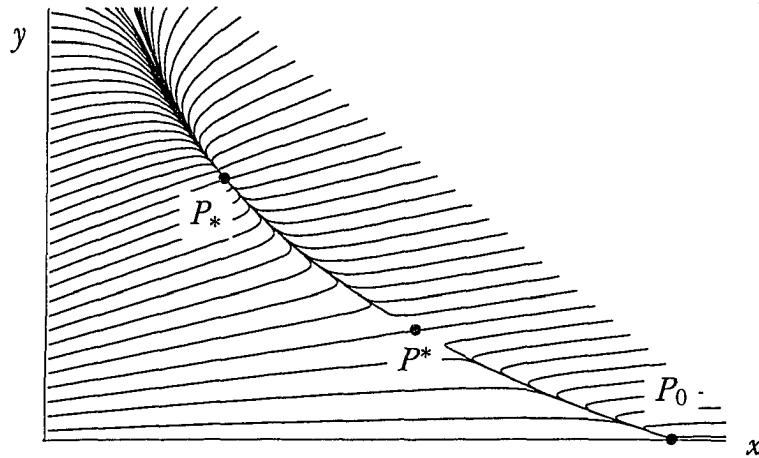


Figure 3.7. Phase-portrait of (3.22) showing multiple stable equilibria.

3.5. Numerical Simulations of the Reduced Model

In this section, we give some biologically relevant conditions to ensure that (3.29) and (3.30) are verified. Firstly, we expect that in the absence of infection, the equilibrium level x_0 of T cells is less than the carrying capacity K , namely

$$x_0 < K. \quad (3.31)$$

It is known that HTLV-I-infected cells are functionally similar to their healthy counterpart [4]. Therefore, it is reasonable to assume that healthy and infected T cells have similar natural growth and removal rates:

$$\mu_1 \approx \mu_2, \quad \nu_1 \approx \nu_2. \quad (3.32)$$

We choose the unit time in system (3.22) as day, and follow a scaling law suggested by Perelson [30]:

$$\beta K \approx 1 \text{ (day)}. \quad (3.33)$$

Under (3.32) and (3.33), conditions (3.29) transform into:

$$\sigma < \frac{\nu_2}{\nu_2 + 1}, \quad \mu_i < \nu_i \leq 1, \quad i = 1, 2. \quad (3.34)$$

Finally, we assume that $v_1 - \mu_1$ and $v_2 - \mu_2$ are in the following range:

$$\frac{v_1 - \mu_1}{2} < \sqrt{\frac{\lambda}{K}} v_1. \quad (3.35)$$

It can be shown that conditions (3.32)-(3.35) imply (3.29) and (3.30). In fact, we can establish the following result.

Corollary 3.5. Conclusions of Theorem 3.4 holds under the assumptions (3.32)-(3.35).

Proof. From (3.32) and (3.33), we have $\vartheta_1 \approx 1 + \frac{1}{v_1} > 1$; thus, $\tilde{m}_1 \approx (v_1 - \mu_1)(1 - \vartheta_1) < 0$. Note that $\tilde{m}_2(\sigma) \approx \frac{-v_1 - \vartheta_1(\sigma - v_1)}{K}$; this observation and (3.34) yield

$$\begin{aligned} \sigma < \frac{v_1}{v_1 + 1} &\iff (v_1 + 1)(v_1 - \sigma) > v_1^2 \iff \left(1 + \frac{1}{v_1}\right)(v_1 - \sigma) > v_1 \\ &\iff \frac{-v_1 - \vartheta_1(\sigma - v_1)}{K} > 0; \end{aligned}$$

therefore, condition (3.29) is verified. Condition (3.30) follows from (3.32), (3.33) and (3.35) since

$$\begin{aligned} \sigma_0 &\approx \frac{v_1 \left[4\lambda\beta - (v_1 - \mu_1)^2 \left(1 - \frac{v_1 + \beta K}{v_1}\right)^2 \right]}{4\lambda\beta(v_1 + \beta K)} \approx \frac{v_1 \left[4\lambda\beta - (v_1 - \mu_1)^2 \frac{\beta^2 K^2}{v_1^2} \right]}{4\lambda\beta(v_1 + \beta K)} \\ &\approx \frac{4\lambda v_1^2 - (v_1 - \mu_1)^2 K}{4\lambda v_1(v_1 + \beta K)} > 0. \end{aligned}$$

Finally, condition (3.30) follows from (3.33), since $\sigma_c < \frac{v_2}{\beta K} \approx v_2 \leq 1$. *q.e.d.*

Next, we will produce numerical simulation of system (3.22). Several researchers have studied CD4⁺ T-cell dynamics because of its relevance for HIV-1 infection. Our parameter estimation follows that of Nelson *et al.* [29]. We choose the production rate of CD4⁺ as $\lambda = 25$ cells/mm³, and the removal rate of CD4⁺ as $\mu_1 = \mu_2 \approx 0.03$ day⁻¹. In the absence of HTLV-I infection, the number of CD4⁺ T cells is expected to be constant and has a normal count around 1000 cells/mm³ [1, 9], and a

carrying capacity constant $K = 1150$ cells/mm³. This gives us $x_0 \approx 1000$ cells/mm³, or $f(x_0) \approx 0$. Using (3.2) we can then estimate that the proliferation constant for CD4⁺ T cells as $\nu_1 = \nu_2 \approx 0.038$ day⁻¹. To estimate β , we use the scaling relation (3.33), $\beta K \approx 1$ day. We choose $\beta = 1.03 \times 10^{-3}$ mm³/cells/day. One can verify that, with these parameter values, condition (3.29) holds, and condition (3.30) gives a range (0.0123, 0.0243) of σ for backward bifurcation to occur, and $R_0(\sigma_0) = 0.58869$. Therefore, infection is able to persist at an equilibrium level if $R_0(\sigma_0) > 0.58869$. Equivalently, total infection control is achieved only when $R_0(\sigma_0) < 0.58869$.

Numerical simulations of the model using these parameter values are carried out on *MATHEMATICA*. In Figure 3.8a and 3.8b, $\sigma = 0.015$ and $R_0 = 0.68066$ are in the range of bistability, and we see that small initial infection leads to total recovery in 3.7a, and higher initial infection leads to persistent infection in 3.7b. In Figure 3.8c, all parameter values are the same as in 3.8a and 3.8b except $\sigma = 0.03$ and $R_0(\sigma) = 1.19527$, which belong to the persistence range. We see that even a low initial infection leads to persistent infection in this case. From 3.8c, we conclude that between 10–20% of the CD4⁺ T cells will carry the provirus, which is consistent with clinical data [3, 4, 11].

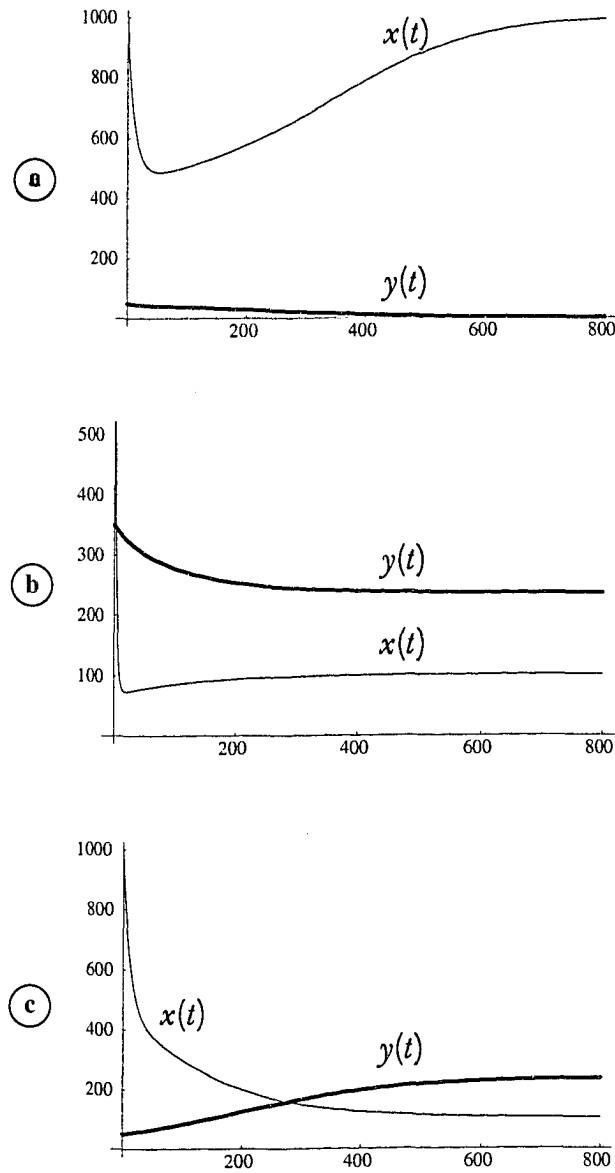


Figure 3.8. *MATHEMATICA* simulations of system (3.22) with parameter values $\mu_1 = \mu_2 = 0.03$, $\nu_1 = \nu_2 = 0.038$, $\lambda = 25$, $K = 1150$, $\beta = 0.00103$, $x_0 = 999.25$. (a) and (b) show the critical dependence on initial conditions due to the instability when $\sigma = 0.015$ and $R_0 = 0.68066$. For $\sigma = 0.03$ and $R_0 = 1.19527$, (c) shows then persistence even when the initial load of infected cells is low. The infected load stabilizes approximately at 20% of the original CD4 T-cell load.

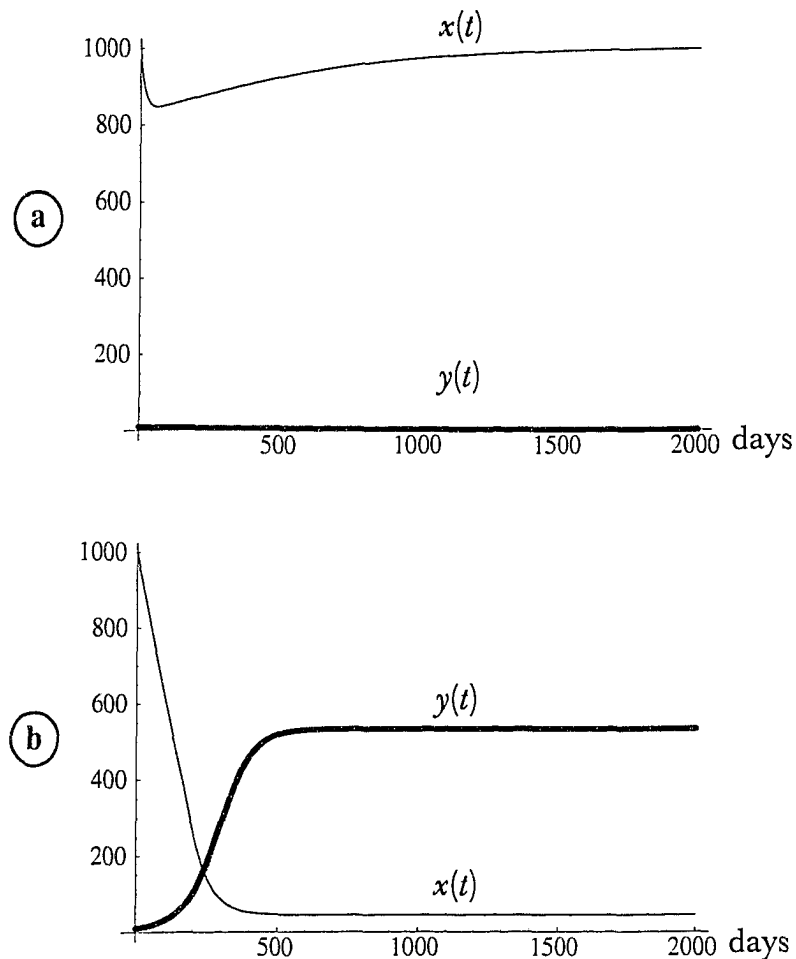


Figure 3.9. *MATHEMATICA*[®] simulations showing a sudden jump of infection level with small change in R_0 . Parameter values are $\mu_1 = 0.03$, $\nu_1 = \nu_2 = 0.038$, $\lambda = 25$, $K = 1150$, $\beta = 0.00103$, $x_0 = 999.25$. In (a) $\mu_2 = 0.032$, $R_0 = 0.92115$ and infection remains low. In (b) $\mu_2 = 0.02$, $R_0 = 1.47385$ and infection has a sudden jump.

In Figure 3.9, simulations are run to demonstrate the catastrophic effect of the backward bifurcation. The same set of parameter values are used. We choose $\sigma = 0.0238$ and $\mu_2 = 0.032$. In Figure 3.9a, $R_0 = 0.92115$, $y(0) = 10$, and infection level remains low for 2000 days. In Figure 3.9b, $\sigma = 0.0238$ remains the same, and we lower μ_2 from 0.032 to 0.02 so that $R_0 = 1.47385$. The same initial infection level $y(0) = 10$ leads to a huge jump in infection level within a year.

3.6. Conclusions

It is known that HTLV-I infection of CD4⁺ T cells is through direct cell-to-cell contact [4, 11]. Current clinical research supports the following theory (see [3, 27, 28, 36]): HTLV-I infection consists of two steps: a transient phase of reverse transcription and a phase of persistent multiplication of infected CD4⁺ T cells. When an infected cell multiplies, the provirus is passed to the daughter cell, as a form of vertical transmission. This two-step process can explain the observed high proviral load and low genetic variability in HTLV-I-infected T cells. In this Chapter, we propose and analyse a mathematical model for the infection of CD4⁺ T cells by HTLV-I based on this two-step process theory. The model incorporates both infectious (horizontal) transmission and mitotic (vertical) transmission. We also assume that a fraction σ of infected cells survive the immune system attack. The genetic stability of HTLV-I suggests that the fraction σ should be very low ($\sigma \ll 1$). Also, the high proviral load in HTLV-I infection suggest that the rate of cellular division should be high ($\nu_2 > \mu_2$). Under biologically sound assumptions, our model exhibits a bifurcation diagram that predicts persistent infection for an extended range of the basic reproduction number $R_0(\sigma)$. However, somewhat surprisingly, the same bifurcation diagram shows that the model undergoes a backward bifurcation as σ increases: a stable chronic-infection equilibrium P_* exists when the basic reproduction number $R_0(\sigma)$ is below unity for an open range of parameter values. The global dynamics for the corresponding parameter range show that P_* and the infection-free equilibrium P_0 are co-existing attractors whose basins of attraction partition the feasible region. Even when the basic reproduction number $R_0(\sigma) < 1$, whether an infection persists or dies out critically depends on which basin of attraction the initial point lies in. This clearly demonstrates the catastrophic behaviour that accompanies the backward bifurcation.

Backward bifurcation in compartmental models have attracted serious research attention only recently. Several mechanisms have been shown to lead to backward bifurcation in epidemic models, see [7, 8, 12, 13, 20, 21, 24, 32]. Dushoff *et al.* [8] provided an intuitive mechanism for backward bifurcation to occur: an increase in

infected population does not lead to a decrease in susceptibles. In our model, vertical transmission through cellular division allows the infected to grow without decreasing uninfected. This seems to agree with the intuition in [8]. We want to comment, however, that the loss of infected T cells due to immune response after viral replication is also important; backward bifurcation does not occur in our model when $\sigma = 1$. When $\sigma = 1$, our model is the same as a SI epidemic model with migration and logistic growth, and bilinear incidence. It is known that such a model only has forward bifurcation and no bistability occurs. In this sense, our analysis indicates that backward bifurcation is a byproduct of the two-step process of HTLV-I infection.

In a standard forward bifurcation (c.f. [10, 34]), when R_0 passes through 1, the level of chronic infection remains low. In contrast, as demonstrated in the bifurcation diagram in figure 3.5, a backward bifurcation results in the following catastrophic effects:

- When R_0 increases through 1, the number of infected T-cell population may experience a sudden outbreak.
- When R_0 decreases through 1, the level of chronic-infection remains high.

As a result, the standard infection-control measure of lowering R_0 below 1 is no longer viable; R_0 needs to be below $R_0(\sigma_0)$ to achieve infection control, which may be very difficult. Other infection-control measures need to be investigated. Based on our model and analysis, such measures might include

- lowering the level of chronic infection y_* to unharmed levels;
- increasing the value $R_0(\sigma_0)$ to close to 1, and hence reduce the parameter range for backward bifurcation to occur;
- identifying basin of attractions and basin boundaries as shown in Figure 3.7. This may help to design tests for development of chronic infection.

In conclusion, our model and analysis suggest that backward bifurcation may be intrinsic to HTLV-I-infection dynamics. Our theoretical results warrant further investigation of the HTLV-I-infection dynamics using more realistic models and through verification by clinical data.

3.7. References

- [1] A. K. ABBAS, A. H. LICHTMAN, AND J. S. POBER, *Cellular and Molecular Immunology*, W. B. Saunders Company, 4 ed., 2000.
- [2] B. ASQUIT, E. HANON, G. P. TAYLOR, AND C. R. M. BANGHAM, *Is human T-cell lymphotropic virus type I really silent?*, Philos. T. Roy. Soc. B., (2000), pp. 1013–1019.
- [3] C. M. R. BANGHAM, *The immune response to HTLV-I*, Curr. Opin. Immunol., 12 (2000), pp. 397–402.
- [4] A. J. CANN AND I. S. Y. CHEN, *Human T-cell leukemia virus type I and II*, in Fields Virology, B. N. Fields, D. M. Knipe, and P. M. Howley, eds., Lippincott-Raven Publishers, 1996, pp. 1849–1880.
- [5] D. R. CLARK, R. J. DE BOER, K. C. WOLTERS, AND F. MIEDEMA, *T cell dynamics in HIV-1 infection*, in Advances in Immunology, F. J. Dixon, ed., Academic Press, 1999, pp. 301–327.
- [6] W. A. COPPEL, *Stability and Asymptotic Behavior of Differential Equations*, D. C. Heath and Company, 1965.
- [7] J. DUSHOFF, *Incorporating immunological ideas in epidemiological models*, J. Theor. Biol., 180 (1996), pp. 181–187.
- [8] J. DUSHOFF, W. HUANG, AND C. CASTILLO-CHÁVEZ, *Backwards bifurcations and catastrophe in simple models of fatal diseases*, J. Math. Biol., 36 (1998), pp. 227–248.
- [9] R. A. GOLDSBY, T. J. KINDT, B. A. OSBORNE, AND J. KUBY, *Immunology*, W. H. Freeman and Company, 5th. ed., 2003.

- [10] H. GÓMEZ-ACEVEDO AND M. Y. LI, *Global dynamics of a mathematical model for HTLV-I infection of T cells*, *Canad. Appl. Math. Quart.*, 10 (2002), pp. 71–86.
- [11] C. GRANT, K. BARMAK, T. ALEFANTIS, J. YAO, S. JACOBSON, AND B. WIGDAHL, *Human T cell leukemia virus type I and neurologic disease: events in bone marrow, peripheral blood, and central nervous system during normal immune surveillance and neuroinflammation*, *J. Cell. Physiol.*, 190 (2002), pp. 133–159.
- [12] D. GREENHALGH, O. DIEKMANN, AND M. C. M. DE JONG, *Subcritical endemic steady states in mathematical models for animal infections with incomplete immunity*, *Math. Biosci.*, 165 (2000).
- [13] K. P. HADELER AND P. VAN DEN DRIESSCHE, *Backward bifurcation in epidemic control*, *Math. Biosci.*, (1997), pp. 15–35.
- [14] J. K. HALE, *Ordinary Differential Equations*, Krieger Publishing Company, 1980.
- [15] J. K. HALE AND H. KOÇAK, *Dynamics and Bifurcations*, Springer-Verlag, 1991.
- [16] E. HANON, S. HALL, G. P. TAYLOR, M. SAITO, R. DAVIS, Y. TANAK, K. USUKU, M. OSAME, J. N. WEBER, AND C. R. M. BANGHAM, *Abundant Tax protein expression in CD4⁺ T cells infected with HTLV-I is prevented by cytotoxic T lymphocytes*, *Blood*, (2000), pp. 1386–1392.
- [17] H. W. HETHCOTE, *The mathematics of infectious diseases*, *SIAM Rev.*, 42 (2000), pp. 599–653.
- [18] D. D. HO, A. U. NEUMAN, A. S. PERELSON, W. CHEN, J. LEONARD, AND M. MARKOWITZ, *Rapid turnover of plasma virions and CD4 lymphocytes in HIV-1 infection*, *Nature*, 373 (1995), pp. 123–126.
- [19] S. JACOBSON, H. SHIDA, D. E. MCFARLIN, A. S. FAUCI, AND S. KOENIG, *Circulating CD8⁺ cytotoxic T lymphocytes specific for HTLV-I pX in patients with HTLV-I associated neurological disease*, *Nature*, 348 (1990).

- [20] C. M. KRIBS-ZALETA AND M. MARTCHEVA, *Vaccination strategies and backward bifurcation in an age-since-infection structured model*, Math. Biosci., 177-178 (2002), pp. 385–424.
- [21] C. M. KRIBS-ZALETA AND J. VELASCO-HERNÁNDEZ, *A simple vaccination model with multiple endemic states*, Math. Biosci., 164 (2000), pp. 183–201.
- [22] A. MANNS, E. L. MURPHY, R. WILK, G. HAYNES, J. P. FIGUEROA, B. HANCHARD, M. BARNETT, J. DRUMMOND, D. WATERS, M. CERNEY, J. R. SEALS, S. S. ALEXANDER, H. LEE, AND W. A. BLATTNER, *Detection of early human T-cell lymphotropic virus type I antibody patterns during seroconversion among transfusion recipients*, Blood, 77 (1991), pp. 896–905.
- [23] L. M. MANSKY AND H. M. TEMIN, *Lower mutation rate of bovine leukemia virus relative to that of spleen necrosis virus*, J. Virol., 68 (1994), pp. 494–499.
- [24] M. MARTCHEVA AND H. R. THIEME, *Progression age enhanced backward bifurcation in an epidemic model with super-infection*, J. Math. Biol., 46 (2003), pp. 385–424.
- [25] G. F. MEDLEY, N. A. LINDOP, W. J. EDMUNDS, AND D. J. NOKES, *Hepatitis-B virus endemicity: heterogeneity, catastrophic dynamics and control*, Nat. Med., 7 (2001), pp. 619–624.
- [26] J. MENA-LORCA AND H. W. HETHCOTE, *Dynamic models in infectious diseases as regulators of population sizes*, J. Math. Biol., 30 (1992), pp. 693–716.
- [27] F. MORTREUX, A.-S. GABET, AND E. WATTEL, *Molecular of cellular aspects of HTLV-I-associated leukemogenesis in vivo*, Leukemia, 17 (2003), pp. 26–38.
- [28] F. MORTREUX, M. KAZANJI, A.-S. GABET, B. DE THOISY, AND E. WATTEL, *Two-step nature of human T-cell leukemia virus type 1 replication in experimentally infected squirrel monkeys (saimiri sciureus)*, J. Virol., 75 (2001), pp. 1083–1089.
- [29] P. W. NELSON, J. D. MURRAY, AND A. S. PERELSON, *A model of HIV-1 pathogenesis that includes an intracellular delay*, Math. Biosci., 163 (2000), pp. 201–215.

- [30] A. S. PERELSON, *Modeling the interaction of the immune system with HIV*, in *Mathematical and Statistical Approaches to AIDS Epidemiology*, C. Castillo-Chávez, ed., vol. 83 of *Lecture Notes in Biomathematics*, Springer-Verlag, 1989, pp. 350–370.
- [31] N. SACHSENBERG, A. S. PERELSON, S. YERLY, G. A. SCHOCKMEL, D. LEDUC, B. HIRSCHL, AND L. PERRIN, *Turnover of CD4⁺ and CD8⁺ T lymphocytes in HIV-1 infection as measured by ki-67 antigen*, *J. Exp. Med.*, 187 (1998), pp. 1295–1303.
- [32] P. VAN DEN DRIESSCHE AND J. WATMOUGH, *A simple SIS epidemic model with a backward bifurcation*, *J. Math. Biol.*, 40 (2000), pp. 525–540.
- [33] ———, *Reproduction numbers and sub-threshold endemic equilibria for compartmental models of disease transmission*, *Math. Biosci.*, 180 (2002), pp. 29–48.
- [34] L. WANG, M. Y. LI, AND D. E. KIRSCHNER, *Mathematical analysis of the global dynamics of a model for HTLV-I infection and ATL progression*, *Math. Biosci.*, 179 (2002), pp. 207–217.
- [35] E. WATTEL, M. CAVROIS, A. GESSAIN, AND S. WAIN-HOBSON, *Clonal expansion of infected cells – a way of life for HTLV-I*, *J. Acquir. Immune Defic. Syndr. Hum. Retrovirol.*, 13 (Suppl. 1) (1996), pp. 92–99.
- [36] E. WATTEL, J.-P. VARTINIAN, C. PANNETIER, AND S. WAIN-HOBSON, *Clonal expansion of human T-cell leukemia virus type I-infected cells in asymptomatic and symptomatic carriers without malignancy*, *J. Virol.*, 69 (1995), pp. 2863–2868.
- [37] D. WODARZ, M. A. NOWAK, AND C. R. M. BANGHAM, *The dynamics of HTLV-I and the CTL response*, *Immunol. Today*, 20 (1999), pp. 220–227.
- [38] Y. YAMANO, M. NAGAI, M. BRENNAN, C. A. MORA, S. S. SOLDAN, U. TOMARU, N. TAKENOCHI, S. IZUMO, M. OSAME, AND S. JACOBSON, *Correlation of human T-cell lymphotropic virus type 1 (HTLV-1) mRNA with proviral DNA load, virus-specific CD8⁺ T cells and disease severity in HTLV-1-associated myelopathy (HAM/TSP)*, *Blood*, 99 (2002), pp. 88–94.

Chapter 4

CD34 Stem Cells as a Reservoir for HTLV-I Infection

4.1. Introduction

Blood cells originate from *stem cells* (also called *hematopoietic cells* or CD34⁺ cells) in the bone marrow. Under cytokine stimulation, hematopoietic cells either renew themselves or differentiate into distinct lineages. CD34 hematopoietic cells can differentiate into lymphoid progenitors, which ultimately turn into lymphocytes, dendritic cells and natural killer cells [1, 2, 4, 10].

In vitro experiments show that CD34⁺ stem cells are susceptible to HTLV-I-infection. Furthermore, CD34⁺-infected cells preserve the proviral genome when they differentiate into mature hematopoietic lineages, e.g. lymphoid progenitors, *in vitro* and *in vivo* [9]. These experiments support the hypothesis that infected CD34⁺ cells can produce infected T cells.

The normal trafficking of T cells between the peripheral blood and bone marrow facilitates the interaction between HTLV-I-infected T cells and CD34⁺ hematopoietic cells. This interaction may lead to a viral invasion of the CD34⁺ population in the bone marrow. Moreover, *in situ* PCR analyses show that HAM/TSP patients harbour high levels of HTLV-I provirus in the bone marrow cells, even though these cells do not show any viral RNA [12, 14]. These analyses suggest that there is a latent HTLV-I infection in the bone marrow maintained by the CD34⁺ cells. Thus, it is reasonable to consider that CD34 hematopoietic cells act as a reservoir for HTLV-I infection, as suggested by Grant et al. [11].

In this Chapter, we propose and analyse a model that incorporates such a reservoir in our basic transmission model.

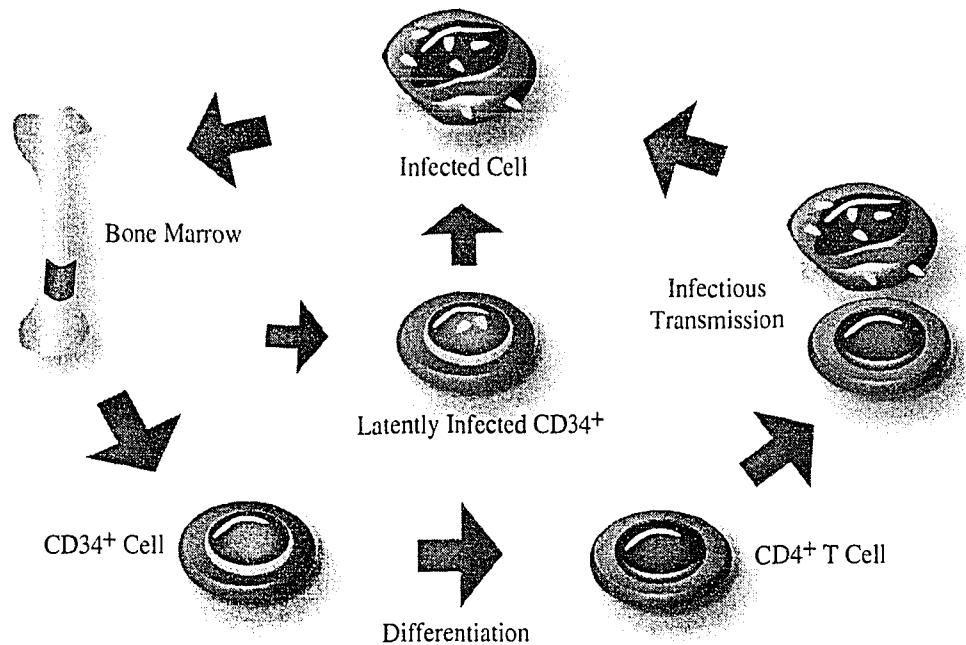


Figure 4.1. CD34⁺ act as a reservoir for HTLV-I infection.

4.2. A Mathematical Model

As in previous chapters, we partition CD34⁺- and CD4⁺-cell populations into compartments. We use the same notation for the CD4⁺ T-cell compartments; namely, x denotes the number of healthy cells and y its infected counterpart. For the CD34⁺ compartments, x_h and y_h denote the number of healthy and HTLV-I-infected hematopoietic cells, respectively. We assume that CD34⁺ cells are produced at a constant rate Λ , and newly generated cells are not infected. We consider a bilinear incidence form $\beta_1 x_h y$ for the infectious transmission among the CD34⁺-cell population, where β_1 is the transmission rate. The removal rate for hematopoietic cells is denoted by

μ_h . Since CD34⁺ differentiation depends primarily on cytokine stimulation, it is reasonable to assume that uninfected and infected CD34⁺ cells mature at the same rate b . The assumptions on CD4⁺ T-cell parameters are the same as in Chapter 2. The diagram below depicts the transmission dynamics:

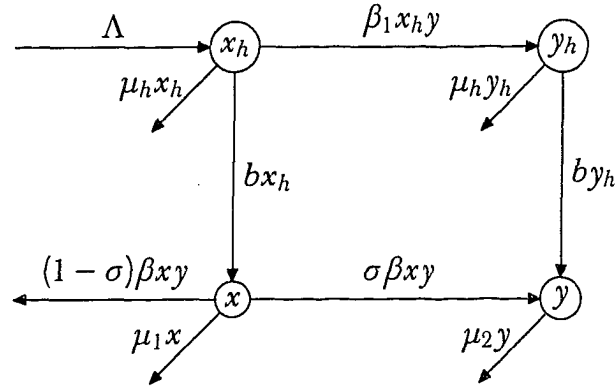


Figure 4.2. Transfer diagram.

The removal rates for uninfected and infected CD4⁺ T cells are μ_1 and μ_2 , respectively. The removal rate μ_1 is due to natural causes, viz. cell aging and positive/negative selection; whereas, μ_2 may account for elimination of HTLV-I-infected cells by the immune system. In the above model, all the parameters are positive constants.

From our assumptions and the transfer diagram, we obtain the following system of non-linear differential equations:

$$\begin{aligned}
 x'_h &= \Lambda - \beta_1 x_h y - (b + \mu_h) x_h, \\
 y'_h &= \beta_1 x_h y - (b + \mu_h) y_h, \\
 x' &= b x_h - \mu_1 x - \beta x y, \\
 y' &= b y_h + \sigma \beta x y - \mu_2 y.
 \end{aligned} \tag{4.1}$$

Adding up the first two equations in (4.1) we obtain

$$(x_h + y_h)' = \Lambda - (b + \mu_h)(x_h + y_h),$$

which implies that, for the initial condition $\xi = x_h(0) + y_h(0)$,

$$x_h(t) = \frac{\Lambda}{b + \mu_h} + \xi \exp(-(b + \mu_h)t) - y_h(t).$$

Therefore, system (4.1) can be rewritten as the following non-autonomous system of differential equations:

$$\begin{aligned} y_h'(t) &= \beta_1 \left(\frac{\Lambda}{b + \mu_h} + \xi \exp(-(b + \mu_h)t) - y_h(t) \right) y(t) - (b + \mu_h)y_h(t), \\ x'(t) &= b \left(\frac{\Lambda}{b + \mu_h} + \xi \exp(-(b + \mu_h)t) - y_h(t) \right) - \mu_1 x(t) - \beta x(t)y(t), \\ y'(t) &= b y_h(t) + \sigma \beta x(t)y(t) - \mu_2 y(t). \end{aligned} \quad (4.2)$$

System (4.2) is an asymptotically autonomous system [18, 25]. By the theory of asymptotically autonomous systems [7, 26], we know that the asymptotic behaviour of (4.2) can be obtained by studying its limiting system as $t \rightarrow \infty$.

$$\begin{aligned} y_h'(t) &= \beta_1 \left(\frac{\Lambda}{b + \mu_h} - y_h(t) \right) y(t) - (b + \mu_h)y_h(t), \\ x'(t) &= b \left(\frac{\Lambda}{b + \mu_h} - y_h(t) \right) - \mu_1 x(t) - \beta x(t)y(t), \\ y'(t) &= b y_h(t) + \sigma \beta x(t)y(t) - \mu_2 y(t). \end{aligned} \quad (4.3)$$

If we add up the last two equations of (4.3), we conclude that

$$\limsup_{t \rightarrow \infty} x(t) + y(t) \leq \frac{b\Lambda}{\bar{\mu}(b + \mu_h)},$$

where $\bar{\mu} = \min\{\mu_1, \mu_2\}$. Thus, we can define a feasible region for (4.3) as:

$$\Gamma = \left\{ (y_h, x, y) \in \mathbb{R}_+^3 : y_h \leq \frac{\Lambda}{b + \mu_h}, x \leq \frac{b\Lambda}{\mu_1(b + \mu_h)}, x + y \leq \frac{b\Lambda}{\bar{\mu}(b + \mu_h)} \right\}.$$

It can be shown that Γ is positively invariant with respect to (4.3).

HTLV-I-infected cells can arise from “maturation” of infected CD34⁺ cells or from contact between uninfected and infected CD4⁺ T cells. Accordingly, the basic reproduction number consists of two summands. The first summand, R_0^h , represents

the infectious (horizontal) transmission, and the second one, R_0^v , represents the mature (vertical) transmission:

$$R_0 = R_0^h + R_0^v = \frac{\sigma\beta x_0}{\mu_2} + \frac{\beta_1 b x_{h0}}{\mu_2(b + \mu_h)}, \quad (4.4)$$

where x_0 and x_{h0} represent the levels of CD34⁺ and CD4⁺ cells in the absence of infection. More precisely,

$$x_0 = \frac{b\Lambda}{\mu_1(b + \mu_h)} \quad \text{and} \quad x_{h0} = \frac{\Lambda}{b + \mu_h}. \quad (4.5)$$

Heuristically, we obtain R_0^h as in previous chapters: R_0^h is the product of the contact rate β , the proportion σ of CD4⁺ cells that evade the immune response, the average infectious period $1/\mu_2$ and the CD4⁺ T-cell population x_0 in the absence of infection. Likewise, R_0^v is the product of the contact rate β_1 , the mean (death-adjusted) maturation period $1/(b + \mu_h)$, the maturation rate b , the average infectious period $1/\mu_2$, and the CD34⁺-cell population in the absence of infection x_{h0} (see [13, 20, 27]).

4.3. Equilibrium Points

We will use the following technical result:

Lemma 4.1. Consider the polynomials $f(x) = ax^2 + bx + 1$, $g(x) = cx + d$, $a > 0$, $b > 0$, $d \in (0, 1)$. There is at least one positive intersection between f and g if and only if $c \geq \zeta$, where $\zeta = 2a\sqrt{\frac{1-d}{a}} + b$. When $d = 1$, there is exactly one positive intersection if and only if $c > \zeta$.

Proof. Put $c = \zeta + \varepsilon$ and $\varepsilon \geq 0$. The polynomial $f(x) - g(x) = ax^2 + (b - c)x + 1 - d$ has a discriminant:

$$(b - c)^2 - 4a(1 - d) = \left(2a\sqrt{\frac{1-d}{a}} + \varepsilon\right)^2 - 4a(1 - d) \geq 0. \quad (4.6)$$

Since $c > b$, $f(x) - g(x)$ has at least one positive root (see Figure 4.3). When $d = 1$, the inequality (4.6) is strict if and only if $\varepsilon > 0$, i.e. when $c > \zeta$. Thus, there is exactly one positive intersection if and only if $c > \zeta$. *q.e.d.*

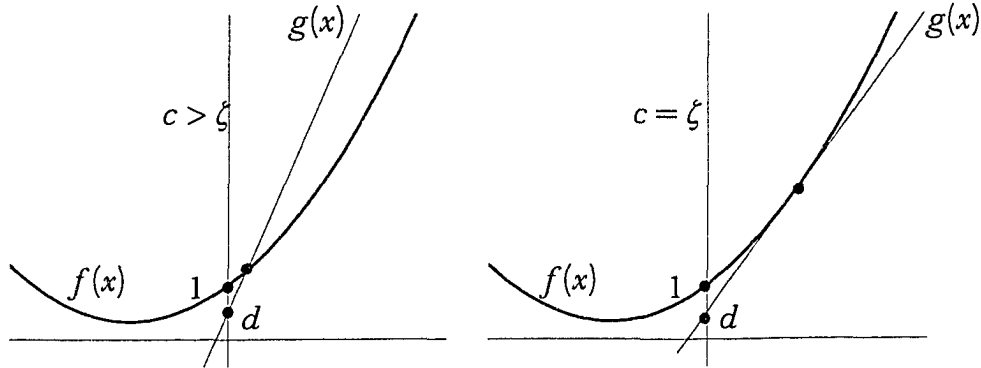


Figure 4.3. Positive roots of $f(x) - g(x)$ when $d \in (0, 1)$.

For any selection of parameters, there is the infection-free equilibrium point $P_0 = (0, x_0, 0)$. Any chronic-infection equilibrium point $P^* = (y_h^*, x^*, y^*)$ must satisfy:

$$\begin{aligned} 0 &= \beta_1 \left(\frac{\Lambda}{b + \mu_h} - y_i^*(t) \right) y^* - (b + \mu_h) y_h^*, \\ 0 &= b \left(\frac{\Lambda}{b + \mu_h} - y_i^*(t) \right) - \mu_1 x^* - \beta x^* y^*, \\ 0 &= b y_h^* + \sigma \beta x^* y^* - \mu_2 y^*, \end{aligned} \quad (4.7)$$

and $y_h > 0$, $y > 0$. From the first equation of (4.7), we have:

$$y_h^* = \frac{\beta_1 \Lambda y^*}{(b + \mu_h)(\beta_1 y^* + b + \mu_h)}. \quad (4.8)$$

Combining the second equation of (4.7) and (4.8), we get:

$$x^* = \frac{b\Lambda}{(\beta y^* + \mu_1)(\beta_1 y^* + b + \mu_h)}. \quad (4.9)$$

Finally, substituting (4.9) in the third equation of (4.7), we conclude that y^* must satisfy:

$$\sigma \beta (b + \mu_h) + \beta_1 \mu_1 + \beta_1 \beta y^* = \frac{\mu_2 (b + \mu_h)}{b\Lambda} (\beta y^* + \mu_1)(\beta_1 y^* + b + \mu_h),$$

or equivalently

$$\tilde{f}(y^*) = \tilde{g}(y^*),$$

where

$$\tilde{g}(Y) = R_0 + \frac{b\Lambda\beta\beta_1}{\mu_1\mu_2(b+\mu_h)^2}Y \quad \text{and} \quad \tilde{f}(Y) = \left(\frac{\beta}{\mu_1}Y + 1\right) \left(\frac{\beta_1}{b+\mu_h}Y + 1\right). \quad (4.10)$$

Assume $R_0 \leq 1$. Since

$$\frac{b\Lambda\beta\beta_1}{\mu_1\mu_2(b+\mu_h)^2} = \frac{\beta}{\mu_1}R_0^v \leq \frac{\beta}{\mu_1} < \frac{\beta}{\mu_1} + \frac{\beta_1}{b+\mu_h} + 2\frac{\beta\beta_1}{\mu_1(b+\mu_h)}\sqrt{\frac{(1-R_0)\mu_1(b+\mu_h)}{\beta\beta_1}},$$

in virtue of the Lemma 4.1, there are no positive roots when $R_0 \leq 1$. On the other hand, when $R_0 > 1$, we have exactly one positive root, see Figure 4.4.

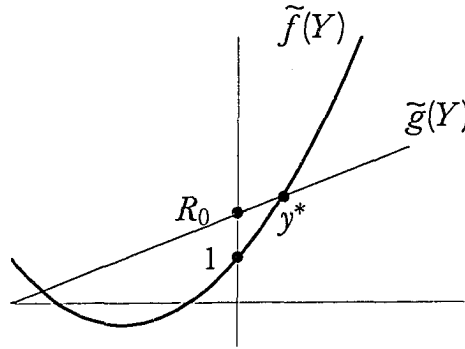


Figure 4.4. Existence of a chronic-infection equilibrium.

We have proved:

Theorem 4.2. If $R_0 \leq 1$, system (4.3) has only the infection-free equilibrium $P_0 = (0, x_0, 0)$. If $R_0 > 1$, there exists exactly one chronic-infection equilibrium $P^* = (y_h^*, x^*, y^*)$.

4.4. Global Dynamics

Theorem 4.3. If $R_0 \leq 1$, then the infection-free equilibrium P_0 is globally stable in the closed region Γ . If $R_0 > 1$, then P_0 is unstable and system (4.3) is uniformly persistent in $\overset{\circ}{\Gamma}$.

Proof. Define $L = (b + \mu_h)y + by_h$. Using the definition of Γ , when $R_0 \leq 1$, we obtain:

$$\begin{aligned} L' &= (b + \mu_h)y' + by_h' = (b + \mu_h)\mu_2 y \left(\frac{\sigma\beta x}{\mu_2} + \frac{\beta_1 b \Lambda}{\mu_2(b + \mu_h)^2} - \frac{\beta_1 b y_h}{\mu_2(b + \mu_h)} - 1 \right) \\ &= (b + \mu_h)\mu_2 y \left(\frac{\sigma\beta(x - x_0)}{\mu_2} + R_0 - 1 - \frac{\beta_1 b y_h}{\mu_2(b + \mu_h)} \right) \\ &\leq (b + \mu_h)\mu_2 y (R_0 - 1) \leq 0, \quad \text{since } x \leq x_0. \end{aligned}$$

The maximal compact invariant set in $\{(y_h, x, y) \in \Gamma : L' = 0\}$ is the singleton $\{P_0\}$, when $R_0 \leq 1$. The global stability of P_0 follows from LaSalle Invariance Principle [15]. Moreover, if $R_0 > 1$, then $L' > 0$ for those points in the interior of Γ that are close enough to P_0 . Solutions starting sufficiently close to P_0 leave a neighborhood of P_0 except those on the invariant x -axis, where solutions converge to the infection-free equilibrium point P_0 . In particular, the largest compact invariant set on the boundary of Γ is the singleton $\{P_0\}$. Uniform persistence can thus be established as in the proof of Theorem 2.2. *q.e.d.*

Theorem 4.4. Assume $R_0 > 1$ and $2\sigma\beta x_0 < \min\{\mu_1, \mu_2\}$, where x_0 is defined in (4.5). Then the unique chronic-infection equilibrium $P^* = (y_h^*, x^*, y^*)$ is globally stable in the interior of Γ .

Proof. We will apply the general method of Li and Muldowney to establish the global stability of P^* (see Appendix B). Note that uniform persistence of (4.3), together with the boundedness of solutions imply the existence of a compact absorbing set in $\overset{\circ}{\Gamma}$ (see [5]), which verifies the assumption (H₂) of Theorem 3.5 of Li and Muldowney. By Theorem 3.1, P^* is the only equilibrium point in $\overset{\circ}{\Gamma}$, therefore the assumption (H₁) is also fulfilled. We need to construct a 3×3 matrix-valued function Q , and select a suitable vector norm $|\cdot|$ in \mathbb{R}^3 so that the corresponding Lozinskiĭ measure μ in such a way that $\bar{q}_2 < 0$ (see Appendices A and B).

The Jacobian matrix of (4.3) along a solution (y_h, x, y) is:

$$J = \begin{pmatrix} -\beta_1 y - (b + \mu_h) & 0 & \beta_1 \left[\frac{\Lambda}{b + \mu_h} - y_h \right] \\ -b & -\mu_1 - \beta y & -\beta x \\ b & \sigma\beta y & \sigma\beta x - \mu_2 \end{pmatrix}.$$

Its second compound matrix, $J^{[2]}$, is given by:

$$\begin{pmatrix} j_{11} & -\beta x & -\beta_1 \left[\frac{\Lambda}{b + \mu_h} - y_h \right] \\ \sigma \beta y & j_{22} & 0 \\ -b & -b & j_{33} \end{pmatrix},$$

where

$$\begin{aligned} j_{11} &= -(b + \mu_h) - \mu_1 - (\beta + \beta_1)y, \\ j_{22} &= -(b + \mu_h) - \mu_2 - \beta_1 y + \sigma \beta x, \\ j_{33} &= -\mu_1 - \mu_2 - \beta y + \sigma \beta x. \end{aligned}$$

Set $Q = Q(y_h, x, y) = \text{diag} \left\{ 1, \sigma, \frac{y_h}{y} \right\}$. Thus,

$$Q_f Q^{-1} = \text{diag} \left\{ 0, 0, \frac{y'_h}{y_h} - \frac{y'}{y} \right\},$$

where Q_f is the matrix obtained by replacing each entry q_{ij} in Q by its directional derivative in the direction of f . Therefore, the matrix $B = Q_f Q^{-1} + Q J^{[2]} Q^{-1}$ can be written in block form as

$$\begin{pmatrix} B_{11} & B_{12} \\ B_{21} & B_{22} \end{pmatrix},$$

where

$$\begin{aligned} B_{11} &= \begin{pmatrix} -(b + \mu_h) - \mu_1 - (\beta + \beta_1)y & -\sigma \beta x \\ \beta y & -(b + \mu_h) - \mu_2 - \beta_1 y + \sigma \beta x \end{pmatrix}, \\ B_{12} &= \left(-\beta_1 \left[\frac{\Lambda}{b + \mu_h} - y_h \right] \frac{y}{y_h}, 0 \right)^T, \quad B_{21} = \left(-b \frac{y_h}{y}, \sigma b \frac{y_h}{y} \right) \text{ and } B_{22} = -\mu_1 - \\ &\mu_2 - \beta y + \sigma \beta x + \frac{y'_h}{y_h} - \frac{y'}{y}. \end{aligned}$$

Choose the vector norm in \mathbb{R}^3

$$|(x, y, z)| = \max\{|x| + |y|, |z|\},$$

and denote μ the corresponding Lozinskiĭ measure. We have the estimate [19]:

$$\mu(B) \leq \max\{g_1, g_2\}, \quad (4.11)$$

where

$$g_1 = \mu_*(B_{11}) + |B_{12}| \quad \text{and} \quad g_2 = |B_{21}| + \mu_*(B_{22}).$$

Here, $\mu_*(B_{11})$ is the Lozinskiĭ measure of the 2×2 matrix B_{11} with respect to the ℓ_1 norm in \mathbb{R}^2 , $|B_{12}|$ and $|B_{21}|$ are the operator norms of B_{12} and B_{21} when they are regarded as mappings from \mathbb{R} to \mathbb{R}^2 and from \mathbb{R}^2 to \mathbb{R} , respectively, and \mathbb{R}^2 is endowed with the ℓ_1 norm. Since B_{22} is a scalar, its Lozinskiĭ measure coincides with itself, i.e.

$$\mu_*(B_{22}) = -\mu_1 - \beta y + \sigma \beta x - \mu_2 + \frac{y'_h}{y_h} - \frac{y'}{y}.$$

Direct calculations yield

$$\mu_*(B_{11}) = -(b + \mu_h) - \beta_1 y + 2\sigma \beta x - \min\{\mu_1, \mu_2\} \quad \text{and} \quad |B_{21}| = b \frac{y_h}{y}.$$

Furthermore, since $y_h \leq \Lambda/(b + \mu_h)$,

$$|B_{12}| = \beta_1 \left[\frac{\Lambda}{b + \mu_h} - y_h \right] \frac{y}{y_h}.$$

We can rewrite the first equation of (4.3) as:

$$\frac{y'_h}{y_h} = \beta_1 \left[\frac{\Lambda}{b + \mu_h} - y_h \right] \frac{y}{y_h} - (b + \mu_h),$$

and the third equation of (4.3) as:

$$\frac{y'}{y} = \sigma \beta x - \mu_2 + b \frac{y_h}{y}.$$

If we substitute the above expression into g_1 , we obtain:

$$\begin{aligned} g_1 &= -(b + \mu_h) - \beta_1 y + 2\sigma \beta x - \min\{\mu_1, \mu_2\} + (b + \mu_h) + \frac{y'_h}{y_h} \\ &= -\beta_1 y + 2\sigma \beta x - \min\{\mu_1, \mu_2\} + \frac{y'_h}{y_h} \leq -\delta - \beta_1 y + \frac{y'_h}{y_h}, \end{aligned} \tag{4.12}$$

where $\delta = \mu_1 \min\{\mu_1, \mu_2\} - 2\sigma \beta \Lambda > 0$. On the other hand, we have:

$$g_2 = -\mu_1 - \beta y + \sigma \beta x - \mu_2 + \frac{y'_h}{y_h} - \frac{y'}{y} + b \frac{y_h}{y} = -\mu_1 - \beta y + \frac{y'_h}{y_h} \tag{4.13}$$

Relations (4.11), (4.12) and (4.13) imply

$$\mu(B) \leq \frac{y'_h}{y_h} - \delta_1,$$

where $\delta_1 = \min\{\mu_1, \delta\} > 0$. Let $K \subset \overset{\circ}{\Gamma}$ be the compact absorbing set. Then there exists $\bar{t} > 0$ such that $(y_h(0), x(0), y(0)) \in K$ implies $(y_h(t), x(t), y(t)) \in K$ for all $t > \bar{t}$. Therefore, for $t > \bar{t}$,

$$\frac{1}{t} \int_0^t \mu(B) ds \leq \frac{1}{t} \ln \frac{y_h(t)}{y_h(\bar{t})} + \frac{1}{t} \int_0^{\bar{t}} \mu(B) ds - \delta_1 \frac{t - \bar{t}}{t}$$

for all $(y_h(0), x(0), y(0)) \in K$, which implies $\bar{q}_2 \leq -\delta_1/2 < 0$, proving Theorem 4.4.

q.e.d.

In terms of our original system (4.1), we obtain the following result:

Theorem 4.5. If $R_0 \leq 1$, system (4.1) has only the infection-free equilibrium $\tilde{P}_0 = (x_{0h}, 0, x_0, 0)$ and it is globally stable in the closed region Γ . If $R_0 > 1$, there is a unique chronic-infection equilibrium $\tilde{P}^* = (x_h^*, y_h^*, x^*, y^*)$, which is globally asymptotically stable in the interior of Γ .

4.5. Numerical Simulations

In this section, we will investigate numerically the consequences of the CD34⁺-cell reservoir in HTLV-I infection. Although many parameters in the model are unknown, we will show that under reasonable assumptions, there is a slow invasion of the bone marrow by HTLV-I-infected cells and such invasion generates high levels of proviral load in the bone marrow and peripheral blood alike.

The time scale selected is days. We choose the production rate of CD34⁺ cells as $\Lambda = 25$ cells/day/mm³, which is in the same order of magnitude as the one proposed by Nelson et al. [22] for CD4⁺ T cells. Since the functional properties of infected and healthy CD4⁺ T cells are similar [6], we assume the removal rates equal i.e., $\mu_1 = \mu_2$; according to Nelson et al. [22] such a rate is 0.03 day⁻¹. Hematopoietic cells can stay

in a resting phase before proliferating [16]; thus, it is reasonable to assume that their life expectancy is longer than that of $CD4^+$ cells. We pick $\mu_h = 0.02 \text{ day}^{-1}$.

In the absence of infection, the normal $CD4^+$ T-cell count is approximately 1000 cells/mm^3 [1, 10]. Using the scaling relation proposed by Perelson [24], we estimate $\beta = 10^{-3} \text{ mm}^3/\text{cells}/\text{day}$. Viral proteins on the surface of HTLV-I-infected cells bind to the receptor GLUT-1 and initiate the infectious process [17]. Such a receptor is expressed after lymphocyte activation [23]. The lack of lymphocyte receptors in $CD34^+$ cells suggests that the infectious transmission is less effective in the $CD34^+$ cells than in the $CD4^+$ T cells. Therefore, we assume $\beta_1 = \beta/3$ in our simulations. Following the parameter values for σ in Chapter 2, we put $\sigma = 0.015$. Finally, we set the maturation rate of $CD34^+$ cells as $b = 0.2 \text{ day}^{-1}$. One can verify that the conditions for Theorem 4.4 hold, i.e. $R_0 = 1.06749$ and $\sigma\beta x_0 = 0.0113636 < 0.015 = \mu_1/2$. Figure 4.5 depicts the solution of (4.1) with initial conditions $x(0) = 1000$, $y(0) = 5$, $x_h(0) = 5$, $y_h(0) = 0$.

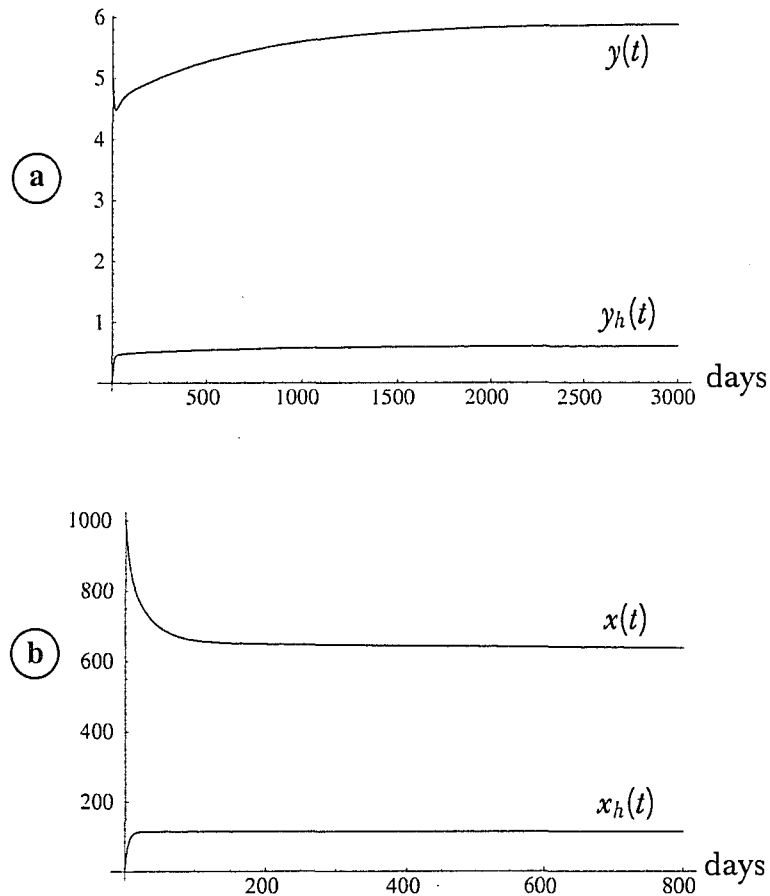


Figure 4.5. *MATHEMATICA*® simulations of system (4.1). (a) shows the count of HTLV-I-infected cells in both the peripheral blood and bone marrow. (b) shows cell counts for the healthy compartments. Parameter values are $\mu_1 = \mu_2 = 0.03$, $\mu_h = 0.02$, $\Lambda = 25$, $\beta = 0.001$, $\beta_1 = \beta/3$ and $b = 0.2$.

We proceed to analyse numerically the relevance of the $CD34^+$ reservoir to HTLV-I infection. We allow the maturation period, b , to change in a feasible range while the rest of the parameters are fixed. The mean maturation period ought to be less than the life expectancy of the $CD34^+$ cells, i.e. $1/\mu_h \geq 1/b$. Thus, with the above choice of parameters, a biologically sound interval for b is $[0.02, \infty)$. Note that when $b \rightarrow \infty$ the mean maturation period $1/b \rightarrow 0$. This extreme case implies that the reservoir is non-existent and the dynamics of (4.1) reduces to the one established in Chapter 2 (with no latency). The graph of the basic reproduction number R_0 as a

function of b is depicted in Figure 4.6. From (4.5), we obtain

$$R_0(\infty) := \lim_{b \rightarrow \infty} R_0(b) = \frac{\sigma \beta \Lambda}{\mu_1 \mu_2}.$$

$R_0(\infty)$ represents the basic reproduction number as described in Chapter 2, i.e., without production of infected cells from the bone marrow. Note that $R_0(0.2) = 1.06749 > 1 > R_0(\infty) = 0.416667$. Thus, the continuous feedback of infected $CD34^+$ cells maintain a chronic infection that otherwise would have been eliminated by the immune system.

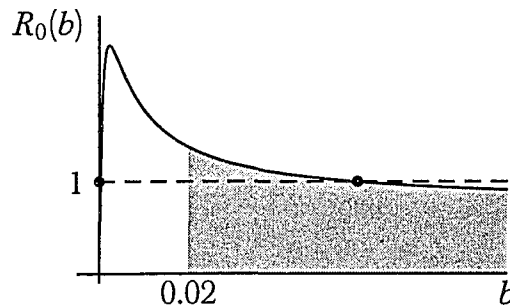


Figure 4.6. Graph of $R_0(b)$. The gray region represents the biologically admissible values for b . Other parameters are the same as for Figure 4.5.

Figures 4.7a and 4.7b depict the percentage of HTLV-I-infected cells in the peripheral blood and the bone marrow, respectively, as b varies. In particular, when $b = 0.1 \text{ day}^{-1}$, the percentage of infected cells in the bone marrow is almost linear and stabilizes after 2 or 3 years; during that time, the viral load in the $CD34^+$ population changes from 1% to 11%, whereas in the peripheral blood increases from 1% to 33%. These proviral load levels coincide with those in the literature [3, 12]. In Figure 4.8 appears the predictions hypothesized by Grant et al. [11]. Note that the long term behaviour of the proviral load coincides with our predictions.

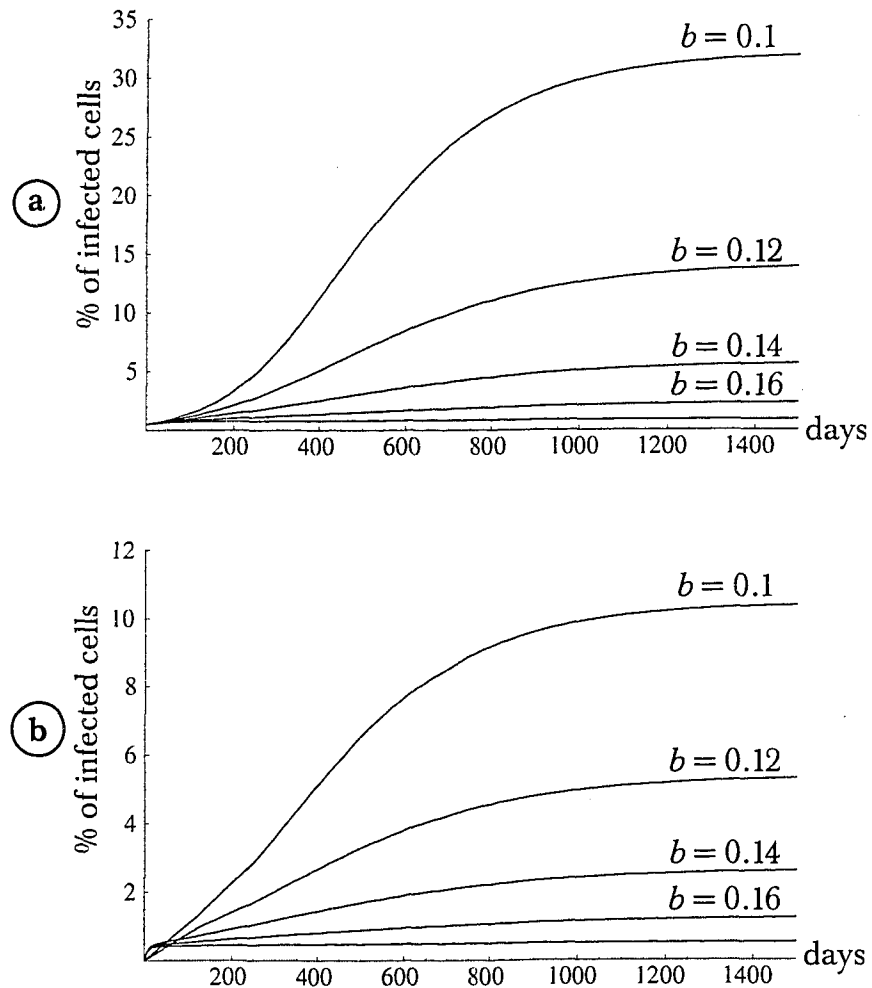


Figure 4.7. *MATHEMATICA** simulations showing the proviral invasion of peripheral blood (a), and bone marrow (b), when the mean maturation period b changes. The rest of the parameters are the same as in Figure 4.5.

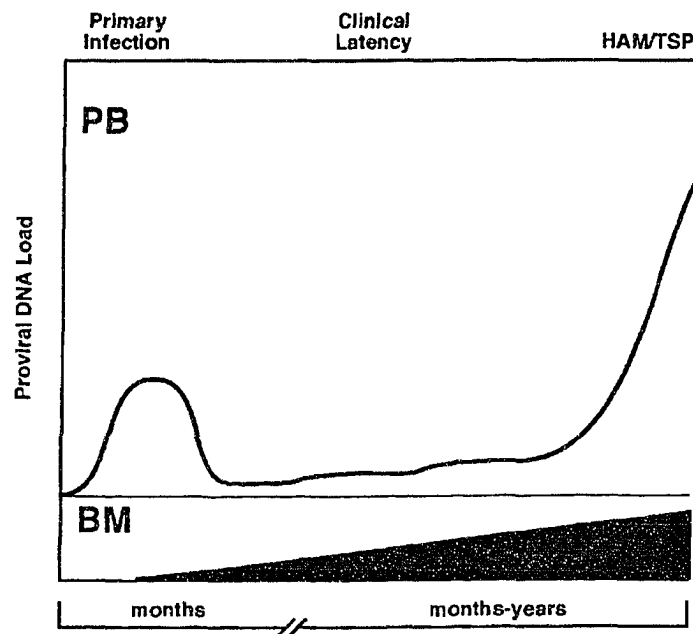


Figure 4.8. Hypothesized correlation between the peripheral blood (PB) and bone marrow (BM) proviral DNA load during HTLV-I infection. (Grant et al. [11]. Copyright ©2002 Wiley-Liss Inc. Reprinted with permission).

4.6. Conclusions

The main target of HTLV-I infection is the $CD4^+$ T-cell population. Lymphocytes routinely circulate in the lymph organs, including the bone marrow. Clinical evidence demonstrates that hematopoietic $CD34^+$ cells are susceptible to HTLV-I infection. Furthermore, HTLV-I-infected $CD34^+$ cells preserve the proviral genome after differentiation into distinct cell lineages [9, 12]. These findings suggest that $CD34^+$ hematopoietic cells may act as a reservoir for HTLV-I infection.

In this Chapter, we propose and analyse a model that considers $CD34^+$ cells as a reservoir for HTLV-I infection. In the model, $CD34^+$ cells are infected by direct contact with $CD4^+$ T cells harbouring the provirus. Therefore, we assume a bilinear incidence term $\beta_1 x_h y$, where β_1 is the infection rate. In contrast with the incidence term for $CD4^+$ T cells, this incidence term does not suffer a reduction σ by the immune system attack. This consideration is in accordance with the fact that HTLV-I-infected $CD34^+$ cells escape the immune system surveillance because of their lack of viral expression [11]. Both populations, uninfected and infected $CD34^+$ cells will mature at

the same rate, b , and will incorporate into their respective $CD4^+$ T-cell compartment. The dynamics of the model is governed by a basic reproduction number R_0 . That is, when $R_0 \leq 1$ HTLV-I infection eventually disappears, whereas when $R_0 > 1$, HTLV-I infection becomes chronic.

Our model analysis set forth the relevance of the $CD34^+$ -cell reservoir to HTLV-I infection. Not surprisingly, the inclusion of the reservoir will augment the basic reproduction number with its concomitant consequences. We simulate the model numerically under reasonable parameter values. From the simulations, we note that the proviral load can increase drastically with changes in the maturation rate. Paradoxically, such an analysis implies that the longer the $CD34^+$ keep undifferentiated, the higher the proviral load levels will be. This is because HTLV-I-infected cells in the bone marrow evade the immune system attack and maintain a constant source which populates the $CD4^+$ infected pool. From the simulations, we also obtain considerable high proviral loads in the range observed in HTLV-I-infected patients [6, 8, 21, 28].

In summary, our model and its analysis suggest that the $CD34^+$ -cell reservoir plays a relevant role in keeping high proviral loads in HTLV-I patients. It is still necessary to tune the parameters with clinical data to get a better understanding of the HTLV-I-infection dynamics.

4.7. References

- [1] A. K. ABBAS, A. H. LICHTMAN, AND J. S. POBER, *Cellular and Molecular Immunology*, W. B. Saunders Company, 4 ed., 2000.
- [2] B. ALBERTS, D. BRAY, J. LEWIS, M. RAFF, K. ROBERTS, AND J. D. WATSON, *Molecular Biology of the Cell*, Garland Publishing, 3rd. ed., 1994.
- [3] B. ASQUIT AND C. R. M. BANGHAM, *The role of cytotoxic T lymphocytes in human T-cell lymphotropic virus type 1 infection*, J. Theor. Biol., 207 (2000), pp. 65–79.
- [4] G. R. BURMESTER AND A. PEZZUTTO, *Color Atlas of Immunology*, Thieme, 2003.

- [5] G. BUTLER, H. I. FREEDMAN, AND P. WALTMAN, *Uniformly persistent systems*, Proc. Amer. Math. Soc., 96 (1986), pp. 425–430.
- [6] A. J. CANN AND I. S. Y. CHEN, *Human T-cell leukemia virus type I and II*, in Fields Virology, B. N. Fields, D. M. Knipe, and P. M. Howley, eds., Lippincott-Raven Publishers, 1996, pp. 1849–1880.
- [7] C. CASTILLO-CHÁVEZ AND H. R. THIEME, *Asymptotically autonomous epidemic models*, in Mathematical Population Dynamics: Analysis of Heterogeneity, O. Arino, D. Axelrod, M. Kimmel, and M. Langlais, eds., vol. 1, Wuerz Publishing Ltd., 1994, pp. 33–50.
- [8] K. ETOH, K. YAMAGUCHI, S. TOKUDAME, T. WATANABE, A. OKAYAMA, S. STUVER, N. MUELLER, K. TAKATSUJI, AND M. MATSUOKA, *Rapid quantification of HTLV-I provirus load: detection of monoclonal proliferation of HTLV-I-infected cells among blood donors*, Int. J. Cancer, 81 (1999), pp. 859–864.
- [9] G. FEUER, J. K. FRASER, J. A. ZACK, F. LEE, R. FEUER, AND I. S. Y. CHEN, *Human T-cell leukemia infection of human hemotopoietic progenitor cells: maintenance of virus infection during differentiation in vitro and in vivo*, J. Virol., 70 (1996), pp. 4038–4044.
- [10] R. A. GOLDSBY, T. J. KINDT, B. A. OSBORNE, AND J. KUBY, *Immunology*, W. H. Freeman and Company, 5th. ed., 2003.
- [11] C. GRANT, K. BARMAN, T. ALEFANTIS, J. YAO, S. JACOBSON, AND B. WIGDAHL, *Human T cell leukemia virus type I and neurologic disease: events in bone marrow, peripheral blood, and central nervous system during normal immune surveillance and neuroinflammation*, J. Cell. Physiol., 190 (2002), pp. 133–159.
- [12] S. JACOBSON, M. KRICHAVSKY, N. FLERLAGE, AND M. LEVIN, *Immunopathogenesis of HTLV-I associated neurologic disease: massive latent HTLV-I infection in bone marrow of HAM/TSP patients*, Leukemia, 11 (Suppl. 3) (1997), pp. 73–75.

- [13] C. M. KRIBS-ZALETA AND J. VELASCO-HERNÁNDEZ, *A simple vaccination model with multiple endemic states*, Math. Biosci., 164 (2000), pp. 183–201.
- [14] R. KUBOTA, M. OSAME, AND S. JACOBSON, *Retrovirus: Human T-cell lymphotropic virus type I-associated diseases and immune dysfunction*, in Effects of Microbes on the Immune System, M. W. Cunningham and R. S. Fujinami, eds., Lippincott Williams & Wilkins, 2000, pp. 349–371.
- [15] J. P. LASALLE, *The Stability of Dynamical Systems*, Regional Conference Series in Applied Mathematics, SIAM, 1976.
- [16] M. C. MACKEY, *Cell kinetic status of haematopoietic stem cells*, Cell Prolif., 34 (2001), pp. 71–83.
- [17] N. MANEL, F. J. KIM, S. KINET, N. TAYLOR, M. SITBON, AND J.-L. BATTINI, *The ubiquitous glucose transporter GLUT-1 is a receptor for HTLV*, Cell, 115 (2003), pp. 449–459.
- [18] L. MARKUS, *Asymptotically autonomous differential systems*, in Contributions to the Theory of Nonlinear Oscillations III, S. Lefschetz, ed., vol. 36 of Ann. Math. Stud., Princeton University Press, 1956, pp. 17–29.
- [19] R. H. MARTIN JR., *Logarithmic norms and projections applied to linear differential systems*, J. Math. Anal. Appl., 45 (1974), pp. 432–454.
- [20] J. MENA-LORCA AND H. W. HETHCOTE, *Dynamic models in infectious diseases as regulators of population sizes*, J. Math. Biol., 30 (1992), pp. 693–716.
- [21] F. MORTREUX, A.-S. GABET, AND E. WATTEL, *Molecular of cellular aspects of HTLV-I-associated leukemogenesis in vivo*, Leukemia, 17 (2003), pp. 26–38.
- [22] P. W. NELSON, J. D. MURRAY, AND A. S. PERELSON, *A model of HIV-1 pathogenesis that includes an intracellular delay*, Math. Biosci., 163 (2000), pp. 201–215.

- [23] J. OVERBAUGH, *HTLV-I sweet-talks its way into cells*, Nat. Med., 10 (2004), pp. 20–21.
- [24] A. S. PERELSON, *Modeling the interaction of the immune system with HIV*, in Mathematical and Statistical Approaches to AIDS Epidemiology, C. Castillo-Chávez, ed., vol. 83 of Lecture Notes in Biomathematics, Springer-Verlag, 1989, pp. 350–370.
- [25] H. R. THIEME, *Convergence results and a Poincaré-Bendixson trichotomy for asymptotically autonomous differential equations*, J. Math. Biol., 30 (1992), pp. 755–763.
- [26] ———, *Asymptotically autonomous differential equations in the plane*, Rocky Mountain J. Math., 24 (1994), pp. 351–380.
- [27] P. VAN DEN DRIESSCHE AND J. WATMOUGH, *Reproduction numbers and sub-threshold endemic equilibria for compartmental models of disease transmission*, Math. Biosci., 180 (2002), pp. 29–48.
- [28] E. WATTEL, J.-P. VARTINIAN, C. PANNETIER, AND S. WAIN-HOBSON, *Clonal expansion of human T-cell leukemia virus type I-infected cells in asymptomatic and symptomatic carriers without malignancy*, J. Virol., 69 (1995), pp. 2863–2868.

Chapter 5

Cytotoxic Response to HTLV-I Infection

5.1. Introduction

Cytotoxic T lymphocytes (CTLs), which normally have the CD8⁺ marker, are the most important effector agents of the immune system. When a CTL recognizes viral peptides on an infected cell, it secretes proteins which either limit the replication of the virus or drive the infected cell to apoptosis. In addition to the cytotoxic function, CTLs produce cytokines such as Interferon- γ (IFN- γ), and Tumour Necrosis Factor (TNF- α). IFN- γ activates macrophages and promotes adhesion of T cells to vascular endothelium, whereas TNF- α recruits neutrophils, induces inflammatory response and promotes the adhesion of leukocytes to endothelial cells [1, 7].

HTLV-I-infected patients harbour different levels of CD8⁺ CTLs in the peripheral blood. Namely, ATL patients show almost negligible levels of anti-HTLV-I CTLs, whereas asymptomatic carriers exhibit high concentrations of CD8⁺ T cells [2, 15]. Furthermore, HAM/TSP patients show extraordinarily high levels of CD8⁺ CTL in the peripheral blood and even HTLV-I-specific CTLs have been detected in the cerebrospinal fluid [14, 18, 21].

CTLs target Tax 11-19 proteins expressed in HTLV-I-infected cells [25, 30]. Clinical evidence suggests that there is a correlation between the HTLV-I proviral load and the frequency of HTLV-I Tax-specific CTLs in HAM/TSP patients [18, 30]. Furthermore, it has been noticed that Tax plays an important role in ATL by accelerating cell growth and inhibiting apoptosis of HTLV-I-infected cells [28]. Therefore, CTL-driven elimination of Tax-expressing CD4⁺ cells may imprint in HTLV-I-related aetiology.

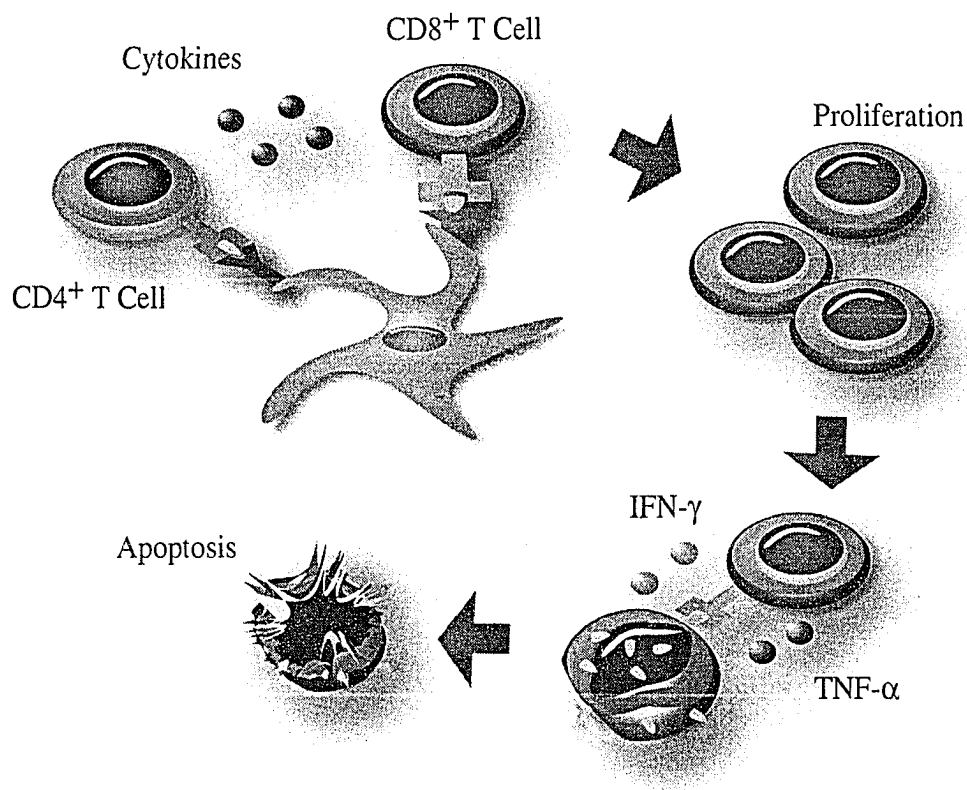


Figure 5.1. CD8⁺ T-cell response in brief.

Interestingly, an elevated CTL level induces cytokine overproduction in the blood stream that may facilitate the migration of T cells across the blood-brain barrier [11]. Once in the central nervous system, HTLV-I-infected CD4⁺ T cells induce CD8⁺ T cell attack with the concomitant production of inflammatory cytokines such as IFN- γ and TNF- α . These cytokines degenerate neurons causing axonal degradation and demyelination [4, 12]. It is still unclear whether the CTL invasion in the central nervous system causes HAM/TSP or vice versa. Bangham and colleagues hypothesize that a strong CTL response reduces proviral load and protects against HAM/TSP [4, 13].

Given the relevance of the CD8⁺ T cells in the development of HTLV-I infection and related diseases, we analyse a model that explicitly incorporates the cytotoxic response in the basic transmission model (see Chapter 2).

5.2. A Mathematical Model

As in the previous chapters, we partition T-cell population into compartments. We use the same notation for CD4⁺ T-cell compartments; namely, x denotes the number of healthy cells and y its infected counterpart. We add an extra compartment, z , that denotes the number of HTLV-I-specific CD8⁺ T cells. Because of the cytotoxic actions of CD8⁺ T cells, we consider a CTL-driven elimination of infected CD4⁺ cells of the form γyz , where γ is the rate of CTL-mediated lysis; such a rate accounts for the overall effects of HTLV-I-infected cell elimination viz. contact frequency and efficiency of pore-forming proteins released by CD8⁺ cells. Anti-HTLV-I CTLs may reduce the proviral load, but this reduction would imply less stimulation for CTL proliferation. Therefore, it is reasonable to consider that CD8⁺ T-cell proliferation is density-dependent [23]. Following Wodarz et al. [29], we assume a CTL proliferation of the form $\nu yz/(z + 1)$, where ν denotes the cytotoxic responsiveness. The CTL responsiveness depends on the contact frequency and attachment effectivity between T-cell receptors and MHC-I molecules. Figure 5.2 illustrates the transmission dynamics.

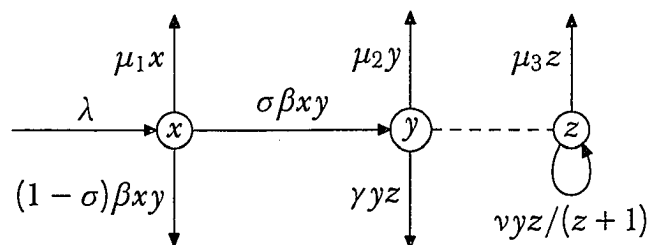


Figure 5.2. Transfer diagram.

The removal rates of uninfected and infected CD4⁺ T cells are μ_1 and μ_2 . The removal rate μ_1 is due to natural causes. Since the model incorporates explicitly humoral and adaptive immune responses, μ_2 represents the removal rate attributable to natural causes, e.g. cell aging, positive/negative selection. The corresponding removal rate for HTLV-I-specific CD8⁺ T cells is μ_3 .

Based on our assumptions and the transfer diagram, we obtain the following system of differential equations:

$$\begin{aligned}x' &= \lambda - \mu_1 x - \beta xy, \\y' &= \sigma \beta xy - \mu_2 y - \gamma yz, \\z' &= v \frac{yz}{z+1} - \mu_3 z.\end{aligned}\tag{5.1}$$

Adding up the above three equations, we obtain:

$$(x + y + z)' \leq \lambda - \mu_1 x - \mu_2 y - \gamma yz + v \frac{yz}{z+1} - \mu_3 z \leq \lambda - \bar{\mu}(x + y + z),$$

when

$$\gamma \geq v,\tag{5.2}$$

and $\bar{\mu} = \min\{\mu_1, \mu_2, \mu_3\}$. Condition (5.2) is likely to be true for biological systems because of the effectiveness of the cytokines released by the CD8⁺ T cells [1, 9]. It follows that $\limsup_{t \rightarrow \infty} x(t) \leq \lambda/\mu_1$ and

$$\limsup_{t \rightarrow \infty} (x(t) + y(t) + z(t)) \leq \frac{\lambda}{\bar{\mu}}.$$

Thus, we will consider the dynamics of our system in the following region:

$$\Gamma = \left\{ (x, y, z) \in \mathbb{R}_+^3 : x \leq \frac{\lambda}{\mu_1}, x + y + z \leq \frac{\lambda}{\bar{\mu}} \right\}.$$

The region Γ is positively invariant and thus, the model is well posed.

The *basic reproduction number* R_0 in the absence of CTL response is given by

$$R_0 = \frac{\sigma \beta \lambda}{\mu_1 \mu_2}.\tag{5.3}$$

Note that the previous expression coincides with the basic reproduction number defined in Chapter 2—without considering latency in the CD4⁺ cells. The parameter

$$R_1 = \frac{\sigma \beta \lambda v}{\mu_2(\mu_1 v + \beta \mu_3)}\tag{5.4},$$

is the *basic reproduction number in the presence of CTL response* plays an essential role in the dynamics of (5.1)(see [24]).

Theorem 5.1. If $R_0 \leq 1$, the only equilibrium point is the infection-free equilibrium $P_0 = (\lambda/\mu_1, 0, 0)$. If $R_1 \leq 1 < R_0$, there is a chronic-infection equilibrium point $P_1 = (\bar{x}, \bar{y}, 0)$ with $\bar{y} > 0$. If $R_1 > 1$, there is another chronic-infection equilibrium point $P_2 = (x^*, y^*, z^*)$ with $y^* > 0$ and $z^* > 0$.

Proof. The infection-free equilibrium $P_0 = (\lambda/\mu_1, 0, 0)$ exists for all the parameters. Let $P = (\bar{x}, \bar{y}, 0)$ be a chronic-infection equilibrium point, i.e. $\bar{y} > 0$. We obtain the following relations:

$$\begin{aligned}\bar{x} &= \frac{\mu_2}{\sigma\beta} = \frac{\lambda}{\mu_1 R_0}, \\ \bar{y} &= \frac{\mu_1(R_0 - 1)}{\beta}.\end{aligned}\tag{5.5}$$

Suppose that a chronic-infection equilibrium point (x^*, y^*, z^*) exists with $z^* > 0$. Such a point must satisfy:

$$\begin{aligned}0 &= \lambda - \mu_1 x^* - \beta x^* y^*, \\ 0 &= \sigma\beta x^* y^* - \mu_2 y^* - \gamma y^* z^*, \\ 0 &= \nu \frac{y^* z^*}{z^* + 1} - \mu_3 z^*.\end{aligned}\tag{5.6}$$

From the second and third expressions of (5.6) we have:

$$x^* = \frac{\gamma z^* + \mu_2}{\sigma\beta} \geq \frac{\mu_2}{\sigma\beta} = \frac{\lambda}{\mu_1 R_0} \quad \text{and} \quad y^* = \frac{\mu_3(z^* + 1)}{\nu}.\tag{5.7}$$

From the first expression of (5.6) and (5.7), we obtain that z^* should be a non-negative root of the quadratic polynomial:

$$\begin{aligned}g(z) &= \lambda - \frac{\mu_1\mu_2}{\sigma\beta} - \frac{\mu_2\mu_3}{\sigma\nu} - z \left(\frac{\mu_1\gamma}{\sigma\beta} + \frac{\mu_3(\mu_2 + \gamma)}{\sigma\nu} \right) - z^2 \left(\frac{\mu_3\gamma}{\sigma\nu} \right) \\ &= \zeta \left[R_1 - 1 - z \left(\frac{\gamma}{\mu_2} + \frac{\beta\mu_3}{\mu_1\nu + \beta\mu_3} \right) - z^2 \left(\frac{\gamma\beta\mu_3}{\mu_2(\mu_1\nu + \beta\mu_3)} \right) \right],\end{aligned}$$

where

$$\zeta = \frac{\mu_2(\mu_1\nu + \beta\mu_3)}{\sigma\beta\nu}.$$

The graph of g is concave down, also $g'(0) < 0$. These conditions imply that there is exactly one positive root of g if and only if $R_1 > 1$ (see Figure 5.3). *q.e.d.*

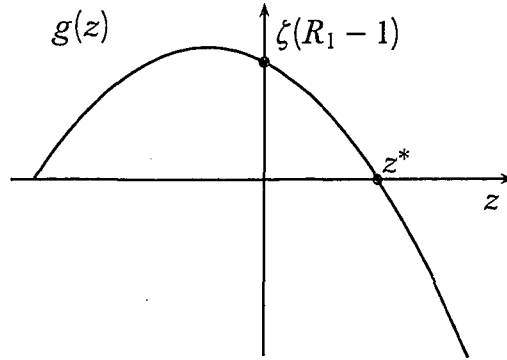


Figure 5.3. Uniqueness of the chronic-infection equilibrium.

5.3. Local Stability Analysis of the Equilibria

Theorem 5.2. When $R_0 < 1$, the infection-free equilibrium point is locally asymptotically stable, whereas when $R_0 > 1$ it is unstable.

Proof. The Jacobian matrix at the infection-free equilibrium point is given by:

$$J(P_0) = \begin{pmatrix} -\mu_1 & -\beta\lambda/\mu_1 & 0 \\ 0 & (R_0 - 1)/\mu_2 & 0 \\ 0 & 0 & -\mu_3 \end{pmatrix}.$$

The conclusion follows from the definition of R_0 . *q.e.d.*

Theorem 5.3. When $R_1 < 1 < R_0$, the chronic-infection equilibrium point P_1 is locally stable, whereas when $R_1 > 1$ it is locally unstable, and P_2 is locally stable.

Proof. Suppose $R_1 < 1 < R_0$. The Jacobian matrix at $P_1 = (\bar{x}, \bar{y}, 0)$ is given by

$$\begin{aligned} J(P_1) &= \begin{pmatrix} -\mu_1 - \beta\bar{y} & -\beta\bar{x} & 0 \\ \sigma\beta\bar{y} & \sigma\beta\bar{x} - \mu_2 & -\gamma\bar{y} \\ 0 & 0 & v\bar{y} - \mu_3 \end{pmatrix} \\ &= \begin{pmatrix} -\mu_1 R_0 & -\frac{\beta\lambda}{\mu_1 R_0} & 0 \\ \sigma\mu_1(R_0 - 1) & 0 & -\frac{\gamma\mu_1(R_0 - 1)}{\beta} \\ 0 & 0 & \frac{\mu_1 v + \beta\mu_3}{\beta}(R_1 - 1) \end{pmatrix}. \end{aligned}$$

Our hypothesis together with

$$\text{Det}J(P_1) = \frac{\sigma\lambda(\mu_1\nu + \beta\mu_3)(R_0 - 1)(R_1 - 1)}{R_0}, \text{ and } c_2 = \frac{\sigma\beta\lambda(R_0 - 1)}{R_0},$$

show that conditions (i)-(iii) of the Routh-Hurwitz criterion hold (see Section 3.3).

Finally, assume that $R_1 > 1$. At the chronic-infection equilibrium P_2 , the Jacobian matrix is given by:

$$J(P_2) = \begin{pmatrix} -\mu_1 - \beta y^* & -\beta x^* & 0 \\ \sigma\beta y^* & 0 & -\gamma y^* \\ 0 & \nu \frac{z^*}{z^* + 1} & -\nu \frac{y^* z^*}{(z^* + 1)^2} \end{pmatrix}.$$

From the above expression we obtain

$$\text{Det}J(P_2) = -\frac{\sigma\nu\beta^2 x^* y^{*2} z^*}{(z^* + 1)^2} - \frac{\nu\gamma(\mu_1 + \beta y^*) y^* z^*}{z^* + 1} < 0,$$

and

$$c_2 = \sigma\beta^2 x^* y^* + \frac{\nu(\mu_1 + \beta y^*) y^* z^*}{(z^* + 1)^2} + \frac{\nu\gamma y^* z^*}{z^* + 1}.$$

Thus, we have:

$$\begin{aligned} \left(\mu_1 + \beta y^* + \frac{\nu y^* z^*}{(z^* + 1)^2} \right) \left(\sigma\beta^2 x^* y^* + \frac{\nu(\mu_1 + \beta y^*) y^* z^*}{(z^* + 1)^2} + \frac{\nu\gamma y^* z^*}{z^* + 1} \right) \\ > \frac{\sigma\nu\beta^2 x^* y^{*2} z^*}{(z^* + 1)^2} + \frac{\nu\gamma(\mu_1 + \beta y^*) y^* z^*}{z^* + 1}, \end{aligned}$$

which proves the conditions (i)-(iii) of the Routh-Hurwitz criterion. Therefore, the chronic-infection point P_2 is locally asymptotically stable when it exists. *q.e.d.*

5.4. Global Dynamics

Theorem 5.4. If $R_0 \leq 1$, then the infection-free equilibrium point P_0 is globally stable in the closed region Γ .

Proof. Consider the Lyapunov function $L = y$. We have:

$$L' = y' = \sigma\beta xy - \mu_2 y - \gamma yz \leq y(\sigma\beta x - \mu_2) \leq \mu_2 y \left(\frac{\sigma\beta x}{\mu_2} - 1 \right) \leq \mu_2 y(R_0 - 1) \leq 0.$$

The maximal compact invariant set in $\{(x, y, z) \in \Gamma : L' = 0\}$ is the singleton $\{P_0\}$ when $R_0 \leq 1$. The global stability of P_0 follows from the LaSalle Invariance Principle [19]. *q.e.d.*

Theorem 4.5. If $R_1 < 1 < R_0$, the equilibrium point $P_1 = (\bar{x}, \bar{y}, 0)$ is globally stable in the closed region Γ .

Proof. We define a Lyapunov function (see [8, 16, 17])

$$V = V(x, y, z) = x - \bar{x} \ln x + \frac{1}{\sigma}(y - \bar{y} \ln y) + \frac{\gamma z}{\sigma v}.$$

It can be verified that V is well defined x and y positive. Moreover, V has a global minimum at the equilibrium point P_1 . Using the relations (5.5), we obtain:

$$\begin{aligned} \frac{dV}{dt} &= x' \left(1 - \frac{\bar{x}}{x}\right) + \frac{y'}{\sigma} \left(1 - \frac{\bar{y}}{y}\right) + \frac{\gamma z'}{\sigma v} \\ &= (\lambda - \mu_1 x - \beta x y) + \left(\beta x y - \frac{\mu_2}{\sigma} y - \frac{\gamma}{\sigma} y z\right) - \left(\lambda \frac{\bar{x}}{x} - \mu_1 \bar{x} - \beta \bar{x} y\right) \\ &\quad - \left(\beta x \bar{y} - \frac{\mu_2}{\sigma} \bar{y} - \frac{\gamma}{\sigma} \bar{y} z\right) + \frac{\gamma}{\sigma} \frac{y z}{z+1} - \frac{\gamma \mu_3}{\sigma v} z. \end{aligned}$$

From the first equation of (5.1), it follows that $\lambda = \mu_1 \bar{x} + \beta \bar{x} \bar{y}$. Therefore,

$$\begin{aligned} \frac{dV}{dt} &= (\mu_1 \bar{x} + \beta \bar{x} \bar{y} - \mu_1 x) - \left(\frac{\mu_2}{\sigma} y + \frac{\gamma}{\sigma} y z\right) - \left(\mu_1 \frac{\bar{x}^2}{x} + \frac{\beta \bar{x}^2 \bar{y}}{x} - \mu_1 \bar{x} - \beta \bar{x} y\right) \\ &\quad - \left(\beta x \bar{y} - \frac{\mu_2}{\sigma} \bar{y} - \frac{\gamma}{\sigma} \bar{y} z\right) + \frac{\gamma}{\sigma} \frac{y z}{z+1} - \frac{\gamma \mu_3}{\sigma v} z \\ &= \mu_1 \bar{x} \left(2 - \frac{\bar{x}}{x} - \frac{x}{\bar{x}}\right) + \beta \bar{x} \bar{y} - \frac{\beta \bar{x}^2 \bar{y}}{x} + \beta \bar{x} y - \beta x \bar{y} + \frac{\mu_2}{\sigma} (\bar{y} - y) \\ &\quad + \frac{\gamma}{\sigma} \frac{y z}{z+1} - \frac{\gamma}{\sigma} y z + \frac{\gamma}{\sigma} \bar{y} z - \frac{\gamma \mu_3}{\sigma v} z. \end{aligned}$$

Since $\sigma \beta \bar{x} = \mu_2$, we have

$$\frac{dV}{dt} = (\mu_1 \bar{x} + \beta \bar{x} \bar{y}) \left(2 - \frac{\bar{x}}{x} - \frac{x}{\bar{x}}\right) + \frac{\gamma}{\sigma} z \left(\bar{y} - \frac{\mu_3}{v}\right) - \frac{\gamma y z^2}{\sigma(z+1)}.$$

From the second equation of (5.5) and the definition of R_1 , we obtain

$$\frac{dV}{dt} = (\mu_1 \bar{x} + \beta \bar{x} \bar{y}) \left(2 - \frac{\bar{x}}{x} - \frac{x}{\bar{x}} \right) + \frac{\gamma(\mu_1 \nu + \mu_3 \beta)}{\sigma \beta \nu} (R_1 - 1) z - \frac{\gamma y z^2}{\sigma(z+1)} \leq 0.$$

For the last step, we use the geometric- and arithmetic-mean inequality. *q.e.d.*

Theorem 5.6. If $R_1 > 1$, the equilibrium point (x^*, y^*, z^*) is globally stable in the closed region Γ .

Proof. Consider the Lyapunov function

$$V(x, y, z) = (x - x^* \ln x) + \frac{1}{\sigma} (y - y^* \ln y) + \frac{\gamma(z^* + 1)}{\sigma \nu} (z - z^* \ln z).$$

We obtain

$$\begin{aligned} \frac{dV}{dt} &= x' \left(1 - \frac{x^*}{x} \right) + \frac{y'}{\sigma} \left(1 - \frac{y^*}{y} \right) + \frac{\gamma(z^* + 1)}{\sigma \nu} z' \left(1 - \frac{z^*}{z} \right) \\ &= (\lambda - \mu_1 x - \beta x y) + \left(\beta x y - \frac{\mu_2}{\sigma} y - \frac{\gamma}{\sigma} y z \right) \\ &\quad + \left(\frac{\gamma(z^* + 1)}{\sigma} \frac{y z}{z+1} - \frac{\gamma(z^* + 1) \mu_3}{\sigma \nu} z \right) - \left(\lambda \frac{x^*}{x} - \mu_1 x^* - \beta x^* y \right) \\ &\quad - \left(\beta x y^* - \frac{\mu_2}{\sigma} y^* - \frac{\gamma}{\sigma} y^* z \right) - \left(\frac{\gamma(z^* + 1)}{\sigma} \frac{y z^*}{z+1} - \frac{\gamma(z^* + 1) \mu_3}{\sigma \nu} z^* \right). \end{aligned}$$

Using $\lambda = \mu_1 x^* + \beta x^* y^*$, we get

$$\begin{aligned} \frac{dV}{dt} &= (\beta x^* y^* + \mu_1 x^* - \mu_1 x) - \left(\frac{\mu_2}{\sigma} y + \frac{\gamma}{\sigma} y z \right) + \left(\frac{\gamma(z^* + 1)}{\sigma} \frac{y z}{z+1} - \frac{\gamma(z^* + 1) \mu_3}{\sigma \nu} z \right) \\ &\quad - \left(\beta \frac{x^{*2} y^*}{x} + \mu_1 \frac{x^{*2}}{x} - \mu_1 x^* - \beta x^* y \right) - \left(\beta x y^* - \frac{\mu_2}{\sigma} y^* - \frac{\gamma}{\sigma} y^* z \right) \\ &\quad - \left(\frac{\gamma(z^* + 1)}{\sigma} \frac{y z^*}{z+1} - \frac{\gamma(z^* + 1) \mu_3}{\sigma \nu} z^* \right) \\ &= \mu_1 x^* \left(2 - \frac{x^*}{x} - \frac{x}{x^*} \right) + \beta x^* y^* - \beta \frac{x^{*2} y^*}{x} + \beta x^* y - \beta x y^* + \frac{\mu_2}{\sigma} (y^* - y) \\ &\quad + \frac{\gamma}{\sigma} (y^* z - y z) + \left(\frac{\gamma(z^* + 1)}{\sigma} \frac{y z}{z+1} - \frac{\gamma(z^* + 1) \mu_3}{\sigma \nu} z \right) \\ &\quad - \left(\frac{\gamma(z^* + 1)}{\sigma} \frac{y z^*}{z+1} - \frac{\gamma(z^* + 1) \mu_3}{\sigma \nu} z^* \right). \end{aligned}$$

From the second equation of (5.6) we get

$$\begin{aligned}
 \frac{dV}{dt} &= \mu_1 x^* \left(2 - \frac{x^*}{x} - \frac{x}{x^*} \right) + \beta x^* y^* - \beta \frac{x^{*2} y^*}{x} + \beta x^* y - \beta x y^* \\
 &\quad + \left(\beta x^* - \frac{\gamma}{\sigma} z^* \right) (y^* - y) + \frac{\gamma}{\sigma} (y^* z - y z) + \left(\frac{\gamma(z^* + 1)}{\sigma} \frac{y z}{z + 1} - \frac{\gamma}{\sigma} y^* z \right) \\
 &\quad - \left(\frac{\gamma(z^* + 1)}{\sigma} \frac{y z^*}{z + 1} - \frac{\gamma}{\sigma} y^* z^* \right) \\
 &= (\mu_1 x^* + \beta x^* y^*) \left(2 - \frac{x^*}{x} - \frac{x}{x^*} \right) + \frac{\gamma}{\sigma} (y z^* - y z) \left(1 - \frac{z^* + 1}{z + 1} \right) \\
 &= (\mu_1 x^* + \beta x^* y^*) \left(2 - \frac{x^*}{x} - \frac{x}{x^*} \right) - \frac{\gamma}{\sigma} \frac{y}{z + 1} (z - z^*)^2 \leq 0
 \end{aligned}$$

This proves the global stability of P_2 when $R_1 > 1$.

q.e.d.

5.5. Relevance of CTL-related Parameters to HTLV-I Infection

Based on our model (5.1), we will analyse the relevance of CTL-related parameters to HTLV-I infection. For instance, we will prove that changes in CTL responsiveness affect the basic reproductive number R_1 , and the CD8⁺ CTL equilibrium levels. *MATHEMATICA*^{*} simulations show fluctuations in the proviral load when the rate of lyse changes. These observations outline the importance of CD8⁺ CTL response in HTLV-I-infection process.

Recall that the basic reproduction number in the absence of CTL response, R_0 , determines whether HTLV-I-infected cells establish a chronic infection or not. Thus, a reasonable control strategy should consider a reduction of R_0 below 1 (e.g. a reduction in the ratio β/μ_2). Macchi et al. [20] have shown that the reverse-transcriptase inhibitor zidovudine (AZT) inhibits transmission of HTLV-I to PBMCs, i.e. reduces β/μ_2 . Therefore, R_0 can be reduced with help of reverse-transcriptase inhibitors.

On the other hand, the basic reproduction number in the presence of CTL response, R_1 , determines whether the anti-HTLV-I CTL response is established or not. When $R_1 < 1$, CD8⁺ T-cell levels eventually vanish and the proviral load reaches a

steady state. Even though the infected cells are not cleared out, the low level of CD8⁺ T cells may imply equally low levels of cytotoxicity in the peripheral blood. Thus, we hypothesize that asymptomatic carriers are more likely to have $R_1 < 1$. In contrast, the high level of CD8⁺ in HAM/TSP patients suggests that R_1 should be bigger than 1 for most of them. Moreover, when $R_1 > 1$, we write the relation (5.7) as

$$y^* = \frac{1}{k}(z^* + 1), \quad (5.8)$$

where $k = \frac{\nu}{\mu_3}$. This condition corroborates the positive correlation between the proviral load and the CD8⁺ T-cell level claimed by Nagai et al. [21]. Furthermore, condition (5.8) also implies that an impaired CD8⁺ responsiveness, i.e. $\nu \ll \mu_3$, can generate high proviral loads. Also note that

$$R_1 = R_0 \left(\frac{h}{h+k} \right),$$

where $h = \frac{\beta}{\mu_1}$. Thus, when the CTL responsiveness augments, R_1 decreases and so does the CD8⁺ CTL level; consequently, the chances of developing HAM/TSP are lessened.

When $R_1 > 1$, the comparison between the equilibrium level y^* and \bar{y} is cumbersome. However, under certain conditions, we will show that $y^* < \bar{y}$. Thus, as suggested by Bangham and colleagues [4, 29], CD8⁺ CTL response plays a protective role in HTLV-I infection.

Corollary 5.7. Assume $R_1 > 1$ and $\mu_2 = \gamma$. Furthermore, suppose that the equilibrium level $z^* \geq 1$. Then $y^* < \bar{y}$.

Proof. Define h and k as before. The value of z^* is given by

$$\begin{aligned} z^* &= \frac{\sqrt{\left(1 + \frac{h}{h+k}\right)^2 + 4(R_1 - 1)\left(\frac{h}{h+k}\right)} - \left(1 + \frac{h}{h+k}\right)}{\frac{2h}{h+k}} \\ &< \frac{\sqrt{\left(R_0 \frac{k}{h+k} - 1\right)\left(\frac{h}{h+k}\right)}}{\frac{h}{h+k}} = \sqrt{\frac{k}{h}(R_0 - 1) - 1} = \sqrt{k\bar{y} - 1}. \end{aligned}$$

Since $z^* = ky^* - 1 \geq 1$, the above inequality yields $y^* < \bar{y}$. *q.e.d.*

For our numerical simulations, we select the time scale as days. We choose a production rate $\lambda = 20$ cells/mm³/day, which is similar to the value selected in previous chapters. Also, we assume that the removal rates of infected and uninfected CD4⁺ T cells are equal i.e., $\mu_1 = \mu_2$, and we select such a rate as 0.015 day⁻¹; this rate is in the same order of magnitude to the value given by Nelson et al. [22]. We also assume the death rate for HTLV-I-specific CD8⁺ cells equal to the CD4⁺ i.e., $\mu_3 = \mu_1$. The average CD4⁺ T-cell count in a healthy adult is approximately 1000 cells/mm³. Using Perelson's scaling relation [26], we assume $\beta = 10^{-3}$ mm³/cell/day. In accordance with our analysis in Chapter 2, we assume that a small fraction $\sigma (=0.05)$ of HTLV-I-infected cells are able to clonally expand and proliferate.

In Figures 5.4-5.7, we select the clearance rate, γ , of infected CD4⁺ T cells by CD8⁺ CTLs as $\gamma = 0.2$ mm³/cell/day. We change the responsiveness ν between 0.0001 and 0.0081 mm³/cell/day. Note that these values agree with the condition (5.2). Figure 5.4 shows the changes in the number of CD4⁺ T cells as ν varies. When R_1 is below 1, the level of CD4⁺ T cells approaches to one third of the normal CD4⁺ T-cell count. In contrast, when $R_1 > 1$ the equilibrium level is attained by damped oscillations approaching to normal CD4⁺ T-cell counts.

Figures 5.5 and 5.6 depict the changes in the proviral load and CTL level as ν varies. When the CTL response is not established, i.e. $R_1 < 1$, CD8⁺ T cells eventually disappear and proviral level augments reaching its equilibrium level. On the other hand, when $R_1 > 1$ the proviral load reduces significantly and CD8⁺ CTLs persist at the equilibrium level. Note that the CD8⁺ T-cell equilibrium level also reduces as the responsiveness augments. This means that high proviral levels stimulate anti-HTLV-I CTL proliferation.

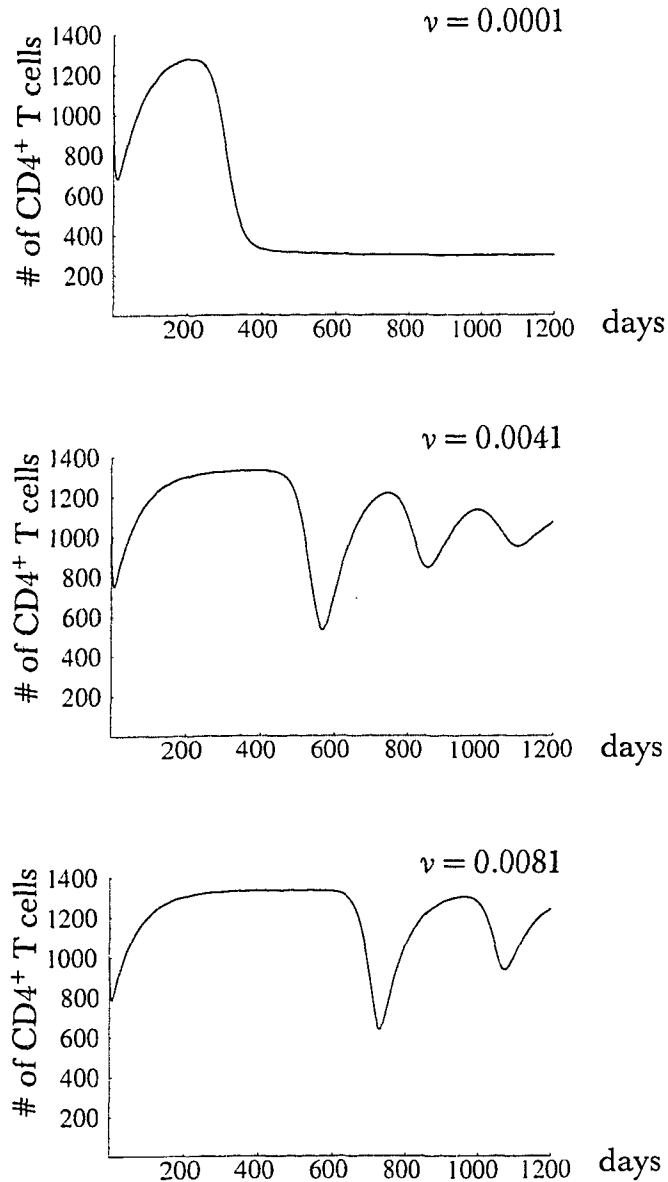


Figure 5.4. *MATHEMATICA* simulations of the healthy CD4⁺ T-cell count as the responsiveness v changes. Parameter values are $\mu_1 = \mu_2 = \mu_3 = 0.015$, $\lambda = 20$, $\beta = 0.001$, and $\gamma = 0.2$. The values of R_1 are 0.404, 3.57 and 3.95 respectively. The initial conditions are $x(0) = 1000$, $y(0) = 10$ and $z(0) = 1$.

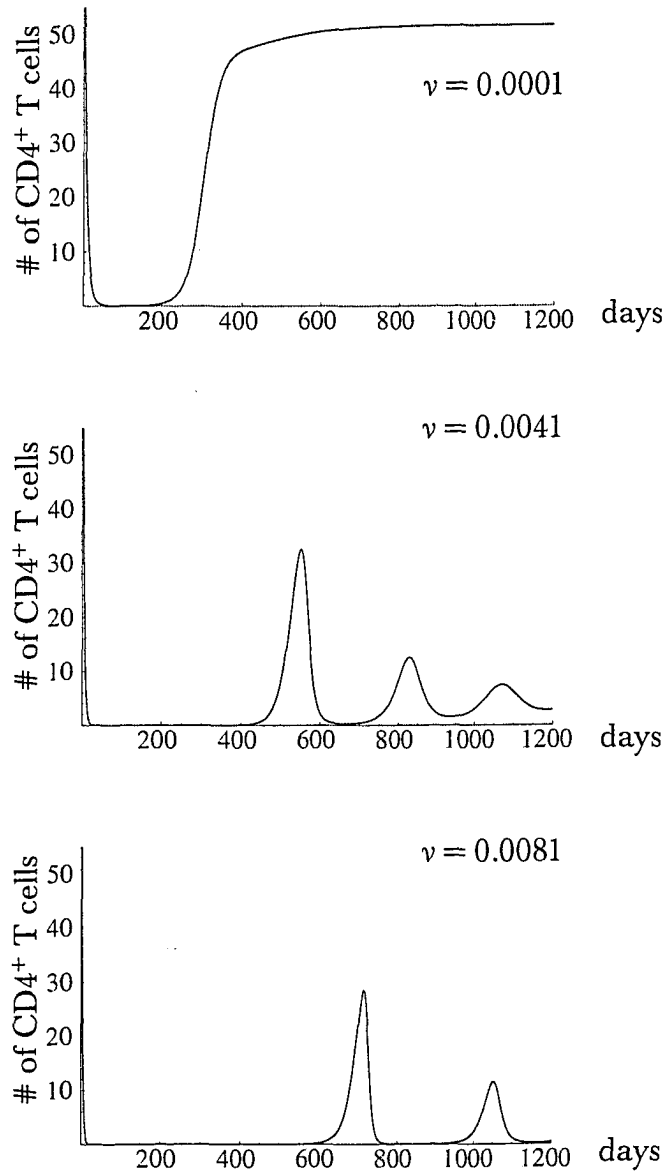


Figure 5.5. *MATHEMATICA** simulations of the proviral load as the responsiveness ν changes. Parameter values and initial conditions are the same as in Figure 5.4.

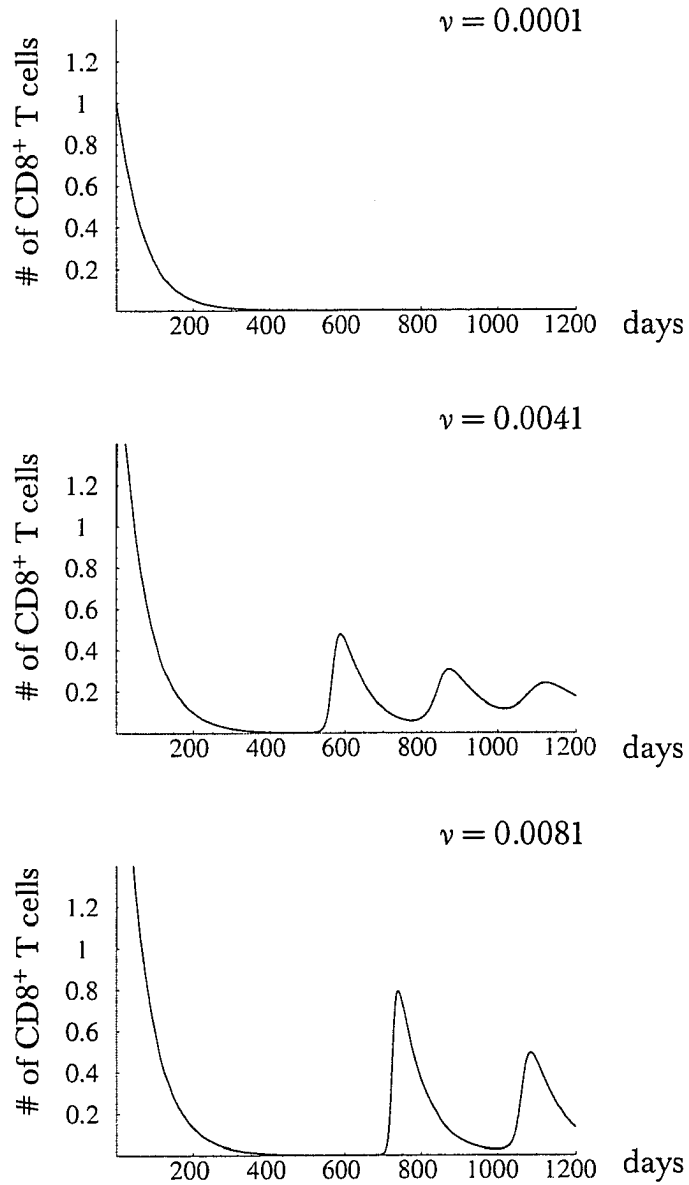


Figure 5.6. *MATHEMATICA*[®] simulations of the CD8⁺ T-cell level as the responsiveness ν changes. Parameter values and initial conditions are the same as in Figure 5.4.

The rate of CTL-driven elimination, γ , does not affect the values of R_1 nor R_0 . Nevertheless, γ can reduce CD8⁺ CTL levels. More precisely,

Corollary 5.8. Assume $R_1 > 1$. The CD8⁺ T-cell level at equilibrium z^* is a decreasing function of γ .

Proof. Write g as

$$g(z) = c - (\gamma + b)z - a\gamma z^2,$$

where a , b , and c are adequate positive constants. Let $z^* = z^*(\gamma)$ be the positive root of g . Then,

$$\frac{dz^*}{d\gamma} = \frac{-b(\gamma + b) - 2a\gamma + b\sqrt{(\gamma + b)^2 + 4a\gamma}}{2a\gamma^2\sqrt{(\gamma + b)^2 + 4a\gamma}} \leq 0.$$

This proves the corollary. *q.e.d.*

Biologically speaking, this means that as the rate γ augments, CTLs lyse more effectively HTLV-I-infected CD4⁺ T cells; then, the stimulation of CD8⁺ decreases and so does the equilibrium level z^* . It is worth mentioning that changes in γ also produce damped oscillations in the solutions. Similar oscillations have been observed in the proviral load of HAM/TSP patients [27]. Also, patients treated with the reverse transcriptase inhibitor lamivudine show similar oscillations in the proviral load [6].

In Figures 5.7-5.9, we change the rate of CTL-driven elimination, γ , keeping the other parameters fixed.

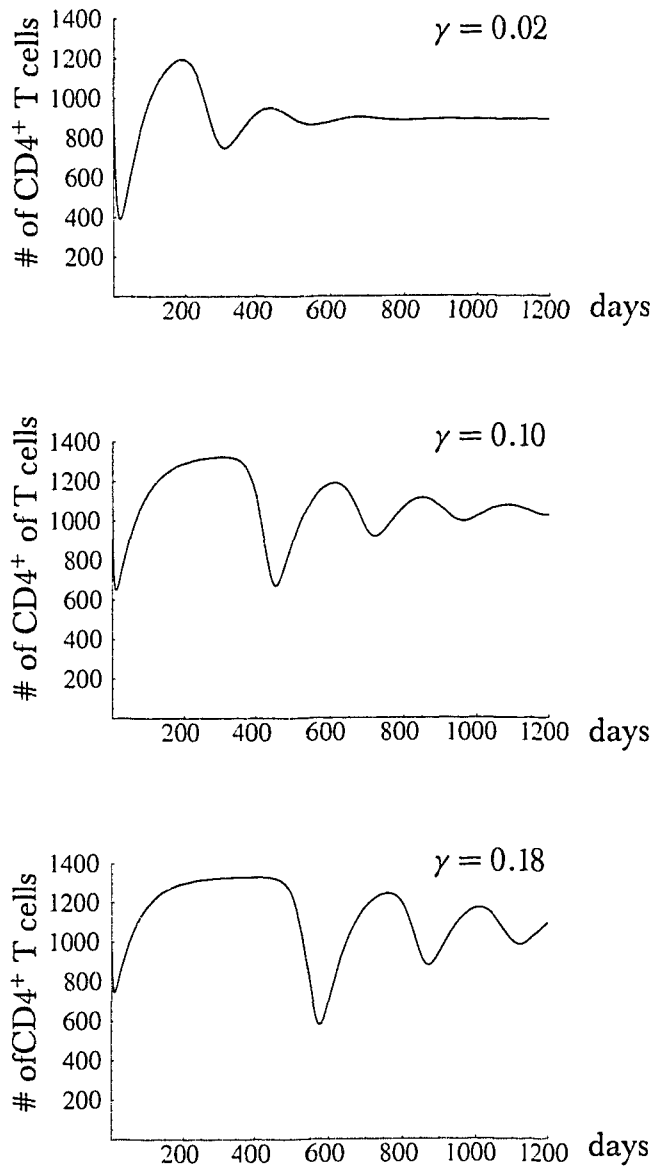


Figure 5.7. Numerical simulations of healthy CD4⁺ T-cell count as the lyse rate γ changes. Parameter values are $\mu_1 = \mu_2 = \mu_3 = 0.015$, $\lambda = 20$, $\beta = 0.001$, and $\nu = 0.005$. Initial conditions are $x(0) = 1000$, $y(0) = 100$ and $z(0) = 1$.

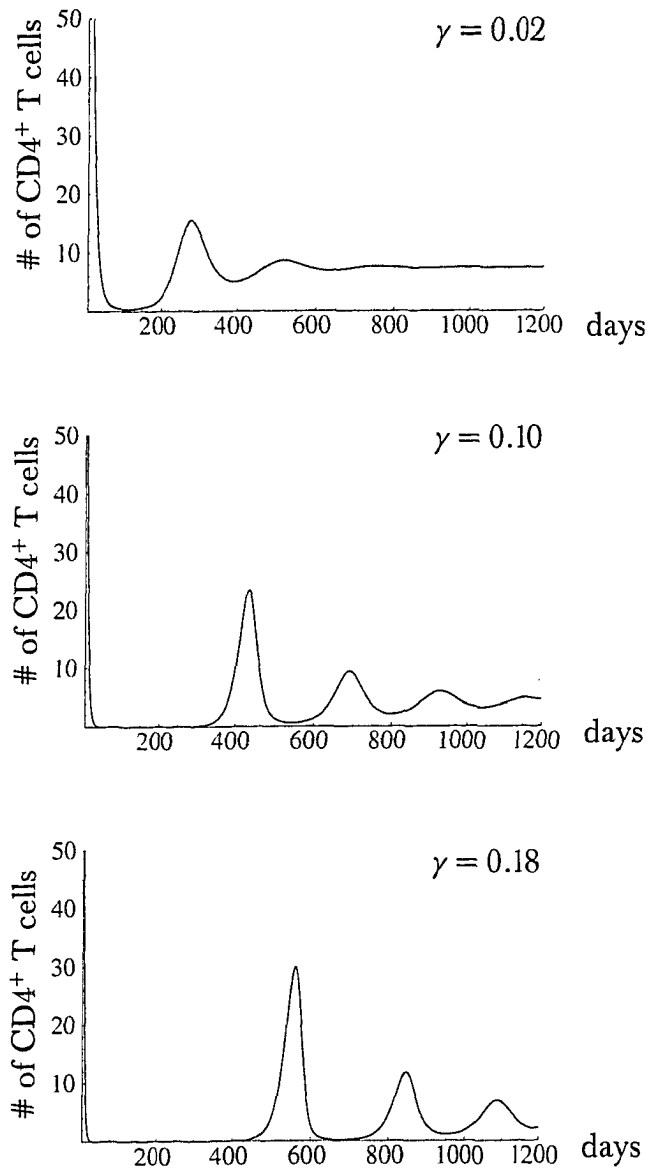


Figure 5.8. Numerical simulations of the levels of HTLV-I-infected CD4⁺ T cells as the lyse rate, γ , changes. The rest of the parameter values and initial conditions are the same as in Figure 5.7.

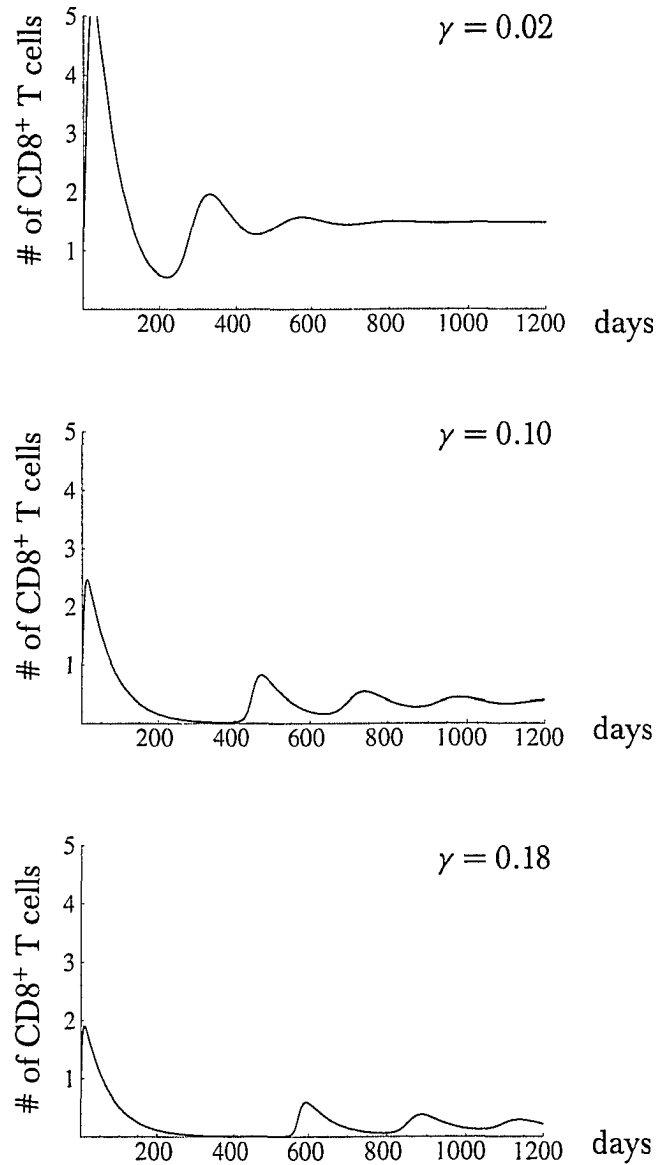


Figure 5.9. Numerical simulations of the levels of $CD8^+$ T cells as the lysis rate, γ , changes. The rest of the parameter values and initial conditions are the same as in Figure 5.7.

5.6. Conclusions

$CD8^+$ cytotoxic T lymphocytes eliminate infected cells by releasing pore-forming proteins and inflammatory cytokines such as $IFN-\gamma$ and $TNF-\alpha$. In HTLV-I infection,

CD8⁺ T cells target primarily the Tax proteins expressed on the surface of infected CD4⁺ T cells [25, 30]. It has been observed that Tax genes accelerate cell growth and delay apoptosis in ATL patients [28]. Asymptomatic carriers and HAM/TSP patients harbour abundant levels of anti-Tax CD8⁺ cells. Furthermore, HTLV-I-specific CD8⁺ T cells have been found in the CNS of HAM/TSP patients [21]; this raises the question whether the high levels of CD8⁺ T cells contribute to the pathogenesis of HAM/TSP or vice versa.

We propose and analyse a mathematical model for the CD8⁺ T-cell response to HTLV-I infection. The model considers that HTLV-I-infected cells are eliminated at rate γ . Since infected T cells stimulate CD8⁺ to proliferate, we consider a density-dependent proliferation with ν as the average rate of proliferation (also called responsiveness) [23]. We demonstrate that the number of equilibria and the global dynamics of system (5.1) depends on the basic reproduction number in the absence of CTLs, R_0 , and the basic reproduction number in the presence of CTL, R_1 . The threshold parameter R_0 determines the widespread of HTLV-I infection among the CD4⁺ T-cell pool. On the other hand, the parameter R_1 determines whether the CD8⁺ CTL response is maintained active or not.

Based on the high levels of CD8⁺ CTL in HAM/TSP patients, we hypothesize that those patients are more likely to have $R_1 > 1$, whereas asymptomatic carriers should have R_1 with values below 1. Moreover, when $R_1 > 1$, we demonstrate that there is a positive correlation between the proviral load and the CD8⁺ T-cell level at equilibrium. This correlation has been clinically verified in HAM/TSP patients [21]. Therefore, a reduction of R_1 would be a control measure for asymptomatic carriers to avoid HAM/TSP development.

There are two important parameters to measure the effectivity of the CD8⁺ CTL response: the rate of lysis of infected cells by HTLV-I-specific CTLs, γ , and the CTL proliferation rate, or responsiveness, ν [3, 24]. We prove that HTLV-I-infected patients with a low responsiveness exhibit high proviral levels. Whereas, patients with a strong responsiveness have smaller values of R_1 and, consequently, they reduce

their chances of developing HAM/TSP. Our numerical simulations and Corollary 5.7 suggest that the proviral levels are reduced when the responsiveness augments. Such a HTLV-I proviral reduction corroborates the protective role of CD8⁺ CTLs in HTLV-I infection claimed by Bangham et al. [5, 10, 29]. Interestingly, the rate of CTL-mediated lysis, γ , can be changed without affecting the basic reproduction number in presence of CTL response R_1 . But, it can be verified that the equilibrium level of anti-HTLV-I CTLs, z^* , is a decreasing function of γ . Thus, as the lysing efficiency augments, the number of CTLs required to eliminate infected cells also declines. In our numerical simulations we show that an increase in the rate of lysis reduces the infected CD4⁺ and CD8⁺ T-cell loads alike.

In summary, based on our analysis and simulations, we conclude that the cytotoxic response to HTLV-I-infection can

- reduce the number of infected cells,
- increase the abundance of healthy CD4⁺ T cells, and
- keep low levels of CD8⁺ CTLs,

when the rate of lysis and proliferation rate are carefully adjusted. Therefore, the risk of developing HAM/TSP is more likely to be related with the ability of the individual to mount an appropriate immune response as suggested by Bangham et al. [3, 5, 29]. Unfortunately, in our model the relevance of CD8⁺ T-cell response to ATL is not evident.

5.8. References

- [1] A. K. ABBAS, A. H. LICHTMAN, AND J. S. POBER, *Cellular and Molecular Immunology*, W. B. Saunders Company, 4 ed., 2000.
- [2] B. ARNULF, M. THOREL, Y. POIROT, R. TAMOUZA, E. BOULANGER, A. JACCARD, E. OKSENHENDLER, O. HERMINE, AND C. PIQUE, *Loss of the ex vivo but not the reinducible CD8⁺ T-cell response to Tax in human T-cell leukemia*

- virus type 1-infected patients with adult T-cell leukemia/lymphoma*, *Leukemia*, 18 (2004), pp. 126–132.
- [3] B. ASQUIT AND C. R. M. BANGHAM, *The role of cytotoxic T lymphocytes in human T-cell lymphotropic virus type 1 infection*, *J. Theor. Biol.*, 207 (2000), pp. 65–79.
- [4] C. M. R. BANGHAM, *The immune response to HTLV-I*, *Curr. Opin. Immunol.*, 12 (2000), pp. 397–402.
- [5] ———, *Genetics and dynamics of the immune response to HTLV-I*, in *Two Decades of Adult T-cell Leukemia and HTLV-I Research*, K. Sugamura, T. Uchiyam, M. Matsuoka, and M. Kannagi, eds., Japan Scientific Societies Press, 2003, pp. 149–170.
- [6] C. R. M. BANGHAM, S. E. HALL, K. J. M. JEFFERY, A. M. VINE, A. WITOKOVER, M. A. NOWAK, K. USUKU, AND M. OSAME, *Genetic control and dynamics of the cellular immune response to the human T-cell leukemia virus, HTLV-I*, *Philos. T. Roy. Soc. B.*, 354 (1999), pp. 691–700.
- [7] S. J. FLINT, L. W. ENQUIST, R. M. KRUG, V. R. RACANIELLO, AND A. M. SKALKA, *Principles of Virology: Molecular Biology, Pathogenesis, and Control*, American Society of Microbiology Press, 2000.
- [8] H. I. FREEDMAN AND J. W.-H. SO, *Global stability and persistence of simple food chains*, *Math. Biosc.*, 76 (1985), pp. 69–86.
- [9] R. A. GOLDSBY, T. J. KINDT, B. A. OSBORNE, AND J. KUBY, *Immunology*, W. H. Freeman and Company, 5th. ed., 2003.
- [10] P. K. C. GOON, A. BIANCARDI, N. FAST, T. IGAKURA, E. HANON, A. J. MOSLEY, B. ASQUIT, K. G. GOULD, S. MARSHALL, G. P. TAYLOR, AND C. R. M. BANGHAM, *Human T cell lymphotropic virus HTLV-1-specific CD8⁺ T cells: frequency and immunodominance hierarchy*, *J. Infec. Dis.*, 189 (2004), pp. 2294–2298.

- [11] C. GRANT, K. BARMAK, T. ALEFANTIS, J. YAO, S. JACOBSON, AND B. WIGDAHL, *Human T cell leukemia virus type I and neurologic disease: events in bone marrow, peripheral blood, and central nervous system during normal immune surveillance and neuroinflammation*, *J. Cell. Physiol.*, 190 (2002), pp. 133–159.
- [12] T. F. GRETEN, J. E. SLANSKY, R. KUBOTA, S. S. SOLDAN, E. M. JAFFEE, T. P. LIEST, D. M. PARADOLL, S. JACOBSON, AND J. P. SCHNECK, *Direct visualization of antigen-specific T cells: HTLV-I Tax 11-19-specific CD8⁺ cells are activated in peripheral blood and accumulate in cerebrospinal fluid from HAM/TSP patients*, *Proc. Natl. Acad. Sci. USA*, 95 (1998), pp. 7568–7573.
- [13] E. HANON, S. HALL, G. P. TAYLOR, M. SAITO, R. DAVIS, Y. TANAK, K. USUKU, M. OSAME, J. N. WEBER, AND C. R. M. BANGHAM, *Abundant Tax protein expression in CD4⁺ T cells infected with HTLV-I is prevented by cytotoxic T lymphocytes*, *Blood*, (2000), pp. 1386–1392.
- [14] S. JACOBSON, H. SHIDA, D. E. MCFARLIN, A. S. FAUCI, AND S. KOENIG, *Circulating CD8⁺ cytotoxic T lymphocytes specific for HTLV-I pX in patients with HTLV-I associated neurological disease*, *Nature*, 348 (1990).
- [15] M. KANNAGI, K. SUGAMURA, K. KINOSHITA, H. UCHINO, AND Y. HINUMA, *Cytotoxic T-cell response and expression of the target antigen in HTLV-I infection*, *Leukemia*, 8 (Supp. 1) (1994), pp. S54–S59.
- [16] A. KOROBENIKOV AND P. K. MAINI, *A Lyapunov function and global properties for SIR and SEIR epidemiological models with nonlinear incidence*, *Math. Biosc. Eng.*, 1 (2004), pp. 57–60.
- [17] A. KOROBENIKOV AND G. C. WAKE, *Lyapunov functions and global stability for SIR, SIRS, and SIS epidemiological models*, *Appl. Math. Lett.*, 15 (2002), pp. 955–960.

- [18] R. KUBOTA, T. KAWANISHI, H. MATSUBARA, A. MANNS, AND S. JACOBSON, *HTLV-I specific IFN- γ^+ CD8 $^+$ lymphocytes correlate with the proviral load in peripheral blood of infected individuals*, J. Neuroimmunol., 102 (2000), pp. 208–215.
- [19] J. P. LASALLE, *The Stability of Dynamical Systems*, Regional Conference Series in Applied Mathematics, SIAM, 1976.
- [20] B. MACCHI, I. FARAONI, J. ZHANG, S. GRELLI, C. FAVALLI, A. MARTINO, AND E. BONMASSAR, *AZT inhibits the transmission of human T-cell leukaemia/lymphoma virus type I to adult peripheral blood mononuclear cells in vitro*, J. Gen. Virol., 78 (1997), pp. 1007–1016.
- [21] M. NAGAI, Y. YAMANO, M. B. BRENNAN, C. A. MORA, AND S. JACOBSON, *Increased HTLV-I proviral load and preferential expansion of HTLV-I Tax-specific CD8 $^+$ T cells in cerebrospinal fluid from patients with HAM/TSP*, Ann. Neurol., 50 (2001), pp. 807–812.
- [22] P. W. NELSON, J. D. MURRAY, AND A. S. PERELSON, *A model of HIV-1 pathogenesis that includes an intracellular delay*, Math. Biosci., 163 (2000), pp. 201–215.
- [23] M. A. NOWAK AND C. R. M. BANGHAM, *Population dynamics of immune responses to persistent viruses*, Science, 272 (1996), pp. 74–79.
- [24] M. A. NOWAK AND R. M. MAY, *Virus Dynamics: Mathematical Principles of Immunology and Virology*, Oxford University Press, 2000.
- [25] C. E. PARKER, S. DAENKE, S. NIGHTINGALE, AND C. R. M. BANGHAM, *Activated, HTLV-1-specific cytotoxic T-lymphocytes are found in healthy seropositives as well as in patients with tropical spastic paraparesis*, Virology, 188 (1992), pp. 628–636.
- [26] A. S. PERELSON, *Modeling the interaction of the immune system with HIV*, in Mathematical and Statistical Approaches to AIDS Epidemiology, C. Castillo-Chávez, ed., vol. 83 of Lecture Notes in Biomathematics, Springer-Verlag, 1989, pp. 350–370.

- [27] J. H. C. TOSSWILL, G. P. TAYLOR, J. P. CHEWLEY, AND J. N. WEBER, *Quantification of proviral DNA load in human T-cell leukaemia virus type I infections*, *J. Virol. Meth.*, 75 (1998), pp. 21–26.
- [28] T. TSUKAHARA, M. KANNAGI, T. OHASHI, H. KATO, M. ARAI, G. NUNEZ, Y. IWANAGA, N. YAMAMOTO, K. OHTANI, M. NAKAMURA, AND M. FUJII, *Induction of Bcl-x(L) expression by human T-cell leukemia virus type 1 Tax through NF- κ B in apoptosis resistant T-cell transfectants with Tax*, *J. Virol.*, 73 (1999), pp. 7981–7987.
- [29] D. WODARZ, M. A. NOWAK, AND C. R. M. BANGHAM, *The dynamics of HTLV-I and the CTL response*, *Immunol. Today*, 20 (1999), pp. 220–227.
- [30] Y. YAMANO, M. NAGAI, M. BRENNAN, C. A. MORA, S. S. SOLDAN, U. TOMARU, N. TAKENOUCI, S. IZUMO, M. OSAME, AND S. JACOBSON, *Correlation of human T-cell lymphotropic virus type 1 (HTLV-1) mRNA with proviral DNA load, virus-specific CD8⁺ T cells and disease severity in HTLV-1-associated myelopathy (HAM/TSP)*, *Blood*, 99 (2002), pp. 88–94.

Chapter 6

Conclusions

6.1. General Discussion

Human T-cell Leukaemia/Lymphoma Virus Type I (HTLV-I) is the causative agent of adult T-cell Leukaemia (ATL) and HTLV-I-Associated Myelopathy/Tropical Spastic Paraparesis (HAM/TSP) [8]. HTLV-I is endemic in several regions around the world, including Japan and Caribbean Islands. It is estimated that between 10 to 20 million people are infected. HTLV-I is a retrovirus with genetic structure similar to HIV. However, HTLV-I spreads horizontally by cell-to-cell contact and its virions are not very infectious. The main target of HTLV-I infection is the $CD4^+$ T-cell population.

During the course of HTLV-I infection, the immune system activates different processes to control the viral replication. Antibodies against HTLV-I either inhibit the virus attachment to cellular receptors or interfere with membrane fusion that allows viral RNA entry to the cytoplasm [9]. These antibodies are detected within a few weeks after the primary infection [5]. Also, asymptomatic carriers harbour high levels of anti-HTLV-I cytotoxic T cells (CTLs) in the peripheral blood [1]. Intensification of the host immune response might lead to prevention of ATL and HAM/TSP [6]. Therefore, it is important to understand the dynamics of the transmission in order to propose effective strategies for the control of HTLV-I infection.

We have proposed and investigated several mathematical models that may help to elucidate the infection dynamics. Our approach is based on the compartmental models amply used in theoretical epidemiology. We have adopted many key concepts

and terminology from epidemiological models such as basic reproduction number, contact rate, incidence form, etc. In spite of these similarities, immunological models in this thesis have peculiarities that deserve their own analysis and interpretation.

In Chapter 2, we analysed a basic model for HTLV-I-infection dynamics. We assumed that the incidence form depends on the total $CD4^+$ T-cell population. The horizontal transmission proposed includes both the bilinear and standard incidence forms alike. We have proved that the basic reproduction number R_0 governs the global dynamics of the system. More specifically, when $R_0 \leq 1$ infected cells always die out. When $R_0 > 1$, a chronic infection is established. This type of behaviour is common in many compartmental models and it is referred to as ‘forward bifurcation’. Interestingly, our analysis showed that the standard incidence form induces higher levels of HTLV-I-infected $CD4^+$ T cells than the bilinear one.

In Chapter 3, we proposed an extension to our basic model that incorporates mitotic division. Unlike other retroviruses such as HIV, HTLV-I shows an extraordinary genetic stability and the bulk of the proviral load is made up of relatively few clones [7]. The high levels of HTLV-I-carrier cells in the peripheral blood may suggest that the high proviral loads are maintained by the mitotic division of HTLV-I-infected cells. We proved that under biologically sound conditions, the model exhibits ‘backward bifurcation’. This bifurcation has ‘catastrophic’ effects on the dynamics, in which a reduction in the basic reproduction number is not necessarily the best measure to control the infection.

In Chapter 4, we proposed and analysed a model that considers the infection of $CD34^+$ stem cells with HTLV-I. Clinical evidence shows that the $CD34^+$ hematopoietic cells are susceptible to HTLV-I infection *in vitro*. Also, infected $CD34^+$ cells can turn into $CD4^+$ T cell and preserve the viral DNA [2]. Thus, $CD34^+$ hematopoietic cells act as a reservoir for HTLV-I. We proved the global dynamics of this reservoir-type of model. We showed that there is a slow invasion of the bone marrow. This invasion may provoke the persistence of the infection and ultimately the high proviral levels observed in HTLV-I-infected patients.

In Chapter 5, we have analysed a model that incorporates $CD8^+$ T-cell immune response to our basic model. $CD8^+$ cytotoxic cells release inflammatory cytokines and pore-forming proteins to eliminate infected cells. However, an overproduction of these proteins can damage bystander cells. HAM/TSP patients show extraordinarily high levels of activated $CD8^+$ T cells in the peripheral blood [3]. Furthermore, $CD8^+$ T cells can be detected in the cerebrospinal fluid of HAM/TSP patients. These findings have opened a controversy about the protective role of the CTL response in HAM/TSP prognosis. We concluded that the global dynamics of the CTL response is determined by two parameters: the basic reproduction number in the absence of CTLs R_0 , and by a basic reproduction number modified by the presence of CTLs R_1 . Also, we proved that when an active CTL response is present, the proviral load and level of CTLs have a positive correlation (see (5.8)). Furthermore, the same condition can be used to calculate the responsiveness in terms of the proviral load and CTLs level. We hypothesized that HAM/TSP patients are more likely to have $R_1 > 1$, whereas most of the asymptomatic carriers should have $R_1 < 1$. This also suggests that, in a chronic infection (i.e. $R_0 > 1$), keeping $R_1 < 1$ may be a more realistic strategy for preventing the development of HAM/TSP .

Mathematically, we strive to establish rigorously the global dynamics of our models. Global stability is a highly nontrivial problem in the theory of Ordinary Differential Equations. Traditionally, Lyapunov's direct method is used to address that issue. For models where no Lyapunov function has been discovered, the method developed by Li and Muldowney to prove global stability is an alternative to address that problem. Both the Lyapunov's direct method and the method of Li and Muldowney are used in our global analysis.

Finally, this work might have shown the relevance of the mathematical modelling in HTLV-I-infection dynamics. At the present, HTLV-I-infection and related diseases have not been as profusely studied as HIV and AIDS. To our knowledge, our modelling parameters have not been calculated experimentally for HTLV-I. It is our wish that this thesis will motivate further interdisciplinary research on HTLV-I infection.

6.2. Future Research

We have proved that proviral loads can be obtained by either mitotic division of HTLV-I-infected CD4⁺ T cells or by maturation of CD34⁺ hematopoietic cells. It may be necessary to clarify which route is more important and easier to control experimentally.

An extension of our models to include ATL progression is necessary. As any other hematological malignancy, transformation from an infected cell to an oncogenic one is a multifactorial process. Nonetheless, the proliferation rate of cancer cells deserves further investigation. The analysis of such a 'generalised' model may usher chemotherapy strategies [4].

Generalisations to our models will pose new challenges for model analysis and give ample opportunities for developing new mathematical methods and techniques to analyse systems of non-linear differential equations.

It would be fruitful if further research is done to establish any cause-effect relationship between HTLV-I-infected cells and the immune system response. It is hoped that other researchers in the area will be encouraged to make use of the models we used in this exploratory effort.

It is in our best interest to motivate interdisciplinary research to get a better understanding of HTLV-I infection, since it affects so many people in this world.

6.3. References

- [1] A. J. CANN AND I. S. Y. CHEN, *Human T-cell leukemia virus type I and II*, in Fields Virology, B. N. Fields, D. M. Knipe, and P. M. Howley, eds., Lippincott-Raven Publishers, 1996, pp. 1849–1880.
- [2] G. FEUER, J. K. FRASER, J. A. ZACK, F. LEE, R. FEUER, AND I. S. Y. CHEN, *Human T-cell leukemia infection of human hemotopoietic progenitor cells: maintenance of*

- virus infection during differentiation in vitro and in vivo*, J. Virol., 70 (1996), pp. 4038–4044.
- [3] C. GRANT, K. BARMAK, T. ALEFANTIS, J. YAO, S. JACOBSON, AND B. WIGDAHL, *Human T cell leukemia virus type I and neurologic disease: events in bone marrow, peripheral blood, and central nervous system during normal immune surveillance and neuroinflammation*, J. Cell. Physiol., 190 (2002), pp. 133–159.
- [4] T. ISHIKAWA, *Current status of therapeutic approaches to adult T-cell leukemia*, Int. J. Hematol., 78 (2003), pp. 304–311.
- [5] A. MANNS, E. L. MURPHY, R. WILK, G. HAYNES, J. P. FIGUEROA, B. HANCHARD, M. BARNETT, J. DRUMMOND, D. WATERS, M. CERNEY, J. R. SEALS, S. S. ALEXANDER, H. LEE, AND W. A. BLATTNER, *Detection of early human T-cell lymphotropic virus type I antibody patterns during seroconversion among transfusion recipients*, Blood, 77 (1991), pp. 896–905.
- [6] M. MATSUOKA, *Somatic alterations in adult T-cell leukemia cells*, in Two Decades of Adult T-cell Leukemia and HTLV-I Research, K. Sugamura, T. Uchiyam, M. Matsuoka, and M. Kannagi, eds., Japan Scientific Societies Press, 2003, pp. 115–126.
- [7] F. MORTREUX, M. KAZANJI, A.-S. GABET, B. DE THOISY, AND E. WATTEL, *Two-step nature of human T-cell leukemia virus type 1 replication in experimentally infected squirrel monkeys (saimiri sciureus)*, J. Virol., 75 (2001), pp. 1083–1089.
- [8] N. E. MUELLER AND W. A. BLATTNER, *Retroviruses-human T-cell lymphotropic virus*, in Viral Infections in Humans: Epidemiology and Control, A. S. Evans and R. A. Kaslow, eds., Plenum Medical Book Company, 1997, pp. 785–813.
- [9] H. SHIRAKI, Y. SAGARA, AND Y. INOUE, *Cell-to-cell transmission of HTLV-I*, in Two Decades of Adult T-cell Leukemia and HTLV-I Research, K. Sugamura, T. Uchiyam, M. Matsuoka, and M. Kannagi, eds., Japan Scientific Societies Press, 2003, pp. 303–316.

Appendix A

A.1. Lozinskiĭ Measure

Let $A = (a_{ij})$ be a $n \times n$ real matrix. For a vector norm $|\cdot|$ in \mathbb{R}^n , the matrix norm of A induced by $|\cdot|$ is defined as

$$|A| = \sup_{|x|=1} |Ax|.$$

The *Lozinskiĭ measure* μ of A with respect to $|\cdot|$ is defined as

$$\mu(A) = \lim_{h \rightarrow 0^+} \frac{|I_n + hA| - 1}{h},$$

where I_n denotes the identity matrix. It can be verified that μ satisfies

$$\mu(\alpha A) = \alpha \mu(A) \quad \text{if } \alpha \geq 0,$$

$$|\mu(A)| \leq |A|,$$

$$\mu(A + B) \leq \mu(A) + \mu(B).$$

For some standard vector norms, the matrix norms and the Lozinskiĭ measures are given below.

$ x $	$ A $	$\mu(A)$
$\sup_i x_i $	$\sup_i \sum_k a_{ik} $	$\sup_i (a_{ii} + \sum_{k, k \neq i} a_{ik})$
$\sum_i x_i $	$\sup_k \sum_i a_{ik} $	$\sup_k (a_{kk} + \sum_{i, i \neq k} a_{ik})$
$\sqrt{(\sum_i x_i ^2)}$	Square root of largest characteristic root of A^*A	Largest characteristic root of $\frac{1}{2}(A^* + A)$

For properties and calculations of Lozinskiĭ measures we refer the reader to [2].

A.2. Compound Matrices

Let T be a linear operator on \mathbb{R}^n and A its matrix representation with respect to the standard basis $\{e_1, \dots, e_n\}$. Let $\wedge^2 T$ denote the exterior power of the operator

T on $\overset{2}{\wedge}\mathbb{R}^n$ (see [1, 3]). T induces canonically a linear operator $T^{[2]}$ on $\overset{2}{\wedge}\mathbb{R}^n$. More specifically, for any decomposable element $v_1 \wedge v_2$ we have

$$T^{[2]}(v_1 \wedge v_2) = T(v_1) \wedge v_2 + v_1 \wedge T(v_2).$$

The matrix associated to $T^{[2]}$ with respect to the canonical basis $\{e_i \wedge e_j\}_{i < j}$ is denoted by $A^{[2]}$ and called the *second additive compound matrix* of A . This is an $\binom{n}{2} \times \binom{n}{2}$ matrix and satisfies the property $(A + B)^{[2]} = A^{[2]} + B^{[2]}$. In the special case when $n = 2$, we have $A^{[2]} = \text{Tr } A$. For $n = 3$, the second additive compound matrix of $A = (a_{ij})$ is

$$A^{[2]} = \begin{pmatrix} a_{11} + a_{22} & a_{23} & -a_{13} \\ a_{32} & a_{11} + a_{33} & a_{12} \\ -a_{31} & a_{21} & a_{22} + a_{33} \end{pmatrix}.$$

For a detailed discussion of compound matrices and their properties, we refer the reader to [2]. A comprehensive survey on compound matrices and their relations to differential equations is given in [4].

References

- [1] O. A. BIBERSTEIN, *Fundamentos de Variedades Diferenciables*, Instituto Politécnico Nacional, México, 2001.
- [2] M. FIEDLER, *Additive compound matrices and inequality for eigenvalues of stochastic matrices*, Czech. Math. J., 99 (1974), pp. 392–402.
- [3] S. LANG, *Real and Functional Analysis*, Springer-Verlag, 3rd. ed., 1993.
- [4] J. S. MULDOWNY, *Compound matrices and ordinary differential equations*, Rocky Mountain J. Math., 20 (1990), pp. 857–872.

Appendix B

Li and Muldowney's Method for Global Stability

We quote a general method of Li and Muldowney for proving global stability. For a detailed presentation of the result see [1].

Let $\Omega \subset \mathbb{R}^n$ be an open subset and $f: \Omega \rightarrow \mathbb{R}^n$ be a C^1 function. Consider the autonomous differential equation

$$x' = f(x). \tag{E}$$

An equilibrium point x^* of (E) is called *globally stable* in Ω if it is locally stable and all trajectories in Ω converge to x^* . Let $x(t, x_0)$ denote the solution of (E) satisfying $x(0, x_0) = x_0$ and $Df(x)$ the Jacobian matrix of f at x . Assume that (E) satisfies the following two conditions:

(H1) (E) has only one equilibrium point x^* in Ω .

(H2) (E) has a compact absorbing set $K \subset \Omega$.

Let $x \mapsto P(x)$ be an $\binom{n}{2} \times \binom{n}{2}$ matrix-valued function that is C^1 on Ω . Assume that $P^{-1}(x)$ exists and is continuous for $x \in K$. For a Lozinskiĭ measure μ , a quantity \bar{q}_2 is defined as

$$\bar{q}_2 = \limsup_{t \rightarrow \infty} \sup_{x_0 \in K} \frac{1}{t} \int_0^t \mu(B(x(s, x_0))) ds, \tag{1}$$

where

$$B = P_f P^{-1} + P(Df)^{[2]} P^{-1},$$

and the matrix P_f is obtained by replacing each entry p_{ij} in P by its direction derivative in the direction f , $\nabla p_{ij}^* f$. The matrix $Df(x)^{[2]}$ is the second additive compound matrix of the Jacobian matrix $Df(x)$ (see Appendix A).

The following global-stability result is due to Li and Muldowney (see [1, Theorem 3.5]).

Theorem. (Li and Muldowney). Assume that Ω is simply connected and that the assumptions (H1) and (H2) hold. Then \bar{x} is globally stable in Ω if there exists a function $P(x)$ and a Lozinskiĭ measure μ such that \bar{q}_2 defined in (1) satisfies $\bar{q}_2 < 0$.

References

- [1] M. Y. LI AND J. S. MULDOWNEY, *A geometric approach to global-stability problems*, SIAM J. Math. Anal., 27 (1996), pp. 1070–1083.